2021

ENTRY AND EARLY INFECTION OF NON-SEGMENTED NEGATIVE SENSE RNA VIRUSES

Jean Mawuena Branttie
University of Kentucky, jean.m.branttie@gmail.com
Digital Object Identifier: https://doi.org/10.13023/etd.2021.248

STUDENT AGREEMENT:

I represent that my thesis or dissertation and abstract are my original work. Proper attribution has been given to all outside sources. I understand that I am solely responsible for obtaining any needed copyright permissions. I have obtained needed written permission statement(s) from the owner(s) of each third-party copyrighted matter to be included in my work, allowing electronic distribution (if such use is not permitted by the fair use doctrine) which will be submitted to UKnowledge as Additional File.

I hereby grant to The University of Kentucky and its agents the irrevocable, non-exclusive, and royalty-free license to archive and make accessible my work in whole or in part in all forms of media, now or hereafter known. I agree that the document mentioned above may be made available immediately for worldwide access unless an embargo applies.

I retain all other ownership rights to the copyright of my work. I also retain the right to use in future works (such as articles or books) all or part of my work. I understand that I am free to register the copyright to my work.

REVIEW, APPROVAL AND ACCEPTANCE

The document mentioned above has been reviewed and accepted by the student's advisor, on behalf of the advisory committee, and by the Director of Graduate Studies (DGS), on behalf of the program; we verify that this is the final, approved version of the student's thesis including all changes required by the advisory committee. The undersigned agree to abide by the statements above.

Jean Mawuena Branttie, Student

Dr. Rebecca Dutch, Major Professor

Dr. Trevor Creamer, Director of Graduate Studies

ENTRY AND EARLY INFECTION OF NON-SEGMENTED NEGATIVE SENSE RNA VIRUSES

DISSERTATION

A dissertation submitted in partial fulfillment of the
requirements for the degree of Doctor of Philosophy in the
College of Medicine
at the University of Kentucky

By
Jean Mawuena Branttie
Lexington, Kentucky
Director: Dr. Rebecca Dutch, Professor of Molecular and Cellular Biochemistry
Lexington, Kentucky
2021

ABSTRACT OF DISSERTATION

ENTRY AND EARLY INFECTION OF NON-SEGMENTED NEGATIVE SENSE RNA VIRUSES

Paramyxoviruses, pneumoviruses, and other non-segmented negative sense (NNS) RNA viruses have historically been of public health concern. Although their genomes are typically small (up to 19kbs) they are able to inflict large-scale detrimental pathologies on host cells. Human metapneumovirus (HMPV) is a widespread pathogen and is a NNS RNA virus. HMPV results respiratory tract infections and is particularly dangerous for preterm infants, the elderly, and immunocompromised individuals. Other viruses within the NNS RNA virus order include the deadly Ebola, Hendra, and Nipah viruses (EBOV, HeV, and NiV), as well as the re-emerging measles virus (MeV). Despite their public impact, there are currently very limited available FDA-approved therapeutics and antivirals against NNS RNA viruses.

During the infectious cycle, viral surface glycoproteins play critical roles in establishing infection. For most NNS RNA viruses, the attachment protein is important for the tethering of a viral membrane to host cells, while the fusion protein is responsible for the membrane merger of the virus and host. The fusion protein of paramyxo-and pneumovirus proteins are class I proteins that are folded into trimers, must be proteolytically cleaved to be functional, and are held in a metastable prefusion conformation until the signal for fusion occurs. Upon being signaled, the fusion protein undergoes dramatic essentially irreversible conformational changes for membrane mixing. Because of its important role in starting infection, F has garnered interest as a potentially powerful target against infection. For paramyxoviruses, the ectodomain regions of F have been well-studied; however, the hydrophobic nature of the transmembrane domain (TMD) of the protein has resulted in difficulties in crystallization. To address this, several biochemical assays have been utilized to address the function of the TMDs of paramyxo-and pneumovirus fusion proteins. Although initially thought to be solely a membrane anchor, the transmembrane domains of several viruses have been shown to be important for the functionality of fusion proteins. For some paramyxoviruses, replacement of the proteinaceous TMD resulted in the premature triggering. Further studies showed that the TMDs of paramyxoviruses and several other viral F proteins exist in isolation as trimers, and these trimeric associations in turn drive trimeric associations of the full protein. Studies of the HeV F TMD in isolation identified a leucine/isoleucine (L/I) zipper as an important motif for TMD-TMD trimerization. Mutations to this L/I zipper motif in the context of the full protein resulted in reduced surface expression, and a loss of functionality. The L/I zipper was found to be present in 140 paramyxo- and pneumovirus fusion protein TMDs. This work examines the importance of the L/I zipper in the context of another paramyxvovirus. We

used the model system, PIV5 F to dissect the role of the TMD L/I zipper fusogenic activity. We found that the (L/I) zipper plays important roles in functionality of the PIV5 F protein, but not surface expression of the protein.

Following membrane merging, a series of events occur that facilitate the release of viral contents into the host cell. The NNS RNA carried by the virus into the cell is used as a template for viral replication and transcription; two important steps in generation of viral progeny. In the life cycle of NNS viruses, viral proteins assume multi-functional roles to optimize their replication and spread. One of the key players during the course of infection is the matrix protein (M). The matrix protein has been identified as a master regulator of viral infection with most studies focusing on its roles in late-stage infection, during assembly and budding of viral progeny. The matrix proteins of many enveloped viruses have been shown to associate in high order oligomers to form a grid-like array underneath the plasma membrane, where they can induce membrane curvature to allow for the budding of viral particles. Not surprisingly, the absence of M in some NNS RNA viruses results in a significant viral titer decrease. Interestingly, some recent studies show that the matrix protein has other critical roles in viral infection such as immune modulation and host cell translation antagonism. One of these newly uncovered roles for viral matrix proteins involves the regulation of viral RNA synthesis. Studies with EBOV and MeV demonstrate that the matrix protein is involved in early infection events, as inhibits viral replication. To study the roles of the HMPV M protein in early infection, we performed a spatiotemporal analysis of M in HMPV-infected cells. We noted the presence of HMPV M within the nucleus during early infection. Our knockdown studies of HMPV M indicate that HMPV M is a positive regulator of viral replication and transcription, as in its absence, the rates of mRNA and viral genomic RNA synthesis are dramatically reduced. Additionally, within the NNS RNA virus order, HMPV M is the only matrix protein found to bind calcium. We created alanine mutants to the calcium coordinating residues of HMPV M and found that these residues were important in properly folding the protein. Together, these findings contribute to our understanding of the mechanisms of NNS RNA viral infection.

KEYWORDS: Paramyxovirus; Pneumovirus; Matrix protein; Fusion protein; Membrane fusion; Viral replication.

Jean Mawuena Branttie

(Name of Student)

6/2/2021

Date

ENTRY AND EARLY INFECTION OF NON-SEGMENTED NEGATIVE SENSE RNA VIRUSES

By
Jean Mawuena Branttie

Dr. Rebecca Dutch
Director of Dissertation

Dr. Trevor Creamer
Director of Graduate Studies

6/2/2021
Date

Dedicated to

My father, Ernest Branttie for giving me the courage to live my wildest dreams.

ACKNOWLEDGEMENTS

My time at the Dutch lab has been an incredibly powerful experience; one that I will continue to appreciate throughout my career. The work presented here would not be possible without the exceptional guidance of Dr. Dutch, whose dedication to my success has encouraged me through the toughest times. This journey began with my incredible undergraduate mentors at Kentucky State University. Dr. Alexander Lai, who I am extremely grateful for, personally nurtured my academic interests and was paramount in building up my confidence to apply to pursue graduate school. Dr. Suzette Polson remains one of my favorite teachers; her talent in teaching organic chemistry and biochemistry allowed me to realize a passion for the subjects. Dr. Kazi Javed and Dr. Tamara Sluss, thank you for always believing in me, for providing resources and opportunities outside of the classroom, and for seemingly having endless amounts of time to prepare me for graduate school. I would also like to thank the mentors of the labs I rotated in during my first year: Dr. Erin Garcia, Tanya Myers-Morales, and Dr. Yvonne Fondufe-Mittendorf, who were some of the first to train me at UK. I am thankful for the particularly encouraging words Dr. Yvonne Fondufe-Mittendorf has provided me throughout my graduate school experience.

In the summer of 2016, I started the IBS program with a summer rotation in the Dutch lab. This was my first experience at a prominent research lab. Even so, I remember how confident Dr. Dutch was in my success. To me, it was remarkable how passionate she was in her commitment to provide high quality training to ensure that I excelled. Dr. Dutch's brilliance and outstanding work have established her as a leader in her field; and I have been privileged to experience her mentorship firsthand. In addition to her dedication to my academic excellence, Dr. Dutch has been a firm supporter of my pursuits outside of research. Her mentorship has allowed me to truly flourish both as an academic and as an individual—for that, I am extremely grateful.

I would also like to thank my committee, Dr. Peter Nagy, Dr. Tianyan Gao, Dr. Yvonne Fondufe-Mittendorf, and my outside examiner, Dr. Brett Spear. Their combined expertise has allowed me to think critically about my projects and have

been instrumental in pursuing key questions to advance our understanding of viral infection.

When I started the IBS program, Dr. Brett Spear was the director of graduate studies (DGS); however, Dr. Spear has gone above and beyond his roles as DGS, to be an unparalleled mentor. As a mentor, Dr. Spear has modeled excellence, while maintaining a formidable dedication to the well-being of his students, a trait I hope to emulate as well. I would also like to thank the DGS of our department, Dr. Trevor Creamer, who has always prioritized our needs and provided us with endless lists of academic resources. I am also particularly grateful to his commitment to our well-being as we shut down due to the pandemic. I would also like to thank Dr. Carole Moncman for training me in microscopy: those skills have been instrumental in my projects at the lab

I would like to thank the members of the Dutch lab, who continue to provide a wonderful support system. Dr. Stacy Webb, Dr. Chelsea Barrett, and Dr. Nicolás Cifuentes-Muñoz, thank you for teaching me everything I know, and thank you doing it with kindness. Dr. Cheng-Yu Wu, thank you for being an amazing collaborator. Dr. Liz Zamora-Reyes, Dr. Kerri Boggs, Dr. Tyler Kinder, Rachel Thompson, Hadley Neal, and Kearstin Edmonds, thank you for doing outstanding work and continuing to inspire me. I appreciate the encouragement and support that you provide every day. I would be remiss if I did not thank the members of the department, especially the members of SEEMS for encouraging me throughout the program.

I would like to thank my family and friends turned family. Paris Wheeler, Candice Davis, and Aria Byrd: thank you for providing the graduate student community that I always craved. I would also like to thank Shravani Prakhya for constant encouragement. Finally, to my amazing family: thank you for your immense love and support. Thank you for believing in my wildest dreams and for encouraging me for fearlessly pursue them. I am incredibly grateful that even though we are separated by many miles, you still remind me every day that you are never far away.

Table of Contents

List of Tables

List of Figures

Chapter 1: BACKGROUND AND INTRODUCTION

Pathophysiology of NNS RNA viruses

Non-segmented negative sense (NNS) RNA viruses display a wide range of pathogenicity in their hosts. [1]. Hendra virus (HeV), Nipah virus (NiV), rabies virus (RV), and Borna disease virus (BDV) can infiltrate the central nervous system, resulting in encephalitis and other serious neurological symptoms [2-4]. Additionally, paramyxoviruses and pneumoviruses are some of the leading causative viral agents of respiratory tract illness [5, 6]. For example, infection with respiratory syncytial virus (RSV) and human metapneumovirus (HMPV) typically result in bronchiolitis but can also manifest as more severe symptoms that may require mechanical ventilation and/or cardiovascular support [7]. RSV and HMPV infections are common in pediatric populations, and studies show that most people by the age of 5 have already been infected; however, re-infections occur throughout life [8]. HMPV and RSV also result in significant morbidity and mortality in the elderly and immunocompromised [9-11]. Additionally, human parainfluenza virus (hPIV) 1 and 3 pose significant health risks in lung transplant patients [12], while PIV5 is non-pathogenic in humans but serves as a potent viral model system for paramyxo-and pneumovirus studies [13, 14]. Other NNS RNA viruses such as EBOV, for instance, affect the vascular system of non-human primates and humans, potentially leading to hypervolemic shock, and can result in multi-organ failure and resulting in a 25-90% fatality rate. Although some NNS RNA viruses such as RV and measles virus (MeV) have effective vaccines [6, 15-17], for many NNS RNA viruses, despite multiple ongoing trials, there are currently no FDA-approved vaccines and therapeutics for humans, and much of their treatment involves supportive therapy [6, 18-22]. However, in a positive turn of events, a three-antibody cocktail treatment against EBOV, REGN-EB$_3$, was approved in October 2020 [23], highlighting important strides in NNS RNA viral research. Together, the current literature points out a dire need for a more detailed understanding of the molecular details of NNS RNA viral infection to elucidate novel therapeutic targets.

Public health impacts of NNS RNA viruses

While the impacts of positive stranded RNA viruses such as the newly emerged SARS CoV-2 are at the forefront currently, NNS RNA viruses have also historically contributed to severe disease not only in humans, but also in livestock, plants, and fungi [2, 3, 24, 25]. Ebola virus (EBOV), RSV, and the re-emerging MeV are some high-profile examples of NNS RNA viruses that have caused global public health concern [26-28]. Although some NNS RNA viruses such as RV have been present for centuries [3], the vast majority of emerging viruses are RNA viruses [29]. With a tendency to jump from other species to humans, NNS and other RNA viruses exploit a naïve host cell population with limited cross-immunity to inflict deleterious effects [4, 29, 30].

Classification and morphology of NNS RNA viruses

NNS RNA viruses belong to the order *Mononegavirales* which consists of eight families: *Bornaviridae, Filoviridae*, *Mymonaviridae*, *Nyamiviridae,* Paramyxoviridae*, Pneumoviridae, Rhabdoviridae*, and *Sunviridae* [31]. These viruses are enclosed in a host-derived viral membrane, with a spherical, rod-like, filamentous, or pleomorphic morphology [1, 2, 24, 25]. Their continuous negative stranded genomes are up to approximately 19kb in length and encode between 5-10 genes [32, 33]. Some genes encode proteins directly involved in the viral structure while others have non-structural properties. In general, the RNA is arranged from ^{3}N-P-M-G-L^{5}; however, some NNS RNA viruses contain other proteins such as SH, M2, NS, and additional as-yet uncharacterized proteins [31-33] (Figure 1.1).

The RNP complex of NNS RNA viruses

NNS RNA genomes are encapsidated in a long, flexible, helical ribonucleoprotein (RNP) complex, composed mainly of the nucleoprotein (N, NP) functioning in close association with the RNA dependent RNA polymerase (RdRp) complex. The RdRp is made up of the large protein (L) and the polymerase cofactor phosphoprotein (P) [32, 34]. N/NP functions primarily by enclosing the viral RNA in a continuous protein chain, providing protection against nucleases

[35], and allowing for the encapsidated NNS RNA to be used as a template for both transcription and replication [32, 35]. This N/NP protein coat also circumvents innate immune recognition such as responses from Toll-like receptors, Rig-I, and interferon mediated response that may otherwise identify and respond to degrade foreign RNA species in the host cell [34-36]. P is a multifunctional protein, and one of its roles is to serve as a cofactor the for the viral polymerase [37]. It is also reported to interact with host cell factors [38, 39]. For P, phosphorylation states, as well as the extent of phosphorylation, play significant roles in viral replication and in its interactions with other viral proteins and/or host factors [39, 40]. L, the largest viral protein has RNA dependent RNA polymerase activity, and in concert, N, P, and L facilitate viral replication of the NNS RNA viruses. [31, 35].

Surface glycoproteins of Paramyxo-and Pneumoviruses

Since NNS RNA viruses are enveloped, infection requires the energetically costly process of fusing the viral membranes with their host target cells [41-43]. While some NNS RNA viruses encode a single protein G/GP that facilitates both attachment and fusion, most require two distinct proteins to engage the process. In general, the fusion protein (F) and attachment protein (G, GP, HN, or H) are critical for entry of viruses into host cells—the attachment protein interacts with cell-surface receptors to enable a virion to tether to a host cell. Then, after a virion is oriented closely with a host cell, the fusion protein undergoes essentially irreversible conformational changes to merge viral membranes with host cell membranes [44-47]. F and G/GP/HN/H are the two surface glycoproteins present on most NNS RNA viruses, are recognized by the host cell as antigens and thus often serve as attractive antiviral targets [33, 47-49]. In addition to the fusion and attachment proteins, some viruses such as parainfluenza virus 5 (PIV5), HMPV and RSV have the small hydrophobic (SH) protein, which is a proposed viroporin for HMPV and RSV [50, 51].

The attachment protein

In addition to roles in antigenicity, viral attachment proteins are important determinants of tropism and may also function in triggering the fusion of viral and

host cellular membranes [52]. Paramyxo- and pneumo-virus attachment proteins are generally classified as type II membrane proteins with a globular head, a stalk, a transmembrane domain and a cytoplasmic tail [53].

Although paramyxo- and pneumo-virus attachment proteins exist as homotetramers (dimer-of-dimers), each monomeric unit can bind to its respective receptor molecule. In addition, certain paramyxo- and pneumo-virus attachment proteins can recognize and bind sialic acid on host cell receptors. Indeed, the designated names, H, HN, or G are based on their binding and/or catalytic activity with sialic acid on the cell surface. For instance, hemagglutinin (H) mediates hemagglutinin activity by binding to sialic acid; hemagglutinin-neuraminidase (HN) mediates both hemagglutinin and neuraminidase by binding and cleaving sialic acid; and glycoprotein (G) neither binds nor cleaves sialic acid. Instead, for some viruses, G can bind ICAM, heparan sulfate, or other glycosaminoglycans. NiV and HeV G proteins bind to ephrinB2 or ephrinB3 [53]. Interestingly, MeV H also recognizes and binds to CD46, SLAM (CDw150), and nectin-4 on host cell surfaces [46, 54, 55].

For paramyxoviruses, the viral attachment protein function not only precedes fusion protein conformational changes, but also in essence triggers the beginning of the fusion process mediated by the fusion protein. Aguilar et al. review five mechanisms through which the attachment protein directly interacts with F, and undergoes conformational changes that consequently start the fusion protein activity [53]. However, it is also critical to note that for HMPV and RSV, despite the overall conserved architecture with other paramyxo- and pneumovirus attachment proteins [53], G is not required for infection to occur in cell culture and in an animal model [56, 57]. To that, Chang and Dutch also detail five roles the attachment protein may have in triggering the fusion protein, either by direct interaction with the attachment protein, or through interactions with F and its own cell surface receptor [46].

The small hydrophobic protein

The SH gene is expressed by a select number of NNS RNA viruses such as PIV5, HMPV, RSV, mumps virus (MuV), J paramyxovirus (JPV), and Tupaia rhabdovirus (TRV). Despite SH being present in all primary isolates in HMPV for example, SH deletion is neither beneficial nor detrimental for entry, replication, or spread in the cell culture and animal models that have been examined [50]. For RSV and HMPV, SH forms higher order structures, can localize to the plasma membrane, and is shown to increase plasma membrane permeability [50, 51]. Additionally, RSV SH forms non-selective cation channels that are permissive to Na^+ or K^+ [51]. These data present SH as a potential viroporin.

Studies have also reported that SH regulates cytopathic effects (CPE) in PIV5. A recombinant PIV5 virus lacking the SH gene showed an increase in TNF-α-induced apoptosis, suggesting that SH inhibits apoptosis and consequent CPE in infected cells [58]. Indeed, further research in RSV also suggest similar functions of SH in preventing virus-induced apoptosis as a host immune response, though these studies did not directly implicate TNF-α [51], pointing to perhaps multiple pathways by which SH acts to protect against CPE and sustain infection in intact cells. Surprisingly, HMPV SH has been shown to co-immunoprecipitate with F, and drastically suppress the fusion activity in fusion reporter system [50].

The fusion protein

Although paramyxoviruses typically couple receptor binding with host cell membrane fusion at the plasma membrane [46], the pneumoviruses HMPV and RSV can enter cells through clathrin-mediated endocytosis, or through induction macropinocytosis of the full viral particle [56, 59-61]. For some strains the HMPV F protein is triggered by low pH within endosomes (Figure 1.2). For these viruses the triggering of the fusion protein is nuanced: even though the post-fusion form is energetically favored, F mainly exists on cell surfaces in the pre-fusion form, suggesting an intricate balance in maintaining prefusion conformation until productive triggering can occur. Indeed, as previously described, the attachment protein may interact with the fusion protein, and as it attaches to host cells, could

change the F protein microenvironment to start a cascade of events that trigger the fusion protein. Alternatively, F may bind its own receptor, and act independently of G, as is shown for HMPV and RSV.

Paramyxo- and pneumoviruses, are synthesized as inactive F_0 forms, folded into homotrimers within the endoplasmic reticulum (ER), and trafficked to the plasma membrane. For PIV5 F activation, furin cleaves F_0 within the *trans* Golgi network (TGN) while F traverses the endocytic pathway before it is expressed on the cell surface in the disulfide-linked fusogenically active form, $F_1 + F_2$. In other cases, such as with HeV and NiV, F_0 is first expressed on the cell surface, then is signaled to be endocytosed and cleaved by cathepsin L in the early endosomes and returned to the plasma membrane to mediate fusion. HMPV F can be cleaved by TMPRSS2, HAT, matriptase, KLK5, and trypsin in cell culture [62, 63] (Figure 1.3). Even after proteolytic cleavage, $F_1 + F_2$ is maintained in a metastable conformation until it is triggered to undergo dramatic, essentially irreversible conformational changes into a more energetically stable post-fusion conformation. These large conformational changes are coupled with merging the viral and host cell membrane, thereby reducing the activation energy required to merge the membranes and create a fusion pore. The fusion pore is subsequently expanded to allow for the mixing of viral and cellular contents (Figure 1.4).

F proteins are class I fusion proteins that form homotrimers. Each monomer contains a fusion peptide FP, heptad repeats A and B (HRA and HRB), a single-pass transmembrane domain (TMD), and a cytoplasmic tail (CT) (Figure 1.3). With the help of a trimeric coiled-coil domain (GCNt) attached to the HRB in lieu of the TMD and CT, Yin et al. successfully crystalized the first prefusion form of a paramyxovirus F, PIV5 F. The prefusion structure of F consists of a large globular head domain and a trimeric coiled coil. The proteolytic cleavage reveals the FP, which is proximal to the HRA and larger (F_1) segment. The FP, HRA, and $F_1 + F_2$ form the globular head domain, and it is supported by the HRB which forms the trimeric coiled coil stalk. The TMD and CT would be immediately adjacent to the HRB but were not present in the structure [64, 65].

When triggered, the cleaved form of F inserts its fusion peptide into the host cell membrane, forming a prehairpin fusion intermediate structure. With the FP being proximal to HRA, in the transient prehairpin structure, the HRA is also released from the globular head, stretching towards the target cell membrane. In this intermediate structure, HRB remains pinned adjacent to the viral membrane. Because of its unfavorably high energy state, the prehairpin intermediate subsequently folds upon itself, driving the FP and HRA towards HRB to form a six-helix bundle (6HB) in a hairpin post-fusion structure. This dynamic process is hypothesized to provide the energy to merge the two membranes (Figure 1.4).

The transmembrane domain of the fusion protein

Although initially postulated to be merely a membrane anchor, the TMD of paramyxovirus F proteins has been shown to be important in function. For example, the TMD plays key roles in signaling for endocytosis and recycling of the HeV fusion protein, a critical process without which F would remain fusogenically inactive [66]. In addition, key residues within the TMD and CT tail were found to be important for formation of virus-like particles (VLP)s. F protein cleavage alone is not sufficient for VLP formation, as there was a clear reduction in the incorporation of a trafficking mutant of Hendra F into VLPs when compared to the wild type (WT) protein [67]. Moreover, replacement of Newcastle disease virus (NDV) F TMDs with TMDs from other closely related viruses resulted in fusion-dead proteins that could no longer associate with their homotypic attachment protein. For NDV, the specific TMD sequence is an important factor in maintaining the structural integrity of the fusion protein [68]. Furthermore, a study of RSV F revealed that the TMD is important for localizing the protein onto the apical surface in polarized epithelial cells [69].

A 2005 study of the hPIV3 fusion protein revealed that removal of the TMD resulted in the formation of a 6HB and the isolation of F in the post-fusion conformation [64]. This unexpected finding suggests that the TMD is important in maintaining the metastable pre-fusion conformation of the F protein. However, when replaced with the GCNt trimerization, the same group was able to stabilize

PIV5 in its pre-fusion form [65]. In fact, when isolated, the TMD of PIV5 F, HMPV F, and HeV F associate in a monomer-trimer equilibrium [70]. Moreover, when the proximal HRB was added to the TMD of HeV F, the TMD-TMD interactions were weakened [71], suggesting that the TMD important for maintenance of the fusion protein trimer. Solid-state NMR and SAXS data have been used to generate a model of the TMD structure. In this model, for each monomer, there is a helical coiled coil which is flanked by two β-strands, creating a stand-helix-strand. The β-strand termini are suggested to be critical for inducing membrane curvature and advancing fusion, whereas the α-helical segment of the TMD is rich in β-branched residues, which are important to drive trimeric interactions [72, 73].

The transmembrane domain leucine/isoleucine zipper

To understand the mechanisms through which TMDs support trimeric association of fusion proteins, an analysis of 19 paramyxoviruses yielded 140 TMDs which contained β-branched residues in a heptad repeat pattern. Specifically, a leucine/isoleucine (L/I) zipper was found in the TMDs of several paramyxo- and pneumoviruses, including HeV, PIV5, HMPV, and RSV, among others. Further studies demonstrated that for HeV F, the TMD is important for surface and total expression, stability, and fusogenic activity of the fusion protein. These data indicate that within the TMD, the L/I zipper is an important association and functional domain for HeV F activity. Indeed, when analyzed in isolation, the L/I zipper was found to be an important driver of trimeric association— F proteins lacking the TMD L/I zipper were found to have a greatly reduced trimeric association compared to the wild type protein [74], suggesting a likely mechanism through which the L/I zipper contributes to stabilizing the trimeric metastable prefusion protein.

The matrix protein of NNS RNA viruses

Even at early stages during infection, the matrix protein interacts with viral proteins and host key host factors to facilitate viral entry. Recent literature indicates that as early as between 6-12 hours post-infection, the HMPV genome is actively transcribed into mRNA, in the process termed transcription, which is then used as a template to generate viral protein [75]. At the same time, the HMPV negative sense genome is used as a template to create a positive sense RNA antigenome, which, unlike mRNA, is it not capped and polyadenylated., The L protein uses this antigenome as a template to generate more negative sense viral genomic RNA (vRNA) [35, 75], a process known as replication. These viral replication and transcription events occur in punctate structures within the cytoplasm termed inclusion bodies, viral factories, or in the case of rabies virus, Negri bodies [76-80]. For the HMPV, inclusion bodies coalesce in an actin-dependent manner and are important for efficient viral replication and translation [75]. Importantly, the M protein can interact with N, and consequently with the RNP, as well as with the cytoplasmic tails of F and G, which allows M to recruit RNPs to the plasma membrane for assembly into viral particles [44]. Furthermore, for many viruses, the M protein alone can form authentic looking virus-like particles (VLPs), suggesting that it plays a critical role in viral morphogenesis [44, 81, 82] (Figure 1.5 and Figure 1.6).

The general architecture of matrix proteins across Mononegavirales

Figures 1.7 and 1.8 show that despite the low sequence conservation across the family, there is a degree of sustained structural similarity, suggesting a possible convergent evolutionary relationship that would explain similarity in their function during their respective life cycles. For paramyxoviruses, even though the *primary M protein sequences are not conserved, studies show that their structures* **are** similar, with two characteristic orthogonal β-sandwiches, flanked by α-helices. [44, 83]. Importantly, Chatterjee et al. discovered that the NS1 protein of RSV, which is a strong inhibitor of transcription and replication [84] as well as a potent suppressor of the innate immune response [85], bears a β-sandwich structure that is very similar to that of M [86].

Structural plasticity is important for the function of pneumovirus matrix proteins

In infected cells, paramyxovirus M forms an ordered layer on the cytoplasmic side of the plasma membrane [44], and HMPV M interacts with the membrane through its concave surface [83, 87]. The EBOV matrix cognate VP40 contains a hydrophobic patch that inserts into the plasma membrane. In addition, VP40 contains a positively charged domain which selects for plasma membrane phosphatidylserine (PS). Although VP40 traverses to the membrane as a dimer, after association of PS it forms a higher order filamentous oligomeric structures that induce membrane curvature [81]. Similar to EBOV M, HMPV and RSV M exist in a dimeric form but also oligomerize to form filaments in the presence of lipids [83, 88]. Interestingly, Leyrat et al. have shown that the N-terminal domain of HMPV contains a high affinity Ca^{2+}-binding site, a feature that has not been reported for other viral M proteins. When HMPV M binds Ca^{2+}, it induces a 25ºC increase in melting temperature, likely increasing the structural rigidity, thereby possibly contributing the structural stability of matrix oligomers for more efficient budding facilitated by the M protein [83].

Nuclear entry of some NNS RNA viruses

With exception of *Bornaviridae*, NNS RNA viral replication and transcription is well-documented to occur in the cytosol. Curiously, despite this, several reports show that the matrix proteins of NNS RNA viruses including Newcastle disease virus (NDV), vesicular stomatitis virus (VSV), Sendai virus (SeV), as well as Hendra (HeV) and Nipah virus (NiV) are trafficked to the nucleus during the infectious cycle [89]. This nuclear entry is unlikely to result from free diffusion of the protein through the nuclear pore, since most matrix proteins exist dimers or higher order structures that exceed the 50kDa upper limit to passively traverse the nuclear pore complex [82, 83, 87, 88, 90, 91]. Instead, for some viruses such as NiV M, there is a bipartite nuclear localization sequence which is recognized by importin-α that regulates nuclear entry and a well-documented nuclear export signal (NES) [90], pointing to a role for nuclear entry or sequestration.

Unlike most viruses that belong to the mononegavirales order, Borna disease virus (BDV) is well-documented to have a nuclear step in viral replication. As reviewed by Honda et al., like other NNS RNA viruses, BDV M binds to viral RNPs [92, 93]. Interestingly, the group discusses results which demonstrate that BDV M binds to and facilitates the nuclear to cytoplasmic shuttling of the BDV RNPs, better orienting them for assembly [93]. Given this observation, and given that BDV M is very similar to the N terminal domain of EBOV VP40 [94], it is possible that the other NNS RNA viruses that do not require a nuclear step during replication have a conserved evolutionary step in maintaining the nuclear sojourn, but in this case with M only; however, since viruses evolve to fine-tune their protein functionalities, and since distinct roles for nuclear entry have been outlined for certain viruses such as NiV and RSV [90, 95], it is unlikely that other NNS RNA viral matrix protein nuclear import is completely benign. It is however important to note that not all NNS RNA viral matrix proteins have a nuclear step during infection.

Matrix nuclear entry supports modification for intracellular signaling, oligomerization, or membrane association.

While within the nucleus, SeV M and NiV M are modified by ubiquitin. The ubiquitin modification on NiV occurs on a critical lysine residue, K258, within the NLS. Replacing K258 with arginine, which maintained the positive charge and thus allowing nuclear entry but not the ability to be ubiquitinated, led to an accumulation of NiV K258R M in the nucleus, resulting in a dramatic reduction in viral budding and spread [89]. It is tempting to assume the reduced cytoplasmic levels of K258R M available after nuclear accumulation was the sole determinant of this reduced budding and spread. However, when nuclear import of NiV M was blocked altogether with a K258A mutation, NiV K258A M was only present in the cytosol, but did not associate with membranes.

To further understand the role of ubiquitin in NiV M membrane association, the authors created a NiV K258R M-ubiquitin fusion protein. This fusion protein allowed M to be duly imported to the nucleus but prevented ubiquitination at the K258 position specifically. Here, the ubiquitin fusion rescued the nuclear

accumulation phenotype and allowed export of protein, despite the K258R substitution. While it was expected that the ubiquitin-rescued K258R mutant would result in plasma membrane localization, notably, this mutant also failed to localize at the membrane [89, 90, 96]. The authors therefore speculated that either both the K258A and the K258R-ubiquitin NiV M mutants block interaction with important host factors that normally allow for additional post-translational modifications that functionalize M or that ubiquitination regulates both the oligomerization interface and the membrane interaction of M, allowing it to form the characteristic helical filamentous ordered layer underneath the plasma membrane [89, 90]. Nevertheless, these data also suggest that majority of newly synthesized M relocates to the nucleus providing more evidence to suggest a nuclear function during infection. While the ubiquitination of M has only been documented for certain paramyxoviruses, it does not exclude the possibility that other post-translational modifications may occur which are not specific to the nucleus. These data also beg the question of why this specific modification must happen in the nucleus, with the abundance of E3 ligases in the cytosol.

Matrix protein nuclear localization allows for interaction with splicing machinery

Studies show that for the paramyxoviruses SeV, MuV, NiV, and HeV, in addition to localizing to the nucleus, M is specifically imported to the nucleolus [89]. For these paramyxoviruses, immunofluorescence studies revealed that both WT and the aforementioned K258R mutation result in localization within the nucleolus; however, the K258R mutant accumulated within the nucleolus to a higher degree than WT. These studies showed that NiV M is detected within the nucleus as early as between 8 and 16 hpi, primarily within punctate structures consistent with the nucleolus [96]. It is currently unclear the mechanisms behind the nucleolar targeting of paramyxovirus matrix proteins. However, biochemical studies support this nucleolar association, as NiV M was shown to interact with upstream binding factor F (UBF), a transcription factor particularly associated with recruiting nucleolar factors [89].

In addition, RSV M and HeV M have been associated with the nucleolar protein nucleophosmin (Npm) B23 [97, 98]. UBF and Npm B23 are known to be associated with ribosomal proteins, and thus may suggest a role between matrix proteins and ribosomal biogenesis [98]. The nucleolus is the hub of ribosomal biogenesis [99], which may suggest the role of several NNS RNA viral matrix participation in co-opting host translational responses; however, the nucleolus also serves as a central processing unit of stress response [99]. Similarly to non-membrane-bound cytoplasmic units such as stress granules, P-bodies, and viral inclusion bodies, it is possible that the nucleolus undergoes liquid-liquid phase separation (LLPS) in response to variable cellular environments (such as stressors associated with heat shock, viral infection, or protein aggregation).

Furthermore, not only was fibrillarin, a nucleolar protein found to be critical for Henipavirus infection, but also, specifically, methylation of fibrillarin is essential for viral RNA synthesis. Thus, fibrillarin may be important in proviral RNA synthesis mechanisms and its association with pre-ribosomes and NOP56 or NOP58 [100] could point to methyltransferase activity of host nucleolar enzymes being of particular importance to certain NNS RNA viral infections. These may suggest a novel druggable target. These findings may not exclude the idea that the matrix protein may also in fact interact with other ribosomal biogenesis machinery to prevent targeting of other important host cellular proteins form being synthesized. It is possible M also associates with hnRNPs, and other spliceosome machinery.

Nuclear matrix protein usurps critical cellular processes

Viral infections notably co-opt cellular processes for their own proliferative benefit. Earlier studies showed that VSV M is instrumental in rapidly shutting down host cell macromolecular synthesis including mRNA and proteins. Experiments showed, that independent of other viral proteins, VSV M has profound inhibitory effects on host cell-directed mRNA and snRNA synthesis [101, 102]. This inhibitory role of M is also genetically distinct from its canonical roles in viral assembly and budding [103]. Upon further investigation, the nuclear import of VSV M was found to directly influence RNA species that specifically needed to be transported across

the nuclear pore complex (NPC) [101], alluding to a role for M in mediating nucleocytoplasmic shuttling of host macromolecules. Indeed, the presence of M in *Xenopus laevis* oocytes highly mimics Ran-GTPase deficiency, and thus was hypothesized to interfere with Ran-GTPase-dependent nucleocytoplasmic shuttling [104].

Nuclear entry of matrix protein supports immune modulation

Unlike RSV, HMPV does not have the NS1 and NS2 proteins, however it is still pathogenic. Evidence suggests that while sequence conservation is low, the secondary structures of RSV NS1 and RSV M are similar: NS1 resembles one half of the orthogonal beta sandwich that constitutes the RSV M protein. When compared, RSV NS1 showed a high degree of alignment with the N-terminal domain of RSV M (RMSD 3.78 Å over 96 residues). Moreover, RSV NS1 is also structurally similar to EBOV VP40 and Newcastle disease virus (NDV) M despite low sequence similarities. Based on their data, Chatterjee et al. speculate that a potential duplication event of the N-terminus of M gave rise to the NS1 protein, which then divergently evolved its functions in immune modulation [86]. These data suggest a conserved functional significance in the structural fold of the NS1 and some NNS RNA M proteins. NS1 is a potent immunomodulator; however, most of its reported function is in facilitating inflammatory responses, IFN antagonization, and inhibition of dendritic cell maturation arise from the C terminal α-helix, which is the portion of the RSV NS1 structure that differs from HMPV M.

The matrix protein regulates viral transcription and translation

Transcription

Matrix proteins of NNS RNA viruses play important roles in regulating transcription and replication of viral genomes: BDV, rabies virus (RV), and measles virus (MeV), matrix proteins inhibit viral transcription. For these viruses, M binds to and condenses viral RNA, making it less accessible as a template for transcription [94, 105, 106]. Curiously, for RV, as M inhibits viral transcription, it performs an opposite stimulatory role in replication [105]; providing insight into how transcription and replication are balanced during infection.

Further work on RV M pinpointed residue 58 as important in interacting with the viral polymerase and consequently on downstream effectors that facilitate the switching viral transcription-viral replication gradient. Importantly, this data highlight that mutations at residue 58 do not affect assembly and budding, further elucidating a distinct role of M outside of the classical budding and egress [107]. In terms of regulation, it is hypothesized that because transcription and consequent translation of viral proteins is prioritized upon entry since genomes require encapsidation [32, 34-36], a critical concentration of matrix protein in the cytosol would inhibit transcription. This inhibition of transcription may allow the viral polymerase to favor replication of the viral genome. Indeed, nuclear sequestration of M coincides with an increase in mRNA production and nuclear exit is consistent with decreased mRNA for RSV [87, 95, 108].

Replication

Interestingly, studies on EBOV, MeV, and RSV suggest that increasing amounts of M is detrimental for viral replication. Viral reporter gene assays suggest that in the presence of increasing M, there is a correlative decrease in viral replication [95, 106, 109]. Like with the transcription model, this may point to a role for sequestration of M in the nucleus to allow for an increase in viral replication. It is not far-fetched to postulate such a mechanism would result in the gradual cessation of viral replication at the time that M is also gradually exported from the nucleus to prepare nascent virions for assembly.

This phenomenon also applies to influenza A virus, which belongs to the family Orthomyxoviridae, an RNA viral family whose genomes are encoded in multiple segments. Influenza A has an obligate nuclear stage and a matrix cognate which supports viral transcriptase negative regulation [110]. It is possible that this is an evolutionary or functionally conserved function. Moreover, the presence of M may mark the beginning of assembly, and its nuclear shuttling sequesters M away while replication occurs exponentially. Interestingly, unlike other NNS RNA virus

counterparts, there is currently no evidence that Henipa matrix proteins affect viral replication and transcription, despite being trafficked to the nucleus [89].

The unique calcium binding site of HMPV M

In 2014, Leyrat et al. published the crystal structure of HMPV M, which was surprisingly found to have a calcium binding site [83] (Figure 1.7).They found that calcium (Ca^{2+}) had a role in the structural stability of M, and also speculated on whether this Ca^{2+} association plays a role in the contacts between M and N, possibly influencing which point in the viral life cycle assembly occurs [83]. Furthermore, reports show that RSV M is translocated into the nucleus during infection, and the function of this sojourn is currently unknown [95, 111]. However, RSV M is known to contain RNA-binding properties [112], and this may modulate interactions with host cell nucleic acids. Compared to mammals, viruses such as HMPV and RSV have a relatively small proteome, encoding 9 and 11 proteins respectively [9, 113]. However, there are still many functions involving viral proteins and the viral genome within infected cells that are not yet well understood.

Calcium signaling may be important component in viral spread

Ca^{2+} plays important roles in paramyxo- and pneumoviral infection and spread. For example, in the absence of Ca^{2+}, RSV infectious virus yield was slightly reduced, and cell fusion and syncytium formation was ablated [114]. Another study corroborated this observation that RSV requires Ca^{2+} for efficient spread in cell culture [115]. In addition, when exposed to low Ca^{2+}, production of SeV was suppressed in infected LLC-MK2 cells. Furthermore, Ca^{2+} was found to be critical for cell surface expression of SeV glycoproteins. In low Ca^{2+} conditions, viral glycoproteins were accumulated within the Golgi. When normal Ca^{2+} conditions were restored, the otherwise accumulated SeV glycoproteins, cell surface expression of SeV glycoproteins was quickly rescued, and consequently, Sendai virion production was restored [116].

Calcium binding may support conformational changes that could allow for membrane association, oligomerization and/or fortification of the viral capsule.

Amarasinghe and Dutch discuss the possibility that Ca^{2+} binding leads to additional conformational changes within HMPV M that potentially regulate interactions with (a) host or viral factor(s). Although M interacts with the plasma membrane through its highly positively charged CTD, it is possible that Ca^{2+} binding at the NTD would lead to conformational changes that could extend to the CTD to potentially affect membrane association, as well as the interactions of M with the CT tails of the surface glycoproteins. Moreover, if Ca^{2+} binding in HMPV M affects protein-protein and/or protein-lipid interactions, then it is likely that viral infection may regulate the intracellular Ca^{2+} environment to favor viral infection [117]. Indeed, the ability of HMPV M to bind Ca^{2+}, and the consequent induction of increased thermostability suggest that Ca^{2+} plays roles in stabilizing viral particles as they traverse the Ca^{2+}-rich extracellular environment. This phenomenon may confer an advantage in the lifespan of the virus. [83]. Additionally, since the Ca^{2+} binding site faces away from the membrane, there is a possibility that variations in Ca^{2+} concentrations inside infected cells at various stages of the viral cycle regulate the assembly of viral nucleocapsids onto M arrays at viral budding sites; but there is also a possibility of its involvement in intracellular transport of M proteins to the membrane [83].

Dissertation overview

The current COVID pandemic brings to light the devastation that relatively small biological entities such as viruses can wreak on the global population. Even so, concerted advancements in science to generate world-saving vaccines highlight how critical viral research is. NNS RNA viruses are major contributors to emerging viruses, pinpointing the specific need to dissect their mechanisms of infection. Events that lead to successful entry, replication, transcription, and spread of viral agents are important in the understanding and identification of novel therapeutic targets. Moreover, understanding the mechanisms of viral infection can also provide more insight into non-pathogenic cellular processes, allowing for the progress of basic science. Keeping the broader impact of our basic research

in mind, the Dutch lab studies the fusion, entry, establishment of infection, and egress of paramyxo- and pneumoviruses, two families containing pathogens of worldwide importance. For the fusion studies, we focus on the biochemistry and biophysical properties of the main fusion catalyst, the fusion (F) protein. My work focuses on PIV5 F, a model paramyxovirus. Our work on established infection focuses on unique mechanisms to which cells react to viral pathogens. In addition, I have studied the HMPV matrix (M) protein to dissect its roles in progression of infection.

HMPV and PIV5 are enveloped viruses, and as such need to undergo the energetically unfavorable process of merging their membranes with host cells before they can successfully infiltrate them. For these viruses, this process requires the fusion protein. Fusion proteins have been extensively studied, and much of their mechanisms of action can be detailed; however, there are still significant gaps in the field that warrant further research. For example, paramyxo- and pneumovirus fusion protein transmembrane domains were initially thought to solely be membrane anchors. However, studies showed that when removed or replaced, major changes in the folding and/or oligomerization of the rest of the protein occurred, suggesting more critical roles of the transmembrane domain in fusion function. Indeed, in isolation, the transmembrane domain of PIV5, HMPV, and HeV F are able to associate in trimeric form, indicating that the transmembrane domains also play roles in trimerization of full proteins.

Additionally, an interesting phenomenon that occurs with viral fusion proteins is that they exist largely on the cell surface in a metastable pre-fusion form until the “trigger” for fusion occurs, allowing them to rearrange into a more energetically stable post-fusion conformation. While much is known about the conformational processes that occur with the fusion protein, much more work is needed to elucidate what maintains the metastable pre-fusion conformation. The Dutch lab has done previous work in identifying potential association motifs within the fusion protein transmembrane domain for a multitude of paramyxo- and pneumovirus fusion proteins. This work identified a heptad repeat of

leucine/isoleucine residues that were important for trimerization and fusion function of the HeV fusion protein. To build on these findings, in chapter 3, I address the functional relevance of the leucine/isoleucine zipper by testing whether it is important for another paramyxoviruses. Based on the works described in this chapter, I hypothesized that the transmembrane domain L/I zipper would be critical in the expression, turnover, and functionality of the PIV5 fusion protein. To address this hypothesis, I used the model system PIV5 to address the expression, fusion, and stability in the context of a mutated leucine/isoleucine zipper. Our data show that unlike with HeV fusion protein where expression is reduced, PIV5 fusion protein expression is maintained, while fusogenic activity is ablated.

While studying the effects of actin on cytoplasmic inclusions with Dr. Nicolás Cifuentes-Muñoz, a former post-doctoral scholar at the Dutch lab, I became interested in the HMPV matrix protein. The matrix protein is a key element in viral assembly as it forms an ordered layer underneath the viral membrane, acting as a scaffolding protein allows the virus to bud and form viral particles which egress from host cells. In addition, matrix proteins are known to have important contacts with the RNP, as well as the cytoplasmic tails of the surface glycoproteins, orienting them with each other for efficient viral assembly.

Although the vast majority of NNS RNA viral replication occurs in the cytosol, with no apparent roles for viral proteins within the nucleus, I noted that HMPV M indeed makes a nuclear sojourn. This is consistent with several other viral systems including the matrix proteins of the deadly HeV and NiV viruses. In chapter 4, I discuss the timing of nucleocytoplasmic transport, and address hypotheses involving the sequestration of the matrix protein within the nucleus at the heights of viral infection. Our work shows that when the matrix protein is knocked down with a peptide-conjugated phosphorodiamidate Morpholino oligomer (PPMO), inclusion body morphology and placement are perturbed. Importantly, we find that a lack of the matrix protein results in a drastic reduction in viral transcription and replication, with the mRNA of all viral proteins being remarkably reduced, and the translation of a representative protein also severely

hindered. Our results represent a novel finding that M early in infection is important in both transcription and replication of HMPV.

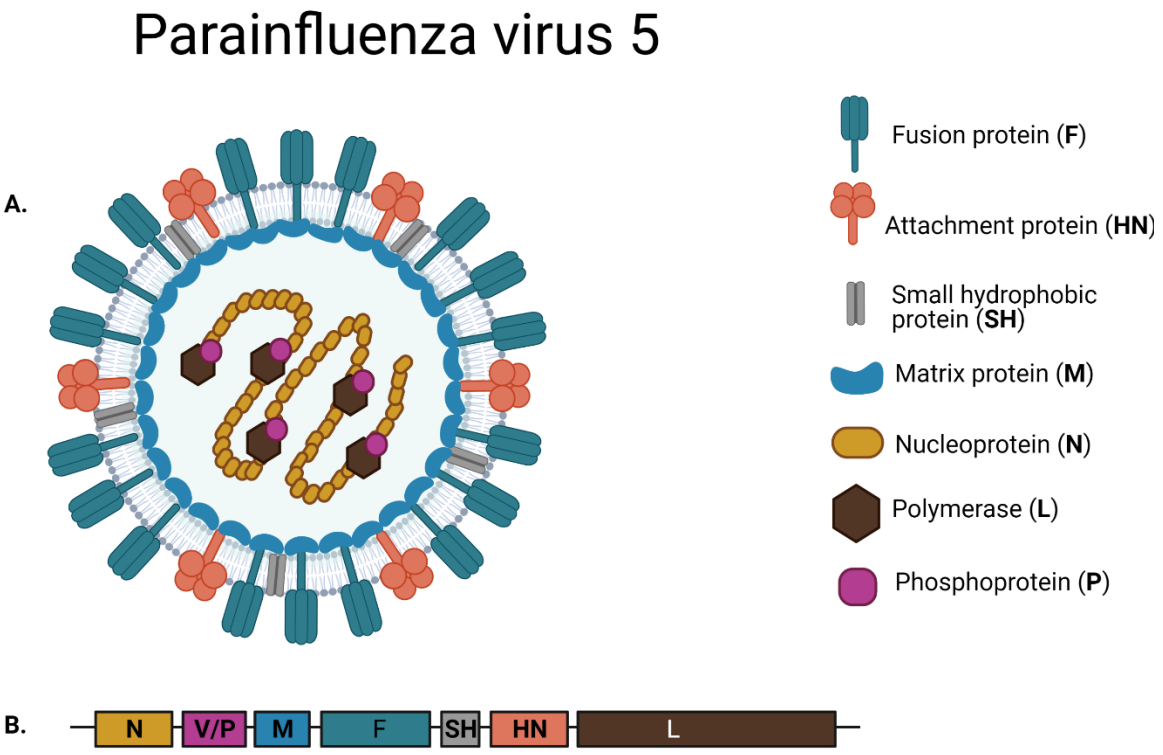

Figure.1.1 The parainfluenza virus 5 particle, a prototypical paramyxovirus. **A.** The non-segmented negative sense NNS RNA genome is encapsidated by nucleoprotein (**N**), along with the polymerase complex that consists of the phosphoprotein (**P**) and the large protein (**L**). These altogether form the ribonucleoprotein complex RNP. The RNP is protected by a host derived membrane, studded with the fusion protein (**F**), the attachment protein with hemagglutinin and neuraminidase activity (**HN**), and the small hydrophobic protein (**SH**). The PIV5 genome also encodes the nonstructural protein (**V**) an immune response agent. B. The genomic arrangement of PIV5.

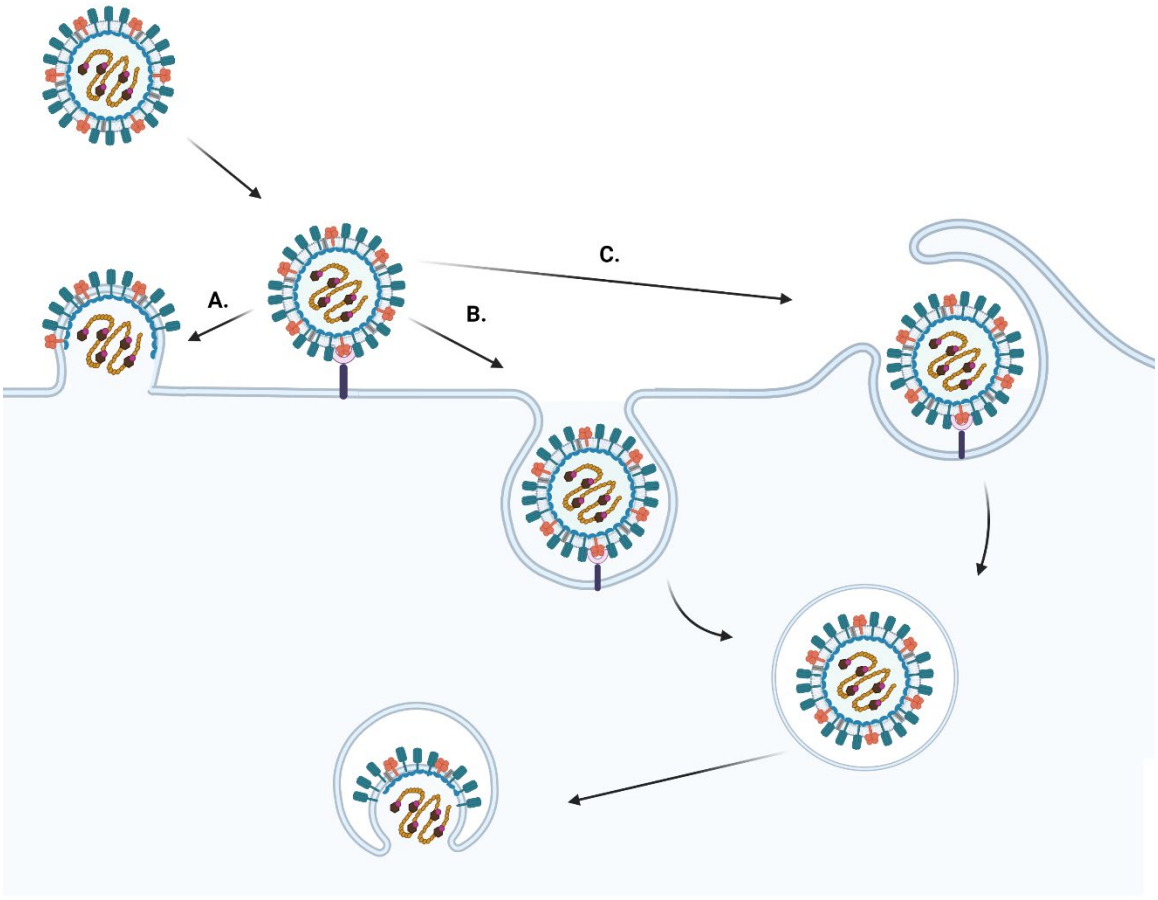

Figure 1.2 The diversity of entry of paramyxo- and pneumoviruses.

After engagement with a cell surface receptor or attachment factor, entry may occur by merger of the viral membrane with the plasma membrane at the cell surface (**A**), endocytosis of the full viral particle, where low pH within endosomes triggers membrane fusion (**B**), macropinocytosis, with the particle passing through the endocytic pathway into low pH endosomes before fusion occurs (**C**).

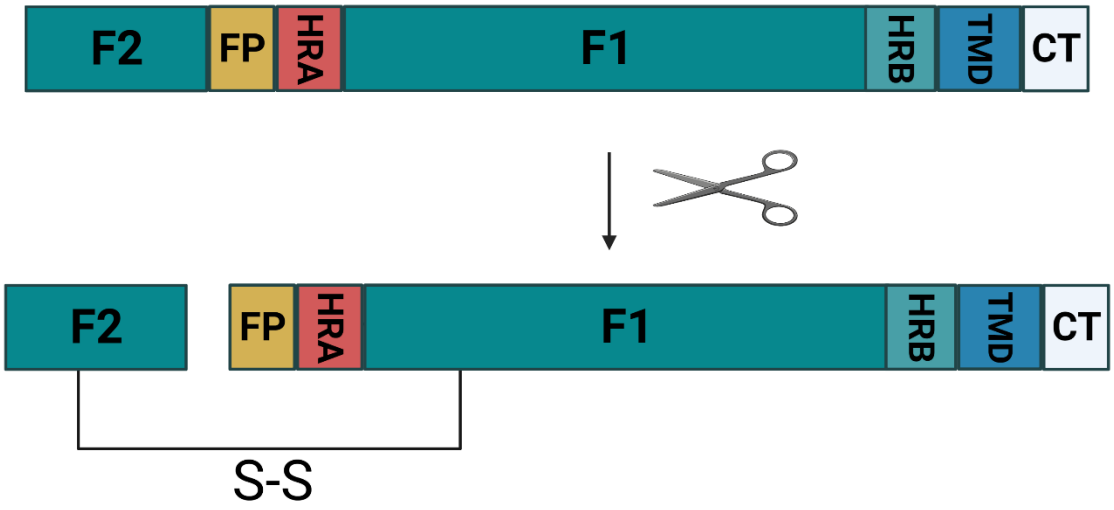

Figure 1.3 Cleavage of the fusion protein.

The fusion protein is initially expressed in a fusogenically inactive form F_0 (**top**). For PIV5, the protein is cleaved within the *trans* Golgi network by furin into the fusogenically active disulfide-linked F_0+F_1 (**bottom**). For other viruses, F can be cleaved by cathepsin L within low pH endosomes, or once incorporated into viral particles or when on the cell surface by extracellular matrix proteases such as matriptase. The fusion protein consists of the **F_1** and **F_2** subunits (***dark teal***), the fusion peptide (**FP**, ***yellow***), heptad repeat A (**HRA**, ***orange***), heptad repeat B (**HRB, *light teal***), the transmembrane domain (**TMD, *blue***), and the cytoplasmic tail (***CT***, ***white***)

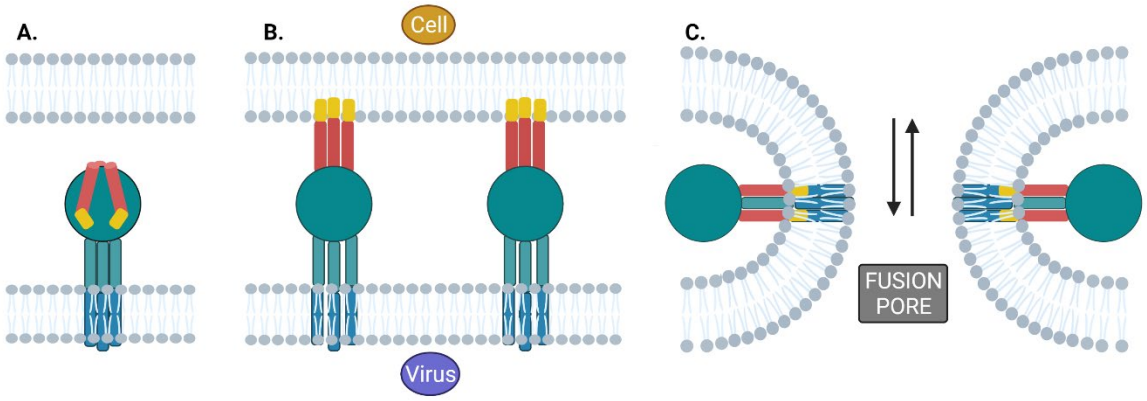

Figure 1.4. Conformational changes that occur during fusion.

Before signaling to begin the fusion process occurs, the fusion protein is held in a metastable prefusion conformation (**A**). As fusion is initiated, the fusion peptide inserts into the host cell membrane, extending the adjacent heptad repeat A region towards the host cell to form a prehairpin intermediate (**B**). Finally, the prehairpin intermediate folds upon itself, with the heptad repeats A and B forming a six-helix bundle and merging the viral and target cell membrane (**C**). This schematic shows two adjacent fusion proteins, providing the two-dimensional view of a fusion pore.

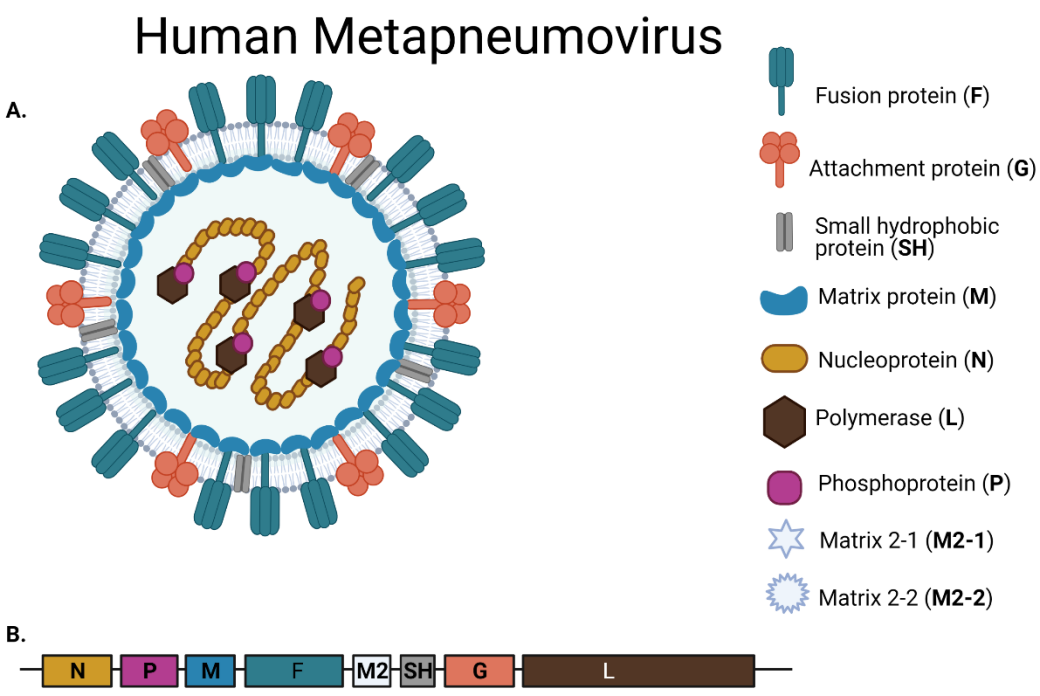

Figure 1.5. The human metapneumovirus particle.

A. Schematic of a HMPV viral particle. The host-derived membrane of the pneumovirus is studded with multiple copies of the fusion protein (F), attachment protein (G), and small hydrophobic protein (SH). Directly underneath the membrane is an ordered layer of matrix proteins (M). The core of the virus consists of the ribonucleoprotein complex, composed of the nucleoprotein (N), which encapsidates the negative stranded single sense RNA genome, the phosphoprotein (P), and the large protein (L), which is an RNA dependent RNA polymerase. The M2 gene encodes two additional proteins (M2-1 and M2-2), which play roles in polymerase processivity and immunomodulation. **B**. The arrangement of the human metapneumovirus genome.

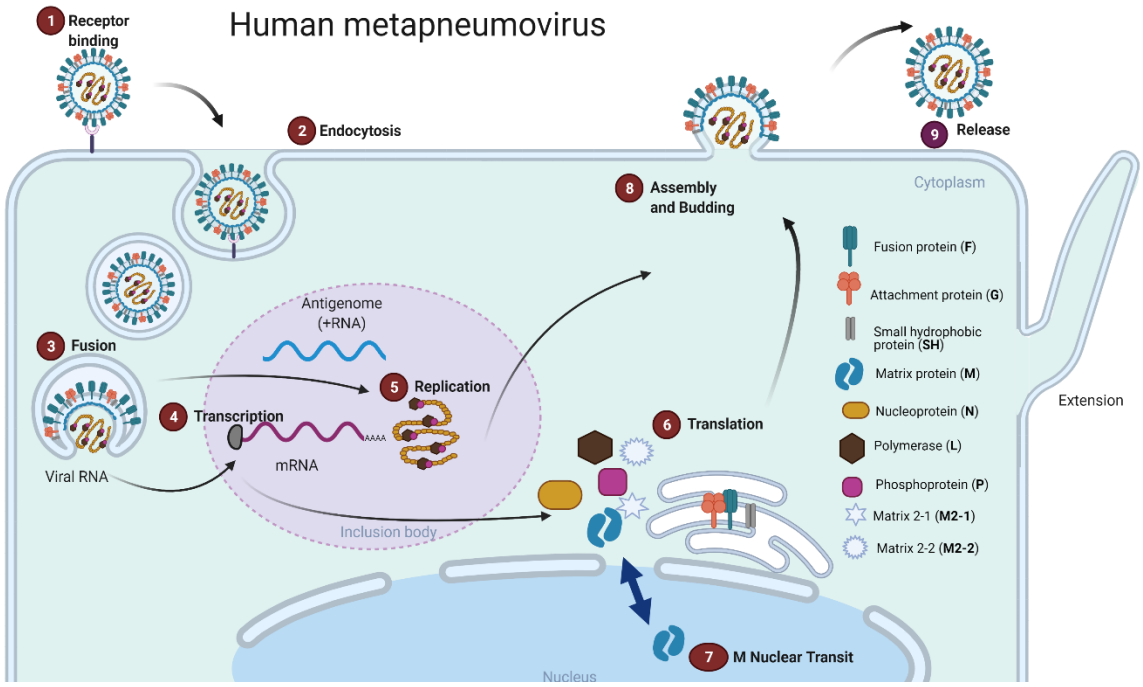

Figure 1.6.The human metapneumovirus life cycle.

Entry is initiated when the viral glycoproteins engage cell surface receptors (**1**). The viral particle is then endocytosed (**2**), where fusion occurs in low pH endosomes (**3**). As the genome is released, transcription (**4**) and replication (**5**) occur in discrete unenveloped compartments within the cytosol termed inclusion bodies. Following transcription, viral mRNA are exported from inclusion bodies, where they gain access to ribosomes to be translated (**6**). Following translation, the matrix protein is promptly delivered into the nucleus. The matrix protein can shuttle between the nucleus and cytoplasm (**7**). After the cell surface glycoproteins traverse the secretory pathway, the matrix proteins assemble them with viral RNA along with additional viral proteins. These assembled proteins bud into viral particles (**8**) and are released (**9**), prime for infection of other cells. In addition to release of nascent viral particles, HMPV induces the formation of extensions that can carry viral genomes from cell-to-cell.

Sequence-based phylogenetic tree

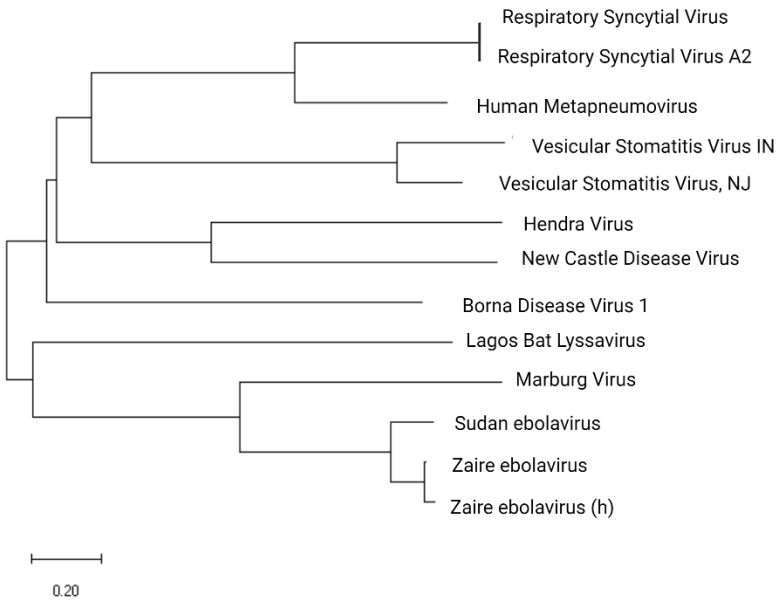

Structure-based phylogenetic tree

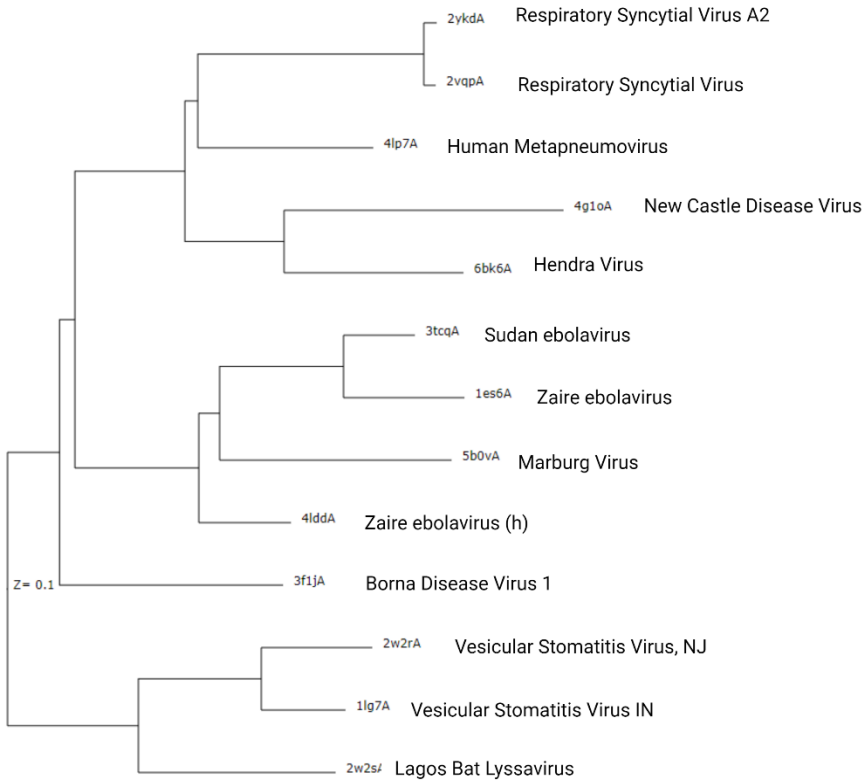

Figure 1.7. Sequence and structure-based relationships of Mononegavirales matrix proteins.

The relationships of mononegavirales matrix proteins based on (top) sequence similarity and (bottom) structure similarity. Top The evolutionary history was inferred using the Minimum Evolution method. The optimal tree is shown. The tree is drawn to scale, with branch lengths in the same units as those of the evolutionary distances used to infer the phylogenetic tree. The evolutionary distances were computed using the Poisson correction method and are in the units of the number of amino acid substitutions per site. The ME tree was searched using the Close-Neighbor-Interchange (CNI) algorithm at a search level of 1. The Neighbor-joining algorithm was used to generate the initial tree. This analysis involved 13 amino acid sequences. All ambiguous positions were removed for each sequence pair (pairwise deletion option). There were a total of 383 positions in the final dataset. Evolutionary analyses were conducted in MEGA X. Bottom: Structural similarity dendrogram. The dendrogram is derived by average linkage clustering of the structural similarity matrix (Dali Z-scores).

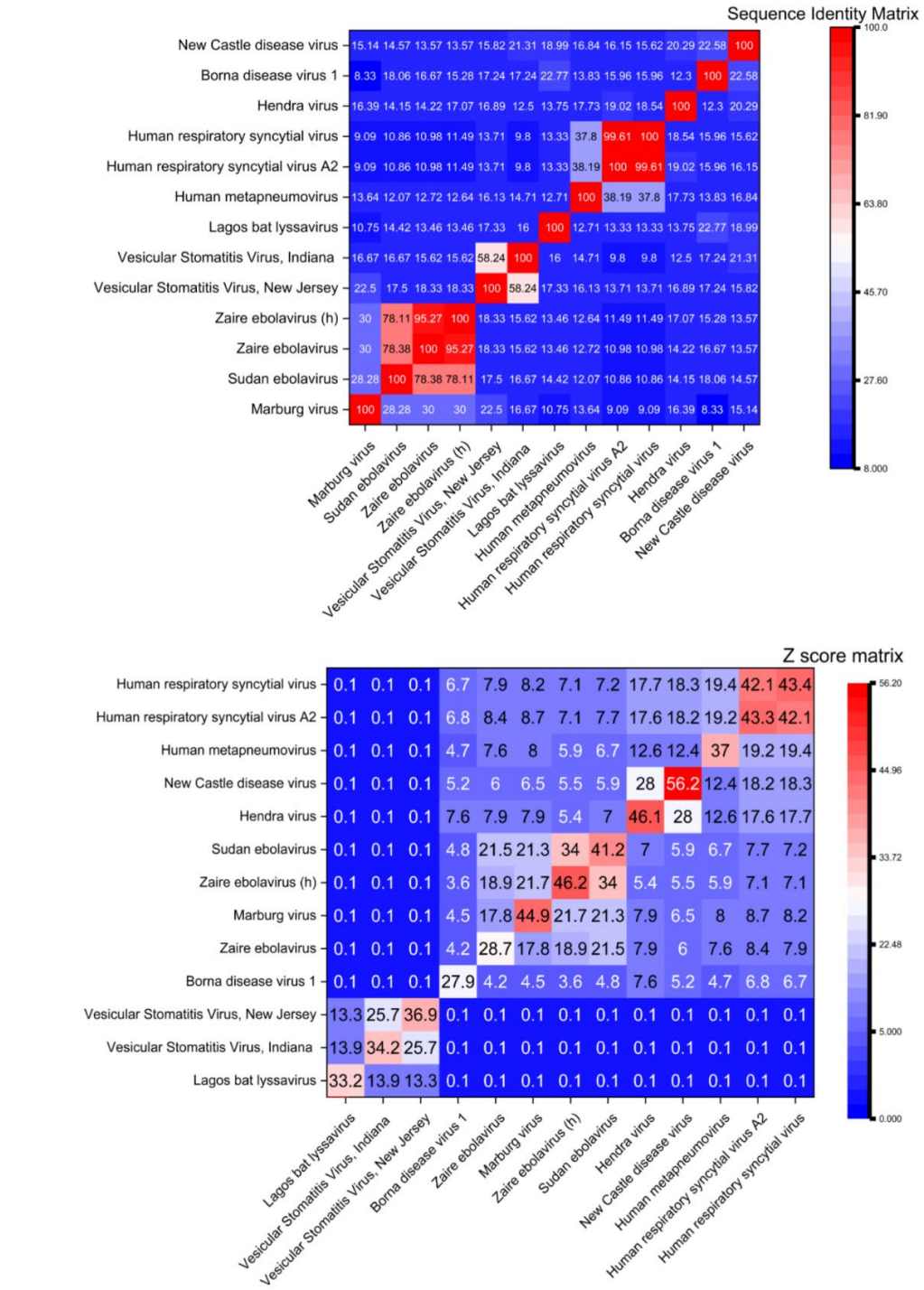

Figure 1.8. Similarity matrix heatmaps of Mononegavirales matrix proteins based on sequence and structural identity.

Top: Sequence identity matrix generated in ClustalW2 and (bottom) structural identity matrix generated by DALI server based of matrix proteins as represented in **Figure 1.7**

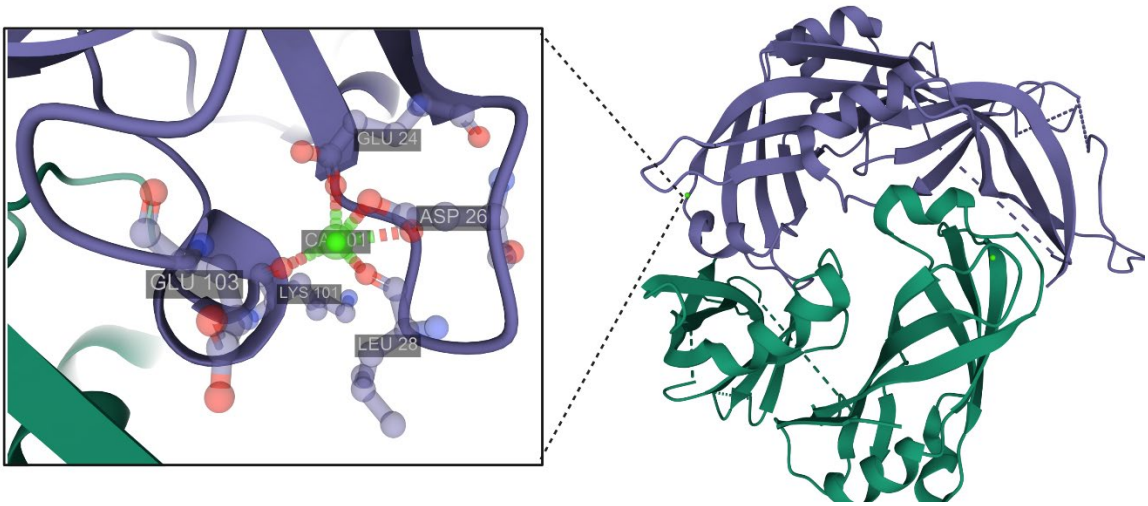

Figure 1.9. The human metapneumovirus matrix protein has a calcium binding site.

Crystal structure of the HMPV matrix protein (right) showing residues that coordinate calcium binding (Glu 24, Asp 26, Leu 28, Lys 101). The diagram shows an adjacent Glu 103 that has not yet been shown to support calcium binding. Calcium shown in green. PDB code:4LP7

Chapter 2 : MATERIALS AND METHODS

PIV5 F Transmembrane domain project

Cell lines and culture

Vero cells were acquired from American Type Culture Collection (ATCC). BSR cells were kindly provided by Karl-Klaus Conzelmann (Max Pettenkofer Institute), and BSR/T7 cells made by constitutively expressing T7 polymerase in BHK cells [118] The cells were maintained in Dulbecco's modified Eagle's media, DMEM (Invitrogen), supplemented with 10% fetal bovine serum, FBS (Sigma). BSR cells were additionally maintained on 0.5 mg/mL of geneticin (Gibco) every third passage, to maintain selection of T7 polymerase.

Plasmids and antibodies

Plasmids with the PIV5 F or HN (W3A) were kindly provided by Robert Lamb (Howard Hughes Medical Institute, Northwestern University) and Hendra F or G-containing plasmids were generously provided by Dr. Lin-Fa Wang (Australian Animal Health Laboratory). Mutants for the study were created using the QuikChange site-directed mutagenesis kit (Stratagene) in pGEM , and subcloned into the eukaryotic expression vector pCAGGS [119], for expression in Vero and BHK cells. For all the analyses, lipofectamine plus and plus reagent (Thermo Fisher) were used per manufacturer's instructions. All constructs used were sequenced (ACGT) to ensure sequence integrity. For PIV5 F analyses, the cytoplasmic tail antibody, which detects residues 516-529 was used, and to detect pre-fusion PIV5 F species, mAb F1a kindly provided by Dr. Richard Randall (University of St. Andrews) were used. HeV F 5G7 antibodies were kindly provided by Dr. Chris Broder (Uniformed Services University of the Health Sciences).

Immunofluorescence

Cells were seeded in 8-well chamber labtek plates (Thermo Fisher) to be at approximately 60-70% confluency for the next day. The following day, cells were transfected with 0.75µg of pCAGGS-MCS, pCAGGS-PIV5 F WT, or pCAGGS-PIV5 F LIZ; pCAGGS-HMPV F WT or pCAGGS-HMPV F LIZ; and pCAGGS-HeV F WT or pCAGGS-HeV F LIZ. 24 hours post-transfection, cells were fixed in 4% paraformaldehyde (PFA) for 20 mins at room temperature, followed by permeabilization in 1% Triton X-100 for 15 mins at 4°C. Cells were then blocked in 1% normal goat serum (NGS) in phosphate buffered saline (PBS), followed by incubation with their respective antibodies overnight (mAb F1a for PIV5 F, and anti HeV F 5G7 for HeV F) at 4°C. The next day, cells were washed seven times with 0.05% Tween 20 in PBS, and incubated with FITC-conjugated secondary antibodies at 1:300 in 1% NGS for 1 hour at 4°C. The cells were washed again seven times with 0.05% Tween 20 in PBS, before being mounted with VECTASHIELD antifade mounting media with DAPI (Vectorlabs). Images were taken using a Nikon A1 confocal microscope and analyzed with NIS-Elements software. Images were processed with Adobe Photoshop with equivalent adjustments made to all channels.

Time course radioimmunolabel assay

Subconfluent Vero cells were transfected with 2.5 µg of pCAGGS-MCS, pCAGGS-PIV5 F WT or pCAGGS PIV5 F LIZ in 6-well plates. The next day cells were washed twice with PBS and starved for 45 min at 37°C in cysteine-methionine-deficient DMEM. Following the starve, cells were labeled for 30 minutes with Tran[^{35}S] metabolic label (100 µCi/mL; MP Biomedicals). Following the label, cells were washed twice with PBS and normal DMEM was replenished on cells. At the indicated time points, the cells were washed three times with PBS and lysed with radioimmunoprecipitation (RIPA) lysis buffer (100 mM Tris-HCl, pH 7.4, 150 mM NaCl, 0.1% SDS, 1% Triton X-100, 1% deoxycholic acid, 1 mM phenylmethylsulfonyl fluoride (Sigma), and 25 mM iodoacetamide (Sigma)). Lysates were collected and centrifuged at 136,500 × *g* for 15 mins at 4°C, and the supernatants collected for subsequent analysis. 8 uL of anti PIV5 F cytoplasmic

tail antibody 516-529 was added to each cleared lysate and incubated for three hours at 4°C with rocking. Antibody-conjugated PIV5 F in the lysate was immunoprecipitated with 30 µL of Sepharose-A beads (GE Healthcare) for 30 minutes at 4°C with rocking. Following the incubation, lysates were washed twice with RIPA + 0.30 M NaCl, twice with RIPA + 0.15 M NaCl, and once with SDS wash II (150 mM NaCl, 50 mM Tris-HCl, pH 7.4, 2.5 mM EDTA). 30µL of 2X SDS loading buffer was added to each sample and boiled for 10 minutes. Samples were run on 15% SDS-PAGE gels, dried, and exposed to a Phosphor screen for three days. The phosphor screens were visualized using the Typhoon imaging system (GE Healthcare). To quantify bands for analyses, band densitometry (ImageQuant 5.2) was used. Total protein expression was determined as the sum of the uncleaved F_0 plus the cleaved larger F subunit, F_1

Surface biotinylation

Vero cells were seeded in 60mm dishes to be approximately 80% confluent for the next day. The following day, cells were transfected with 4.0 µg of pCAGGS-MCS, pCAGGS-PIV5 F WT or pCAGGS-PIV5 F LIZ with lipofectamine plus and plus reagent (Thermo Fisher) according to manufacturer's instruction. At 18-24 hours post transfection, cells were washed twice with PBS, and starved for 45 mins in cysteine-methionine-deficient DMEM. The cells were then labeled in conditioned cysteine-methionine-deficient DMEM containing Tran[^{35}S]-label (100 µCi/ml; MP Biomedicals) for three hours. At this time, cells were washed three times in ice-cold PBS, pH 8, followed by a 35 minute biotinylation with 1mg/mL of EZ-Link Sulfo-NHS-Biotin (Pierce) in PBS pH 8 with rocking at 4°C. The cells were then brought to room temperature for 15 minutes and washed twice with ice-cold PBS pH 8. Cells were lysed in 500 µL of RIPA lysis buffer, scraped, and centrifuged at 136,500 × *g* for 15 mins at 4°C. The supernatant was transferred to a 1.5mL Eppendorf tube, where 8 µL of PIV5 F antibody 516-529 were added to incubate with rocking for three hours. The fusion protein was then immunoprecipitated by incubating with 30 µL of protein Sepharose-A beads (GE Healthcare) for 30 minutes and washed twice with RIPA + 0.30 M NaCl, twice with RIPA + 0.15 M NaCl, and once with SDS wash II. After the beads were washed, 60 µL of

10% SDS was added, and the samples were boiled for 10 min, transferred to a separate tube, and washes repeated with 40 µL of 10% SDS for a total of 100 µL. 10 µL, denoting 10% of the supernatant, was moved to a separate tube to be used to analyze the total protein population. To the remaining supernatant, 30 µl of streptavidin beads (Pierce) and 400 µl of biotinylation dilution buffer (20 mMTris (pH 8), 150 mM NaCl, 5 mM EDTA, 1% Triton X-100, 0.2% bovine serum albumin) were then added for 1 h at 4°C with rocking. Streptavidin was used to label the biotinylated surface population, which was subsequently precipitated and washed with RIPA buffers as noted above for the total population. Samples were analyzed with 15% SDS-PAGE and visualized using the Typhoon imaging system (GE Healthcare). Band densitometry using ImageQuant 5.2 was performed for each experiment to quantitate the amount of F expressed, which was calculated as the sum of F_0 and F_1, normalized to WT. (Figure 2.1)

Surface expression with prefusion conformation-specific antibody: flow cytometry

Subconfluent Vero cells were transfected with pCAGGS-PIV5 F WT or pCAGGS-F LIZ using Lipofectamine plus and Lipofectamine reagent according to the manufacturer's protocol (Thermo Fisher). Cells were washed twice with ice cold PBS twenty-four hours after transfection. The remainder of the experiment was performed on ice unless otherwise indicated. After washing, transfected cells were incubated with rocking with 1:300 of mAb F1a antibody, which detects the prefusion form, for 1 h. Cells were subsequently washed and incubated with a FITC-conjugated secondary antibody at 1:1000 for 30 minutes with rocking, away from light (covered in tin foil). Cells were once again washed with PBS, lifted with 50mM EDTA in PBS for 15-20 minutes at 37ºC and then transferred to 4ºC for 3 hours. Following lifting, cells were fixed at in 2% PBS and transferred to FACS tubes for processing at the UK flow cytometry core.

Syncytia assay

Subconfluent BHK cells in a 6 well plate were transfected with pCAGGS-PIV5 F WT or pCAGGS PIV5 F LIZ and pCAGGS-PIV5 HN in a ratio of 1:1 for PIV5 F:PIV5 HN. Twenty-four hours after infection, cells were imaged for syncytia with a Nikon

TS100 microscope with 10× objective. Syncytia were captured with a Nikon digital camera attached to the microscope.

Luciferase reporter gene assay

Subconfluent Vero cell monolayers in 12-well plates were transfected with T7 promoted Luciferase plasmid, pCAGGS-PIV5 F WT or LIZ, and pCAGGS-PIV5 HN. Transfection was performed at 1:1:0.8 for F:HN:luciferase under T7 promoter. At 24 hours post-transfection, BSR T7 cells expressing the T7 RNA polymerase were overlaid onto the Vero cells and incubated at 37°C for 3 hours. The monolayers were then washed twice with PBS, lysed in a luciferase lysis buffer (Promega), and clarified by centrifugation per the manufacturer's instructions (Promega). For each sample, lysate was loaded into a 96-well plate, where luciferin was added at a 1:1 ratio of lysate:luciferin. Where there was successful fusion, T7 RNA polymerase from BSR cells would gain access to and synthesize the Luciferase mRNA under the control of the T7 promoter. Luciferase enzyme activity was quantified in a luciferin-dependent reaction and quantified as luminescence with a L_{max} luminometer (Molecular Devices). Luciferase reporter activity for mutants were normalized to WT. (Figure 2.2)

Thermal triggering assay

Subconfluent Vero cells in a 12 well plate were transfected with either pCAGGS-PIV5 F WT of LIZ according to manufacturer's protocol (Lipofectmaine plus and lipofectamine reagent; Thermo Fisher). The following day, at 24 hours post transfection, transfected Vero cells were utilized in a thermal triggering assay as follows: for 15 minutes, cells were incubated at 4ºC, 37ºC, 55ºC, 60ºC, and 65ºC. Cells were immediately placed on ice after thermal treatment for 15 minutes to halt triggering, before they were prepared for flow cytometry. The rest of the procedure was performed on ice as detailed above in the flow cytometry protocol used to quantify surface expression of the prefusion F. The thermal triggering assay addressed changes in expression of the prefusion conformation of F at the surface of the cell in response to triggering with heat. (Figure 2.3)

HMPV matrix protein project

Cell lines and culture

A549, BEAS-2B, and Vero cells were acquired from ATCC. A549 cells were maintained in F-12 (Kaighn's) medium (GE Healthcare), supplemented with 10% FBS (Sigma) and 1% penicillin/streptomycin. BEAS-2B cells were grown in bronchial epithelial cell growth medium (BEBM) supplemented with the reagents from a BEGM SingleQuot kit growth factors (Lonza), and Vero cells were maintained in DMEM supplemented with 10% FBS (Sigma). BSR cells were a kind gift from Karl-Klaus Conzelmann (Max Pettenkofer Institute) and were maintained in Dulbecco's modified Eagle's media (DMEM) and 10% FBS.

Plasmids and antibodies

Mutants for the study were created using the QuikChange site-directed mutagenesis kit (Stratagene) in pGEM, and subcloned into the eukaryotic expression vector pCAGGS [119], for expression in A549 and Vero cells. pTM1 L, M2-1, N, P and CAT-Luciferase minigenome reporter assay plasmids for HMPV were a kind gift from Dr. Rachel Fearns (Boston University). For all the transfection analyses, lipofectamine 3000 (Thermo Fisher) was used per manufacturer's instructions. All constructs used were sequenced (ACGT) to ensure sequence integrity. We used the conformational antibody mAb JOJ (obtained from Thermo Fisher) for immunofluorescence experiments and conformational studies, and a polyclonal against antibody avian metapneumovirus M protein, which also cross-reacts with HMPV M, kindly provided by Sagar M. Goyal (University of Minnesota), for Western blotting and radioimmunolabeling. HMPV N antibodies were obtained from Abcam, HMPV F 54G10 antibody was a kind gift from Dr. John Williams (University of Pittsburgh).

FISH probe design

Forty-eight fluorescence *in situ* hybridization (FISH) probes that target the HMPV RNA sequence between nt 1 and 5467, which contain the genes for N, P, M, F, and M2 were synthesized and obtained from Biosearch Technologies. Each probe

was 20 nt long and linked at the 3' end to the Quasar 570 fluorophore for probes complementary to vRNA [120].

PPMO design

Peptide-conjugated phosphorodiamidate Morpholino oligomers (PPMO) were designed to target and knockdown the HMPV matrix protein. The PPMO was designed based on the several strains of HMPV, and ultimately, the HMPV strain CAN97-83 strain used in this study. The 25 nucleotide (nt) PPMO sequence was designed to encompass 13 nts upstream of the AUG start sequence in the 5'UTR, and span the first 12 nts of the matrix protein nucleotide sequence. Phosphorodiamidate Morpholino oligomers (PMO) were obtained from Gene-Tools. An arginine-rich peptide was added to PMOs to create PPMO by Hong Moulton and David Stein (Oregon State University). The peptide is a potent aid in cellular delivery of PPMO [121-123].

Viral propagation

WT HMPV strain CAN97-83, generously provided by of Guy Boivin (Université Laval, Canada) and recombinant, GFP-expressing HMPV (rgHMPV) strain CAN97-83 (a kind gift of Peter Collins and Ursula Buchholz, National Institutes of Health) were propagated in Vero cells. WT HMPV and rgHMPV were propagated at a starting multiplicity of infection (MOI) of 0.01, and incubated at 32°C with Opti-MEM, 200 mM L-glutamine, and 0.3 µg/ml tosylsulfonyl phenylalanyl chloromethyl ketone (TPCK)-trypsin, which was replenished every day. On days 7-9, cells were scraped and collected in 1X SPG (218mM Sucrose, 4.9 mM L-glutamic acid, 3.8 mM KH_2PO_4, 7.2 mM K_2HPO_4) and frozen at −80°C. The cells were then thawed at 37 °C and subjected to a total of three freeze/thaw cycles before centrifugation at 2,500 × *g* for 20 minutes at 4°C on a Sorval RT7 tabletop centrifuge to clear cellular debris. The supernatant was then centrifuged on a 20% sucrose cushion in TNE (50 mM Tris-HCL, pH 7.4, 100mM NaCl, 0.1mM EDTA) for 2 h and 30 minutes at 27,000 × *g* and 4°C using a SW28 swinging-bucket rotor on a Beckman Optima L90-K ultracentrifuge. Following centrifugation, the supernatant was removed, and the pellet was resuspended in 100 uL Opti-MEM per tube and

incubated at 4°C overnight with rocking to resuspend the viral particles. Samples were aliquoted, flash frozen and stored at −80°C.

Recombinant GFP-expressing PIV5, a kind gift from Robert Lamb (Howard Hughes Medical Institute, Northwestern University) and Jessica Robach (Northwestern University) was grown in MDCK cells. RSV A2 expressing GFP (rgRSV) was kindly gifted by Medimmune/Astrazeneca. For propagation, an MOI of 0.1 of rgRSV was added to Hep-2 cells in Opti-MEM. After 3 h incubation, Opti-MEM with 2 mM L-glutamine was added and cells were incubated for 4 to 5 days at 37 ºC. Cells were then scraped and treated with one freeze-thaw cycle. Cell debris was spun down at 2500rpm and the supernatant made up to 1X of sucrose phosphate (Hyclone, special order from Astrazeneca/Medimmune). Samples were aliquoted and flash frozen to be kept at −80°C. Viral titers were determined by performing serial dilutions and infecting Vero cells in a 96 well plate. The number of fluorescent cells were counted at 24 h.p.i to determine number of plaque forming units that were present per mL (pfu/mL).

Time course immunofluorescence assay

Ten mm coverslips were coated with 1 mg/mL of bovine serum albumin, 10 µg/mL of fibronectin, and 30 µg/mL of collagen in BEBM at 37°C overnight. The following day, the coating was aspirated, and BEAS-2B cells were seeded on coated coverslips to be between 65 – 75% confluency by the next day. Infection was carried out as follows: starting with a multiplicity of infection (MOI) of 4, cells were inoculated with WT HMPV in Opti-MEM. Cells were immediately incubated at 4°C for 2.5 hours to synchronize infection. After this, the inoculum was removed and replaced with fresh Opti-MEM and cells were immediately incubated at 37°C. The time of media replacement and 37°C incubation denotes 0 hours post-infection (h.p.i). Following infection, cells were rinsed twice with PBS and fixed in 4% PFA for 20 minutes at indicated times post-infection. After fixing, cells were washed three times with PBS and incubated for 15 minutes with permeabilization buffer (1% Triton-X-100 in PBS) at 4°C. Cells were subsequently washed twice in PBS, and blocked in 1% NGS for 1 hour. Following blocking, cells were incubated with

the JOJ anti HMPV M monoclonal antibody at 1:100 in 1% NGS overnight at 4°C. Cells were then washed seven times with 0.05% Tween 20 in PBS, and incubated with a TRITC-conjugated secondary antibody at 1:300 in 1% NGS for 1 hour at 4°C. The cells were washed again seven times with 0.05% Tween 20 in PBS, before being mounted with VECTASHIELD antifade mounting media with DAPI (Vectorlabs). Images were taken using a Nikon A1 confocal microscope and analyzed with NIS-Elements software. Images were processed with Adobe Photoshop with equivalent adjustments made to all channels.

HMPV minigenome luciferase assay

BSR cells expressing T7 polymerase were transfected with pCITE-HMPV N, pCITE-HMPV P, pCITE-L, pCITE-M2-1, and a minigenome reporter cassette that encodes a luciferase reporter minigenome construct under control of the T7 promoter using the lipofectamine 3000 system per manufacturers instruction. The amounts transfected are as follows: minigenome: 1.2 µg; P: 0.12 µg; N 0.12 µg, M2-1 0.1 µg. For these conditions, an increasing amount of M, up to 2.0 µg was added to observe effects on minigenome reporter activity. For each condition, the total amount of DNA transfected was kept constant by making up the difference with empty pCAGGS. At 24 hrs post-transfection, cells were lysed in a luciferase lysis buffer and clarified by centrifugation per the manufacturer's instructions (Promega). For each sample, lysate was loaded into a 96-well plate, where luciferin was added at a 1:1 ratio of lysate:luciferin. In this case, reporter activity is read out as the luminescence of enzyme produced with luciferase mRNA is produced by the minigenome, and the effect of increasing amounts of M on luciferase activity is measured (Figure 2.4).

Infected cell count after PPMO treatment

Subconfluent Vero cells in 6-well plates were infected with HMPV at an MOI of 4. The process of infection is described above. At times indicated post-infection, a final concentration of 5µM of either scrambled (control) PPMO or HMPV M-specific PPMO diluted in Opti-MEM were added to cells. At 24 hrs post-infection, cells were lifted with 50mM EDTA for 20 minutes at 37°C. Cells were then transferred to

FACS tubes, where samples were made up to 2% PFA in solution with EDTA and PBS. Samples were analyzed using flow cytometry to determine viral titer as a result of adding PPMO.

Cell toxicity assay

Vero cells were seeded in a 96 well plate. The next day, two-fold serial dilutions of control or HMPV M-specific PPMO were made in Opti-MEM and added to cells. At 24 hours post-treatment, propidium iodide (Thermo Fisher) was subsequently added to quantify the ratios of cell death in PPMO-treated samples compared to untreated samples. Live cells were counted using flow cytometry as a percentage of the total population (live and dead cells) at the UK flow cytometry core.

Immunofluorescence with fluorescence in situ hybridization (FISH)

Subconfluent A549 and BEAS-2B cells grown on 10mm coverslips were infected with WT HMPV as described above. At 0 h.p.i., cells were treated with control or M-specific PPMO as earlier detailed. Cells were then fixed for immunofluorescence in the protocol detailed above, except FISH was performed before cells were mounted. After the final washes following incubation with the secondary antibody for the immunofluorescence portion, cells were once again fixed in 4% PFA for 15 minutes at room temperature. After fixing, cells were washed twice with PBS, and once with 2x SSC-10% formamide buffer, and then transferred to a humidified chamber, where they were incubated overnight at 25°C in FISH vRNA probes diluted at 1:100 in hybridization buffer (4x SSC, 1x Denhardt's solution, 150 µg/mL ssDNA, 2mM EDTA, 50% formamide in DEPC treated water). After 24 hours, cells were washed two times for 20 minutes per wash with 2x SSC-10% formamide buffer and coverslips were mounted using VECTASHIELD antifade mounting media with DAPI (Vectorlabs). Images were taken using a Nikon A1 confocal microscope and analyzed with NIS-Elements software. Images were processed with Adobe Photoshop with equivalent adjustments made to all channels.

RNA extraction and quantitative real time PCR

A549 cells were grown in 6-well plates overnight until a 75-85% confluency was reached. Cells were infected using the method described above, and treated with

PPMO at indicated times post infection. At the indicated times post infection, the cells were washed twice with PBS and then lysed with 500 µl of TriPure isolation reagent (Sigma). The total RNA was extracted according to the manufacturer's instructions. RNA was immediately treated with amplification-grade DNase I (Sigma) for 15 min at room temperature, followed by inactivation at 70°C for 10 min. Reverse transcription was performed starting with 500 ng of DNase-treated RNA, 1.25 mM deoxynucleoside triphosphates, 10 U avian myeloblastosis virus reverse transcriptase (Promega), and 1.25 µM of indicated primers listed in table 2.1. The reaction mixtures were incubated at 80°C for 10 min and then at 42°C for 60 min. For quantitative PCR, 2 µl of freshly made cDNA from the reverse transcription described above was mixed with 1.25 µM each specific primer, Perfecta SYBR green Supermix, and low-carboxy-X-rhodamine reagent (Quanta Biosciences) according to the manufacturer's instructions. The assays were performed using a stratagene Mx 3005P system (Agilent Technologies). The following cycle parameters were used for the experiment: 95°C for 2 min and 40 cycles of 95°C for 30 s, 55°C for 30 s, and 72°C for 60 s. The results were normalized to the average level of expression of the housekeeping gene control, glyceraldehyde-3-phosphate dehydrogenase (GAPDH) and tubulin.

Protein expression studies

Detecting viral proteins in HMPV infection in response to PPMO treatment: Subconfluent A549 cells were infected with rgHMPV or WT HMPV, followed by PPMO treatment at 0 h.p.i. as described above. 1.5 hours before indicated time points, cells were rinsed twice with PBS and starved with cysteine-methionine-deficient media for 30 minutes at 37ºC. Following the starve, cells were labeled with Tran[^{35}S] metabolic label (100 µCi/mL; MP Biomedicals) for 1 hour. Following the label, the cells were washed three times with PBS and lysed with radioimmunoprecipitation (RIPA) lysis buffer, and radioimmunoprecipitation was performed as described in the PIV5 F methods section.

Detecting HMPV M calcium coordinating residue mutants*:* Subconfluent A549 cells were transfected with pCAGGS-HMPV M using Lipofectamine 3000 according to the manufacturer’s protocol. HMPV M expression (WT and mutants) was determined by either radioimmunoprecipitation, described above or by

Western blotting the total lysate. For Western blots, cell lysates were run on 15% SDS PAGE gels, and transferred to polyvinylidene difluoride (PVDF) membranes (Fisher) at 50 V for 80 min at 4°C. Membranes were subsequently blocked with 5% milk in Tris buffered saline with 0.05% Tween-20 (TBS-T). Then, membranes were incubated with anti-AMPV M antibody in 5% milk TBS-T. Membranes were washed with TBS-T and incubated with anti-rabbit secondary antibody at 1:10,000 (Jackson). Membranes were washed again with TBS-T and visualized with the LiCor imaging system.

Statistical analyses

The average value and standard deviation from each indicated experiment were computed. Analyses were generally performed using a two-way ANOVA for multiple comparisons, or the Student *t* test for pairwise comparisons. *p* values are indicated for each individual experiment. All statistical analyses were performed using GraphPad Prism software.

Table 2.1 List of primers used for qPCR experiments.

Target	Primer
RT/HMPV vRNA	AACGCGTATAAATTAAGTTAC
qPCR/HMPV Pvm/F	ACCTACCAAACCGACCATATTG
qPCR/HMPV Pvm/R	CTTCAGTTTTGATTGCCCCAC
qPCR/hmpv N m/F	GTGCTGGTCAAACAATGCTG
qPCR/hmpv N m/R	ACTCAGCTTGGACAGATACATG
qPCR/hmpv M m/F	CTATCAAGGAGAGTGAATCAGCC
qPCR/hmpv M m/R	GATCAGTCCCGCATAAGGTG
qPCR/hmpv F m/F	GAGAACATTGAAAACAGCCAGG
qPCR/hmpv F m/R	AGAGCCAAGGACAGCAATTAG
qPCR/hmpv M2-1 m/F	GCCTGCTACAGTCTACACAAC
qPCR/hmpv M2-1 m/R	AGATGCGGGAGTTTTGCTC
qPCR/hmpv M2-2 m/F	TGACTCTTCATATGCCCTGC
qPCR/hmpv M2-2 m/R	GAGACTTCACTATCCCATCGG
qPCR/hmpv SH m/F	AGACTCACCATCAAATACCACATC
qPCR/hmpv SH m/R	TTATTTTCCAGCATGTGTCCTTG
qPCR/hmpv G m/F	TCACAGCATCCAACTCAACAG
qPCR/hmpv G m/R	TGCTGGTTCTGTTTCTGATGG
qPCR/hmpv L m/F	GCAAGTTCAACCAAGCCTTTAG
qPCR/hmpv L m/R	GTGTTCCATGTAATTCGTCTGC
Oligo(dT)20	TTT TTT TTT TTT TTT TTT TT

Designed by Dr. Cheng-Yu Wu

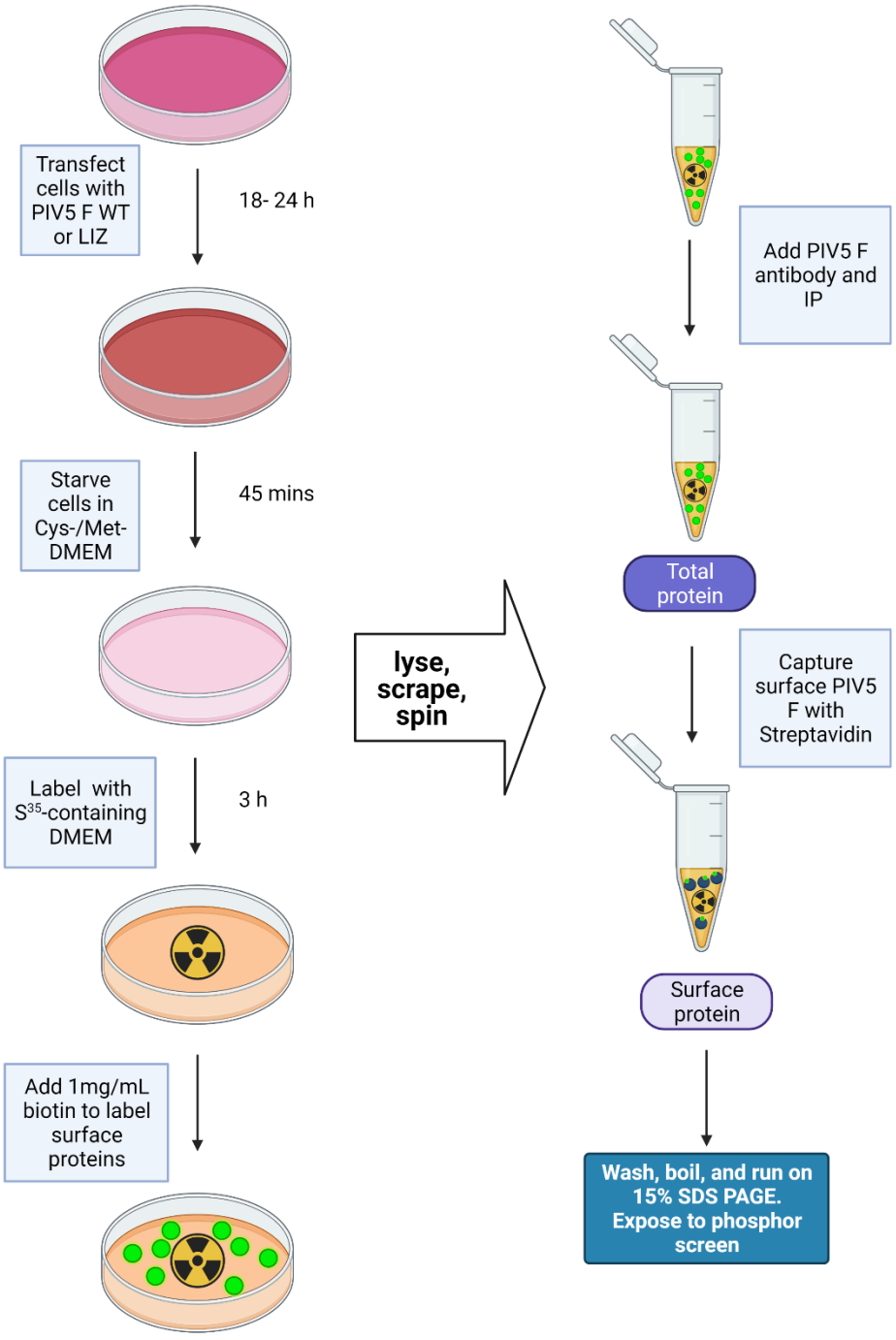

Figure 2.1. Workflow of the surface biotinylation protocol.

Cells are transfected with pCAGGS-PIV5 F and incubated overnight. Cells are then starved, metabolically labeled with radioactive sulfur-containing cysteine and

methionine. Following the radioactive label, the surface population of cells is also labeled with biotin before cell lysis and lysate clarification. F proteins are immunoprecipitated, and at this point 10% is reserved to be analyzed as “total protein”. The remaining 90% is incubated with streptavidin to distinguish surface-expressed F only. The surface protein is boiled to be released from beads, run on a gel and analyzed by autoradiography.

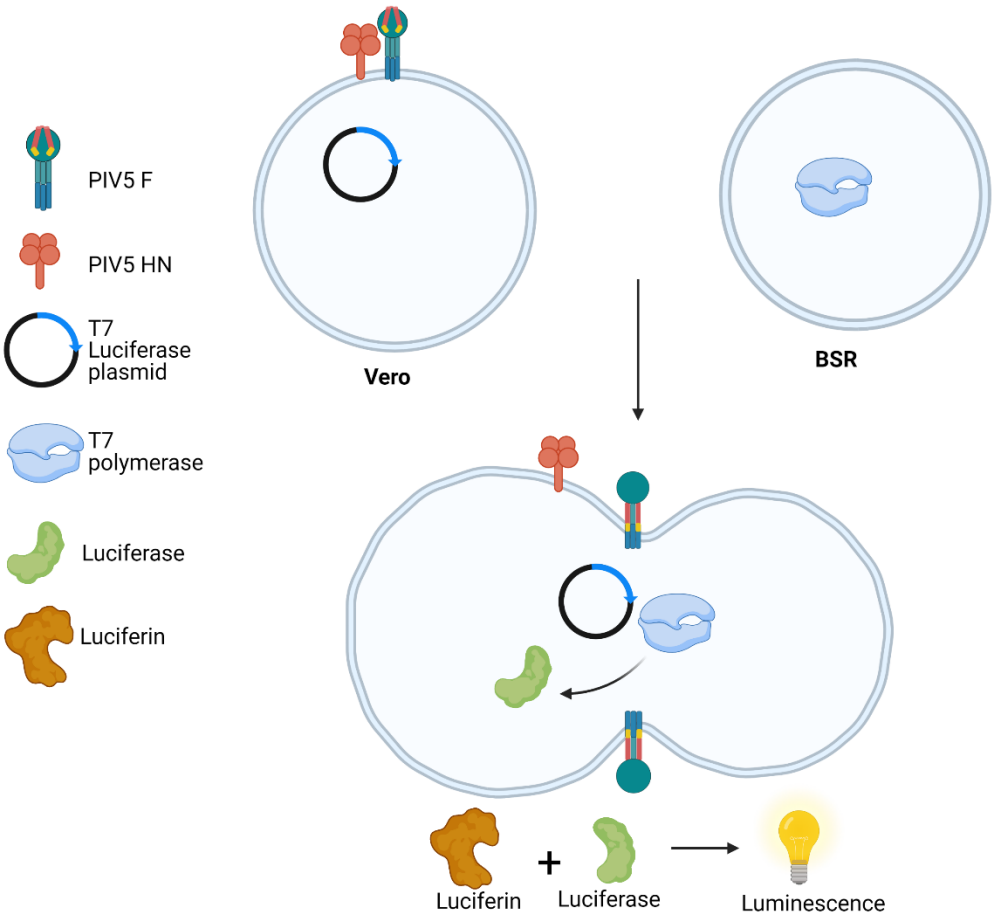

Figure 2.2. Schematic representation of luciferase reporter fusion assay. BSR cells constitutively expressing T7 polymerase were overlaid onto Vero cells transiently expressing PIV5 F (WT or LIZ), PIV5 HN, and containing plasmids with luciferase under a T7 promoter. Where PIV5 F is functional, F would merge the membranes of BSR and Vero cells, giving the T7 polymerase access to the luciferase in Vero cells under the T7 promoter. Thus, if fusion occurs, luciferase is synthesized. The readout of fusogenic activity is observed from the reaction of luciferin in the cell lysates reacting with luciferin. The reaction produces luminescence, which is quantified by a luminometer.

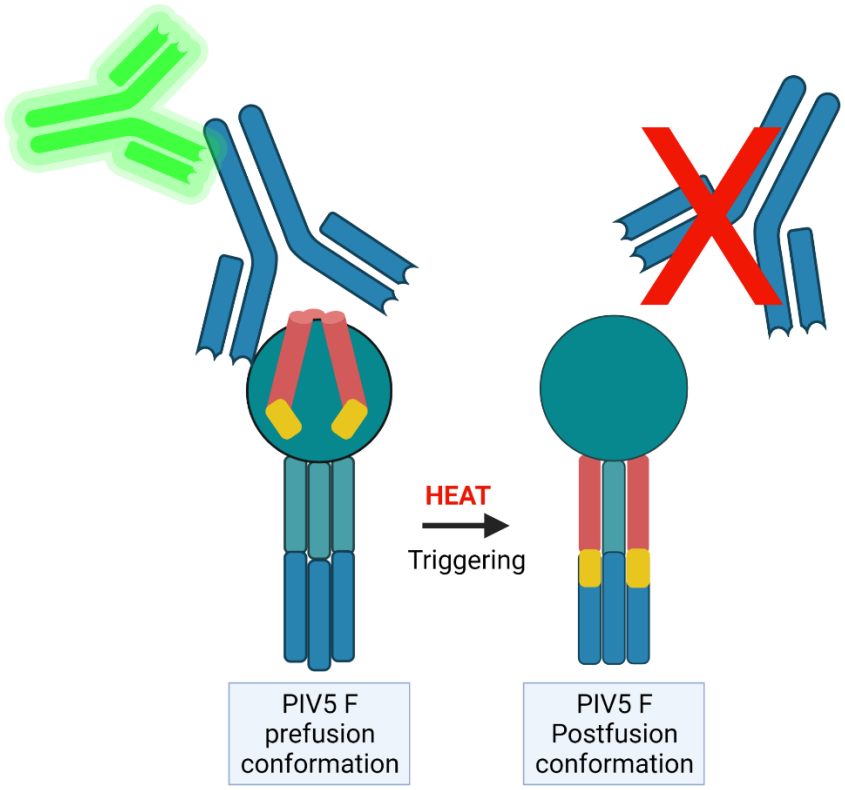

Figure 2.3. Principle of thermal triggering assay.

To test the thermostability of the PIV5 F WT or LIZ, cells transfected with either construct is subject to heat treatment at indicated temperatures for 15 minutes. If the protein remains in the prefusion conformation, mAb F1a, the prefusion antibody will still bind, thus secondary antibodies bound can be quantified by flow cytometry. The lack of mAb F1a binding is a direct function of the amount of F that is triggered at the surface of cells.

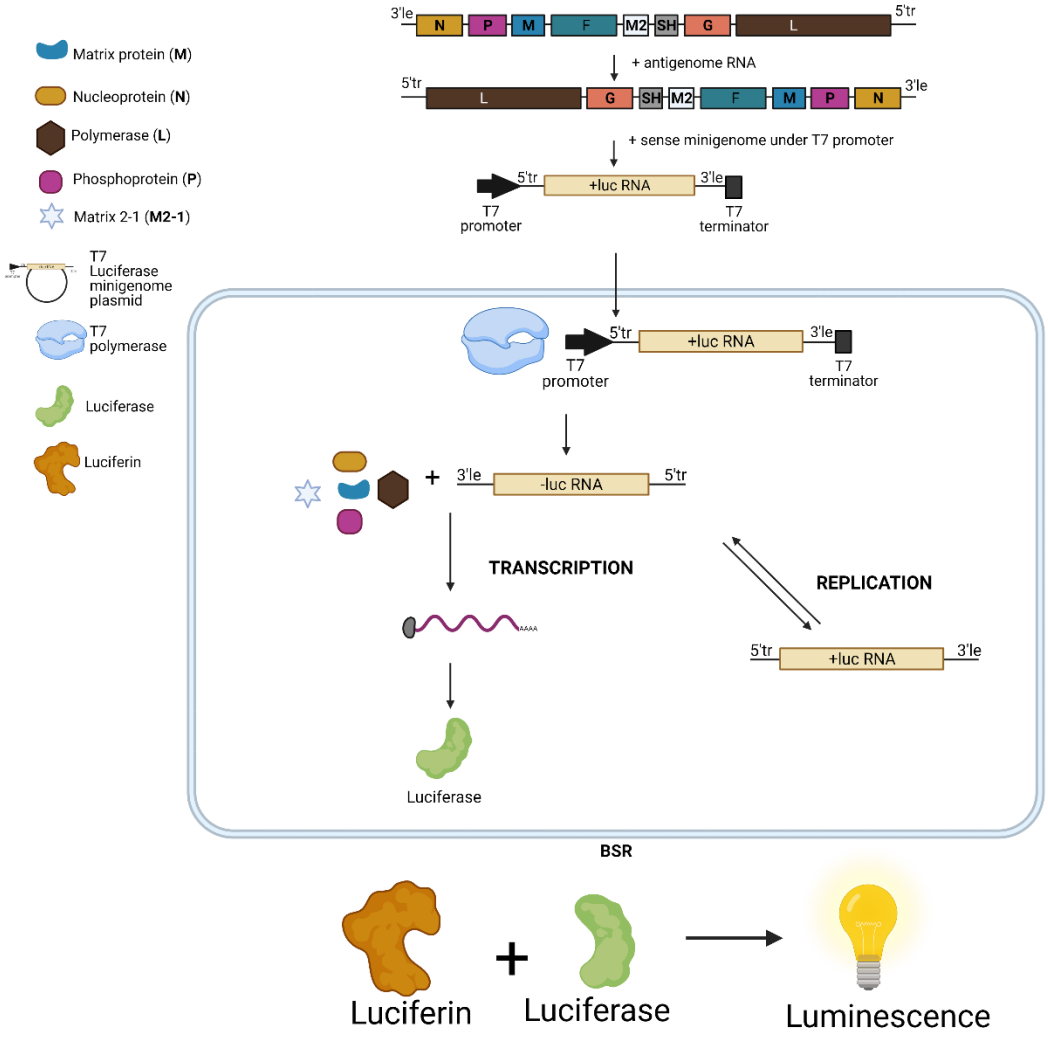

Figure 2.4. Schematic of the minireplicon system mechanism.

BSR cells constitutively expressing T7 polymerase are transfected with a positive sense luciferase minigenome under a T7 promoter, along with the viral components required for viral replication: N, P, L, and M2-1. Once the minigenome is delivered, T7 polymerase from BSR cells gains access to the +strand minigenome, and makes a negative sense RNA copy. At the same time, N,P,L, and M2-1 that are freshly synthesized in the transfected cell can access and read the -luciferase genome leader and trailer elements, transcribing the minigenome

into luciferase mRNA. This mRNA is translated into luciferase protein. The -luc RNA genome is also used as a template for replication: it also directs formation of +luciferase RNA, which is in turn used to generate more -luciferase template for mRNA and protein production. Lysates from this when incubated with luciferin produce varying degrees of luminescence, as a direct readout of the efficiency of viral elements to support replication and transcription. In this assay, increasing amounts of M was added to examine its effect on baseline transcription and replication efficiency of the minigenome system.

Chapter 3 : PARAINFLUENZA VIRUS 5 FUSION PROTEIN MAINTAINS PREFUSION STABILITY BUT NOT FUSOGENIC ACTIVITY FOLLOWING MUTATION OF A TRANSMEMBRANE LEUCINE/ISOLEUCINE DOMAIN

*Portions of this chapter were adapted and reprinted with permission from the Microbiology Society: **Branttie JM**, Dutch RE. Parainfluenza virus 5 fusion protein maintains pre-fusion stability but not fusogenic activity following mutation of a transmembrane leucine/isoleucine domain. J Gen Virol. 2020 May;101(5):467-472. doi: 10.1099/jgv.0.001399. Epub 2020 Feb 25. PMID: 32100701; PMCID: PMC7414451.*

Introduction

Parainfluenza virus 5 (PIV5), measles virus (MeV), and the zoonotic Hendra virus (HeV) and Nipah virus (NiV), are enveloped viruses that belong to the family Paramyxoviridae [124]. MeV, HeV, and NiV are highly pathogenic viruses of worldwide significance [125], while PIV5 serves as an important *Paramyxoviridae* viral model system [126]. Although there are vaccines against MeV and its rampant spread has been mainly checked, there is still a troubling proportion of the global population that remains unvaccinated [127]. In fact, lack of MeV vaccination is the leading worldwide cause of preventable deaths in children. For these unvaccinated groups, MeV causes a range of symptoms, with one of the deadliest being encephalitis [128]. HeV and NiV similarly can result in encephalitis upon disease onset, but patients may also have repeated cases of encephalitis following initial recovery [129]. A combination of HeV and NiV being bat-borne, the high morbidity and mortality rate, along with the lack of human vaccines or therapeutics [130, 131], make apparent the potential risk of a global henipavirus pandemic. Moreover, the voluntary lack of vaccinations against MeV potentially poses a threat to herd immunity, particularly putting immunocompromised individuals at risk. These observations highlight the need for basic and clinical research in paramyxoviruses in order to elucidate attractive and novel therapeutic targets.

Paramyxoviruses contain a non-segmented negative sense (NNS) RNA genome. Within the paramyxovirus family, virion structures are generally highly pleomorphic in size and shape [125, 132, 133]. In contrast, cryo-electron microscopy has demonstrated that PIV5 particles are mostly spherical [133], similar to Sendai virus (SeV) particles [132]. Paramyxovirus particles range from between 110 and 540nm in size, with some particles bearing more than one copy of the viral genome [125, 132]. Data also shows that when compared to other negative sense RNA viruses such as Influenza and Marburg viruses, the genomic packaging of SeV appears to be less ordered, in some cases forming a “tangled knot” [132]. For paramyxoviruses, the RNA copies are encased in nucleoprotein (N) and are associated with the phosphoprotein (P), which is a polymerase cofactor, and a large RNA dependent RNA polymerase protein (L) also forming part of the RNP. Altogether, the viral RNA and its encapsidated proteins form helical ribonucleocapsid filaments, further protected by a viral glycoprotein-rich double layered membrane. The two most prominent glycoproteins within the family are the attachment protein (G/HN/N) and the fusion protein (F), which is largely responsible for successful entry of viral particles to host cells. The PIV5 attachment protein is denoted by HN for its hemagglutinin neuraminidase activity [134].

For these enveloped viruses, successful infection requires fusion of their membranes with target cell membranes to allow for content mixing [41, 53]. Since membrane fusion is energetically costly [135] , F and G/HN/H serve as critical viral surface proteins that lower the kinetic barrier to drive the fusion and entry process. The fusion proteins of PIV5 and other paramyxoviruses are folded into homotrimers within the endoplasmic reticulum (ER) as they are synthesized. These proteins contain a fusion peptide (FP), heptad repeats A and B, the transmembrane domain (TMD) and a cytoplasmic tail. For fusion to occur, the attachment protein tethers the viral particle to the host cell via interactions with cellular receptors; subsequently, the F protein drives the fusion process by undergoing large-scale, essentially irreversible conformational changes from a metastable pre-fusion structure to a highly stable post-fusion conformation that results in the merging of the viral and target cell membranes [44, 45, 134]. These

conformational changes entail the unraveling of the HRA and FP from the ectodomain head and movement of these regions towards the target cell, where the FP is initially inserted to form a pre-hairpin intermediate. As this state is less energetically favorable, the protein then refolds into a low energy conformation, creating a six-helix bundle of the HRA and HRB domains, and merging the two membranes to create a fusion pore [53]. This fusion pore must expand before viral RNA can pass into the host cell, with expansion postulated to be mediated in part by the cytoplasmic tail (CT) of the paramyxovirus fusion protein [136].

Like other class I fusion proteins, paramyxovirus F proteins are synthesized in a metastable prefusion state and folded in ER into the homotrimer that must be proteolytically cleaved to become fusogenically active [135]. The cleavage event unveils a FP that interacts with the target membrane to facilitate the aforementioned fusion process [137, 138]. Upon synthesis, the HeV F is trafficked through the secretory pathway to be expressed on the cell surface in its fusogenically inactive form (F_0). Subsequently, HeV F_0 is endocytosed and cleaved by the protease cathepsin L within endosomes and retrafficked to the surface in a disulfide-linked fusogenically active form (F_1 +F_2) [41, 139]. Conversely, PIV5 F trafficking is more straightforward: it is similarly synthesized in the secretory pathway, but undergoes cleavage within the *trans*-Golgi network (TGN) by furin during transport to the cell surface to be expressed as F_1 + F_2 [41, 44, 134, 139, 140]. Importantly, throughout the trafficking process, paramyxovirus F proteins must be maintained in a metastable pre-fusion state, as premature triggering renders the protein fusion inactive [74].

Although certain paramyxovirus F proteins such as SeV F can trigger in the absence of their homotypic attachment proteins [141], most paramyxoviruses engage in complex interactions with their attachment proteins to begin refolding from the pre-fusion to the post-fusion state [134, 142]. Indeed, the triggering of fusion by initiation of conformational changes still presents as a significant gap in our knowledge fusion regulation. A number of studies have focused on how external domains and cytoplasmic tails of F proteins impact fusion. Many of these

focus on possible interactions with the attachment protein in transmitting conformational changes after attachment to signal the F protein to trigger. [53, 143, 144]. Interestingly, an unsuspected player, the transmembrane domain (TMD), which was initially thought to mainly serve as a membrane anchor, has recently been shown to play critical roles in the pre-fusion stability of the paramyxovirus F proteins [41, 74, 145-149]. In isolation, the TMDs of HeV F, PIV5 F and the closely related pneumovirus human metapneumovirus (HMPV) F self-associate in trimers. For HeV F, an AXXXG motif, similar to the GXXXG motif known to support association of hydrophobic residues, was found to be important for maintaining surface levels of the cleaved prefusion form [41]. On further investigation, another important association motif, the leucine/isoleucine (L/I) zipper was identified in the TMD of HeV F and similar β-branched residues in heptad repeats were found for 140 other paramyxoviruses, including PIV5 F. Studies on HeV F showed that not only is the L/I zipper important for the self-association of the TMDs in isolation, but it is also important in the pre-fusion stability of the full HeV F protein, and circumvents premature triggering and misfolding. These studies showed a severe reduction in surface and total expression for the HeV L/I zipper mutants, termed LIZ mutants. Not surprisingly, HeV F LIZ mutants are also deficient in forming syncytia, a consequence of not being stably present on the cell surface ([74, 145, 146].

This exciting finding of a potential TMD target that could abrogate viral infection led our group to probe the extent to which the L/I zipper drives fusogenic activity in other closely related viruses. To examine this, we used PIV5, a model paramyxovirus. We introduced alanine mutations to the L/I zipper of PIV5 F to create a PIV5 F LIZ mutant. Our data show that the PIV5 LIZ mutant is expressed on the surface and total levels in similar ways to WT. Surprisingly, despite the relative abundance of potentially fusogenically active pre-fusion PIV5 F LIZ on the surface of transfected cells, there is a considerable decrease in the functionality of the fusion protein, suggesting that the L/I zipper is a potentially relevant target in preventing entry of paramyxoviruses.

Results

HeV F LIZ and PIV5 F LIZ localize differently from WT

Understanding the roles of the transmembrane domain in facilitating functional activities of the fusion protein requires extensive study of its oligomeric associations. Recently, SAXS and solid state NMR data have corroborated studies from the Dutch lab that PIV5 F TMD associates in a trimer [41, 74, 145, 148]. Our lab has shown that for HeV F, these trimeric associations are at least in part supported by the hydrophobic interactions mediated by the heptad repeat L/I zipper [74]. Given these observations, we were interested in whether LIZ mutations affected the placement of the fusion protein of HeV in transfected cells. Surface expression of the fusion protein is important in orienting it for proper assembly into viral particles and for positioning for syncytia formation. Additionally, we were interested in the role of the TM L/I zipper motif in paramyxovirus F proteins to examine whether the L/I zipper functionality observed in HeV F is conserved across the family. To address these questions, we introduced TM L/I zipper alanine mutations to create PIV5 F LIZ (Figure 3.1). With this mutant, we performed immunofluorescence on cells to analyze the intracellular localization compared to PIV5 F WT. Our results demonstrate that while HeV F WT displays a ubiquitous cellular distribution, HeV F LIZ is mostly confined in pockets around the nucleus consistent with the placement endoplasmic reticulum (Figure 3.2 A). These observations corroborate previous data that showed that surface and total expression of HeV F LIZ was considerably lower than for HeV F WT [74].

Interestingly, we found that PIV5 F WT primarily localizes at the surface of the cell and is present within membrane ruffles, while PIV5 F LIZ shows a higher level of intracellular distribution. We further examined multiple focal planes of cells transfected with PIV5 F WT and LIZ using Z-stacks (Figure 3.2 B). We found that PIV5 F WT is mostly absent from the immediate perinuclear region in different optical slices, but PIV5 F LIZ is distributed more evenly throughout the cells and is present in puncta close to the nucleus. These results suggest a more subtle yet significant effect of the PIV5 F L/I zipper in trafficking and intracellular localization

of the protein. Likewise, these data indicate a more modest effect of the TM L/I zipper in protein folding for PIV5 F than for HeV F.

PIV5 F LIZ is expressed comparably to PIV5 F WT in time course

Our data showed that not only was HeV F trafficking impaired, but levels of expression were dramatically affected by the L/I zipper [74]. Sustained expression and stability of the fusion protein is paramount to its biological activity and could affect the ability of the full viral particle to be infectious over longer periods of time. We were interested in whether the role of the L/I zipper in stable HeV F expression is preserved across the paramyxovirus family. If paramyxovirus fusion proteins need TMD L/I zipper interactions to be stably maintained in their pre-fusion form during infection, their removal would reduce the lifespan of the fusion protein. Therefore, to biochemically assess the effect of the L/I zipper on PIV5 F synthesis and stability, we performed a pulse-chase time course assay, using PIV5 cytoplasmic tail antibody 516–529, to examine PIV5 F WT and PIV5 F LIZ stability (Fig. 3.3). Previous studies showed that total expression over time for HeV F LIZ was significantly decreased compared to WT [74]. Surprisingly, between 0 and 8 h, PIV5 F LIZ expression was comparable to WT, suggesting that the PIV5 F L/I zipper is not critical for stability, unlike the L/I zipper of HeV F [74]. This observation indicates that the L/I zipper is not critical for all paramyxovirus fusion protein stability.

Surface expression of pre- and post-fusion PIV5 F is moderately affected by the L/I zipper

Since the presence of F at the membrane is crucial for biological activity, we probed the surface expression of PIV5 F WT and LIZ in transfected cells using a surface biotinylation assay. We found that after radiolabeling newly synthesized F protein for 3 h with S^{35} at 18–24 h post-transfection, PIV5 F LIZ surface expression is decreased by more than 30% when compared to WT. In contrast, total amounts of protein between PIV5 F WT and LIZ remain comparable (Figure 3.3 A and B). The antibody, anti PIV5 F 516–529, that was used in this experiment is able to detect both pre-and post-fusion forms of the protein, indicating that the sum of pre-fusion and post-fusion forms of PIV5 F WT is slightly higher at the cell

surface than for PIV5 F LIZ. From these findings, we conclude that L/I zipper interactions do not significantly affect the overall sum of protein expressed; however, taken with Figure 3.2, the data show that the PIV LIZ mutant shows some redistribution throughout the cell compared to the PIV5 F WT. Surprisingly, PIV5 F LIZ mutations displayed a slightly higher cleavage ratio for surface expressed F than for WT. This may be a result of increased intracellular localization because of the LIZ mutations, as longer retention of PIV5 F LIZ within the TGN would provide extended exposure to the cleavage protease furin before the F protein is finally transported to the cell surface.

The L/I zipper mutations ablate fusogenic activity of the fusion protein

While data shown in Figure 3.4 show that PIV5 F WT and LIZ are expressed at comparable levels at the cell surface, we were interested in selectively quantifying the population of potentially fusogenically active protein at the surface. We performed flow cytometry with the pre-fusion-specific PIV5 F mAb F1a. These data also show that the pre-fusion form of PIV5 F LIZ is only slightly lower than for PIV5 F WT (Figure 3.5). This suggests that although there is a slight decrease in metastable, pre-triggered PIV5 LIZ F on the surface of cells, there is still a significant presence of potentially fusogenically active PIV5 at the surface of cells in the absence of the L/I zipper.

Having established that pre-fusion PIV5 F LIZ can still be trafficked to the surface of cells, we utilized a syncytia assay to test the fusogenic activity of PIV5 F LIZ in comparison to WT. When expressed with its homotypic attachment protein, PIV5 F can form syncytia *in vitro*. We used this model to examine functionality of the PIV5 F LIZ mutant in comparison to WT. We observed that PIV5 F WT is highly fusogenic, as the expression of PIV5 F WT with HN resulted in BHK cells fusing into a few, very large syncytia. Remarkably, syncytial activity was abolished in the PIV5 F LIZ mutant (Figure 3.6 A). Further characterization of fusogenic activity using a luciferase reporter system also showed quantitatively that the PIV5 F TM L/I zipper is critical for fusion (Figure 3.6 B). Notably, a leucine residue at position 468 (L486) has been reported to be important for fusogenic

activity. L486 was shown to be critical for both membrane mixing and content mixing, thus identifying L486 as essential in the events leading up to the merge of lipid bilayers driven by F [147]. L486 is present in the proposed L/I zipper of PIV5 F, corroborating this finding in the context of the L/I zipper.

PIV5 F LIZ mutants are triggered more readily at 55 and 60 ºC

The comparable PIV5 F WT and LIZ pre-fusion surface expression levels, in contrast to the dramatic decrease in HeV F LIZ versus HeV F WT, show that L/I zippers in the TMDs of HeV F and PIV5 F play distinct but critical roles in maintaining biological activity. While these studies suggest that fusion, rather than surface or total expression, is significantly affected by residues within the PIV5 F TM L/I zipper, the exact mechanism by which these LIZ mutations abrogate fusion is currently unknown. To understand whether PIV5 F LIZ is capable of being triggered from its pre-fusion form to undergo the conformational changes that are critical for membrane fusion, we transfected cells with either PIV5 F WT or PIV5 F LIZ for a thermal triggering assay.

Previous studies show that PIV5 F can be triggered in the absence of its cognate attachment protein when exposed to heat [144, 150]. Thus, PIV5 F WT- and LIZ-expressing cells were exposed to increasing temperatures (Figure 3.7), and flow cytometry using the pre-fusion-specific mAb PIV5 F1a was utilized to quantitate the levels of pre-fusion F. Triggering of conformational changes in response to heat would lead to loss of F1a binding. Our results show that as the temperature increased, the detected levels of pre-fusion F decreased for both the WT and LIZ F proteins. Interestingly, at 55 and 60°C, a statistically significant increase in the triggering of PIV5 F LIZ compared to WT was observed, potentially indicating a role for the TM L/I zipper in stabilizing PIV5 F in the pre-fusion conformation. This stabilization is less dramatic than was observed for HeV F [74], but does suggest that a role for the LIZ in pre-fusion stability may be a property across the viral family. However, it is unlikely that this small decline in the thermostability of pre-fusion PIV5 F LIZ would fully account for the drastic loss of fusogenic activity shown in the syncytia and reporter gene assays.

Discussion

A number of studies map out the conformational changes that paramyxovirus fusion proteins undergo once triggered [41, 45, 53, 136, 140, 144, 147, 150-152]. However, there is still a gap in our knowledge of what supports the maintenance of the pre-fusion conformation in a metastable, less energetically favorable conformation than the post-fusion structure until the appropriate window for fusion opens. Our studies sought to understand the relevance of a TMD L/I zipper, an association motif found to be important in stability, expression, and functionality of HeV F [41, 74, 145], in stabilizing the fusion protein for proper function across the paramyxovirus family. We performed mutagenesis of the L/I zipper of PIV5 F and probed whether the TMD L/I zipper potentially affected stability of this second paramyxovirus protein. Our examination into L/I zipper potentially affecting protein stability involved two questions:

1. Does the L/I zipper affect fusion protein turnover for PIV5 F?; and

2. Do mutations in the L/I zipper confer changes to readiness of F to be triggered?

Our results demonstrate that there is no significant difference in the protein turnover of the PIV5 F protein once LIZ mutations were made (Figure 3.2). These results are in direct contrast to our previous observation of HeV F [74], highlighting a difference in the mechanism of potential function of the L/I zipper within the paramyxovirus family. However, our data interestingly showed that for both HeV F and PIV5 F, the L/I zipper contribute to F surface expression, albeit to varying degrees (Figure 3.2; Figure 3.4; Figure 3.5). Previous studies in our lab have implicated the TMDs of paramyxovirses in appropriate trafficking of the fusion protein [66, 67]. Although data from HeV F largely suggest that improper trafficking results from a higher tendency of the fusion protein to dissociate or misfold [74], this current study shows that total amounts of PIV5 F are maintained, and only the proportion of protein that is expressed on the surface is reduced for LIZ mutants. It is tempting to suggest then, that based on this data and on cumulative data from TMD trafficking studies across the paramyxovirus family, the TMD L/I zipper plays

a role in trafficking of the virus to the cell surface. From this study, another important parallel in the role of paramyxovirus TMD L/I zippers is drawn: the TMD L/I zipper is critical for functionality of the fusion protein for both HeV F and PIV5 F. In our studies, although there is ample pre-fusion F present at the cell surface with the PIV5 F TMD L/I zipper was mutated to alanine, we found that fusion activity was ablated (Figure 3.6).

Reports show that for class I fusion proteins such as Ebola virus GP2, influenza virus HA and PIV5 F, the FP and TMDs interact in the post-fusion conformation [138, 148, 153, 154]. It is possible that for PIV5 F, the L/I zipper within the TMDs contributes to making essential contacts with the fusion peptide to hold the post-fusion conformation in place and merge viral and target membranes. Additionally, studies demonstrate that the TMs of class I fusion proteins induce local membrane changes that decrease the energy barrier needed for fusion [137, 148, 155] – as such, the L/I zipper of PIV5 F may contribute in this local disruption. Finally, it is important to note that PIV5 F is known to make contact with HN through an Ig-like domain at the ectodomain [144]. The L/I zipper may be involved in transmitting conformational changes that result from this initial contact, and thus in refolding. Alternatively, F could have important interactions with HN through contacts with the TMD L/I zipper, which are disrupted by the LIZ mutations.

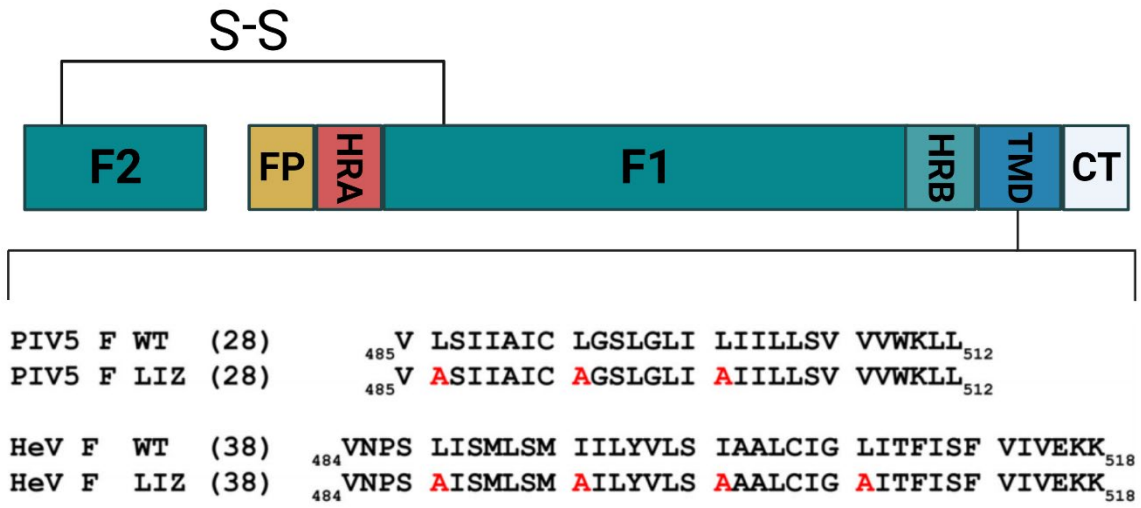

Figure 3.1. Mutations to the L/I zipper of HeV F and PIV5 F.

Schematic of the paramyxovirus fusion protein highlighting the TMD L/I zipper of HeV F and PIV5 F, and the mutant constructs. FP, fusion peptide; HRA, heptad repeat A; HRB, heptad repeat B; TMD, transmembrane domain; CT, cytoplasmic tail); S–S, disulfide bond.

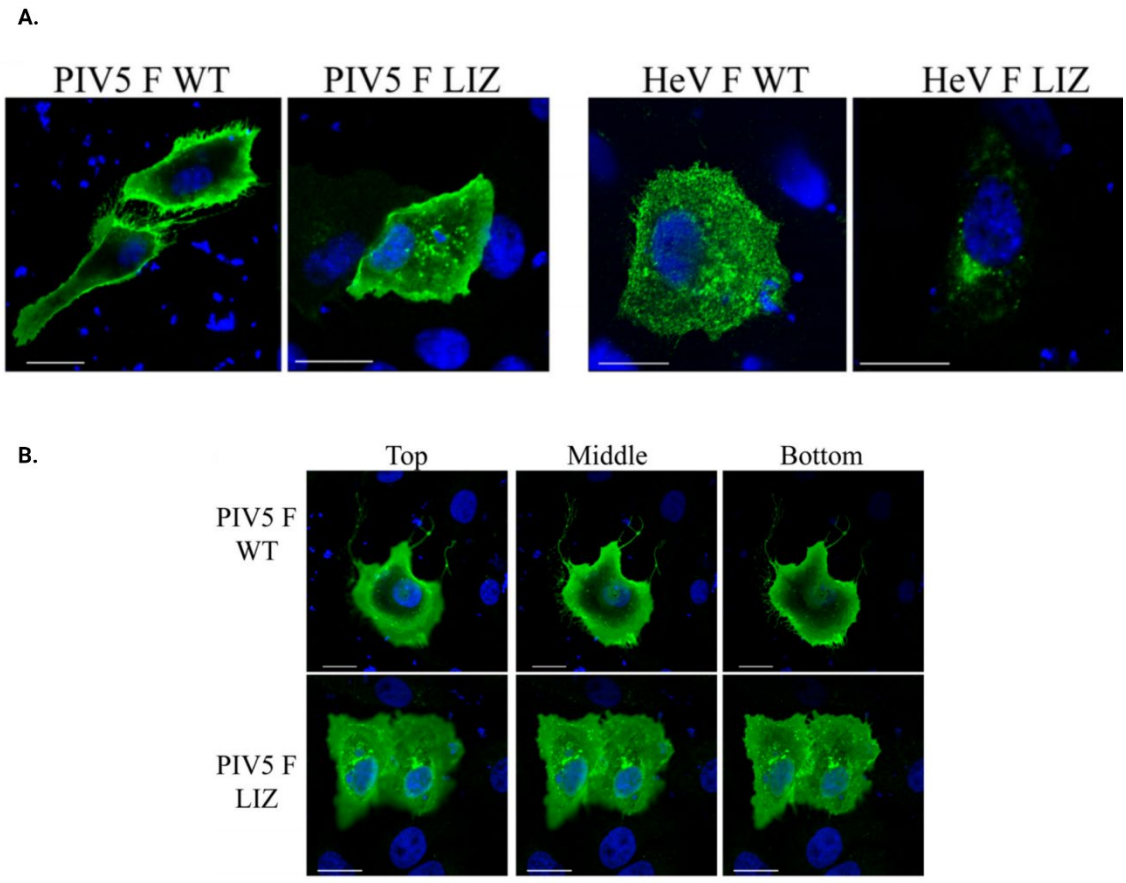

Figure 3.2. **Immunofluorescence to visualize localization of HeV and PIV5 F proteins.**

Vero cells were seeded in eight-well chamber plates and transfected with PIV5 F WT or LIZ mutant (left), and HeV F WT or LIZ mutant (right). Localization of HeV F was analyzed with anti-F 5G7 antibodies, and PIV5 F analysed with mAb F1a (green) (**A**). Images were taken with a Nikon 1A confocal microscope. Images are representative. Scale bars represent 10 µm. (**B**). Z-stack images from (**A**) were collected in 0.3 µm sections, and images corresponding to top, bottom and middle slices are shown. Images are representative of two independent experiments carried out in triplicate. Scale bars represent 10 µm.

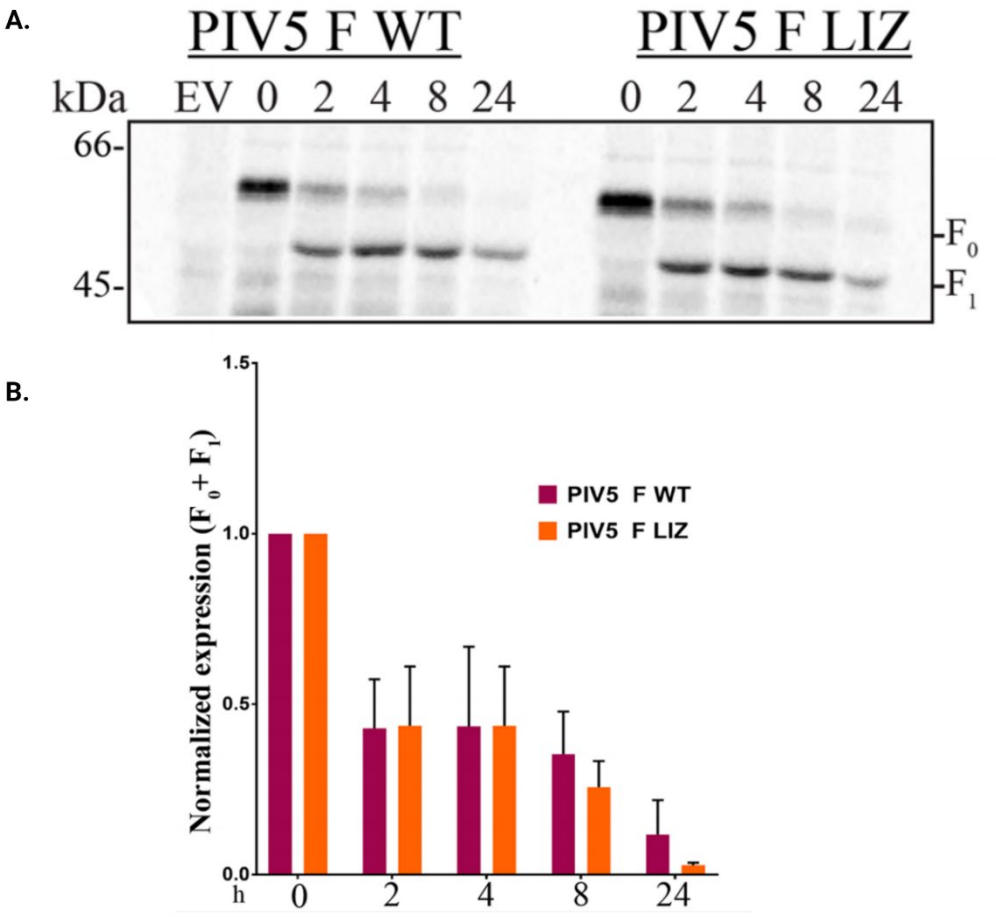

Figure 3.3. **Expression and stability of PIV5 F WT and LIZ are comparable.** **A**. A pulse-chase experiment was carried out 18 h after cells were transfected with 2.5 µg of indicated DNA for Vero cells in six-well plates. Following a 30-minute S^{35} metabolic radiolabel, samples were chased for indicated times. (**B**). Quantitation of PIV5 F and LIZ expression shown in (**A**). Expression levels of total F protein (F_0+F_1) were determined by band densitometry normalized to WT levels. The averages represent three independent experiments, each carried out in duplicate.

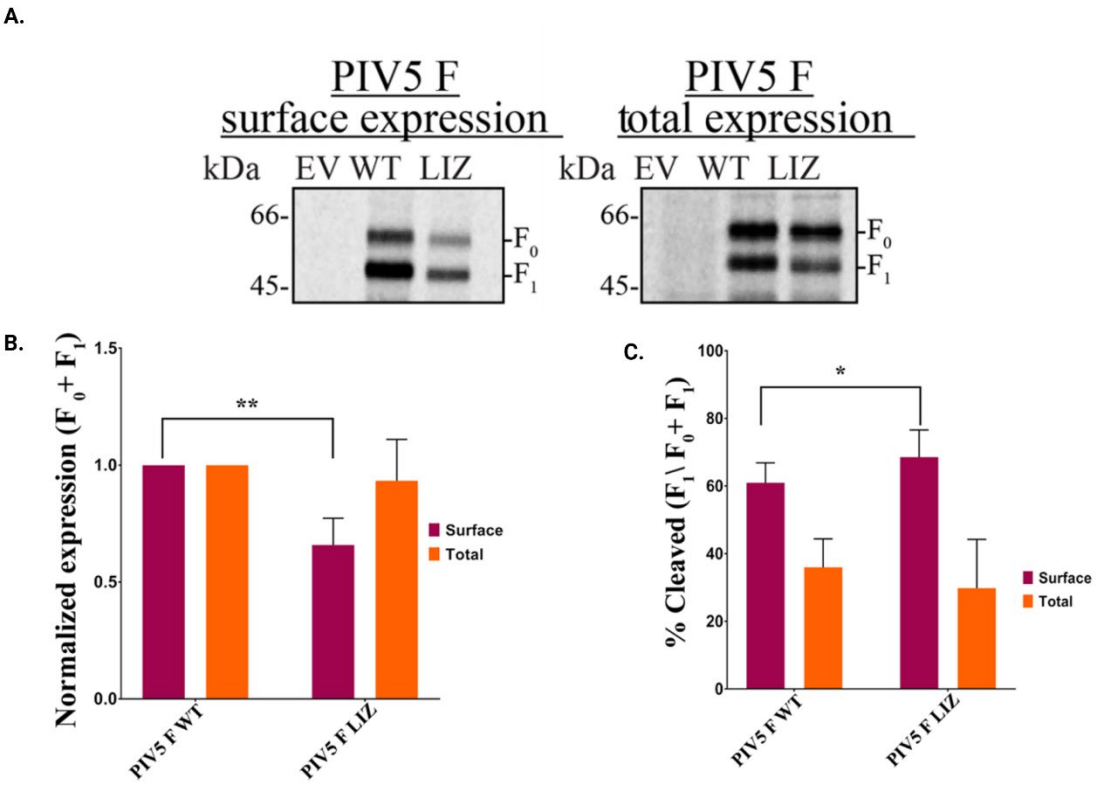

Figure 3.4. Surface and total expression of PIV5 F protein.

(**A**) Surface (left) and total (right) expression levels of PIV5 F WT versus PIV5 F LIZ. (**B**) Quantitation of expression levels (left) and percentage cleavage (right) of surface and total PIV5 F protein. The averages represent three independent experiments, each carried out in duplicate. The LIZ mutant was compared to WT using Student's t-test. *, $P<0.05$; **, $P<0.005$

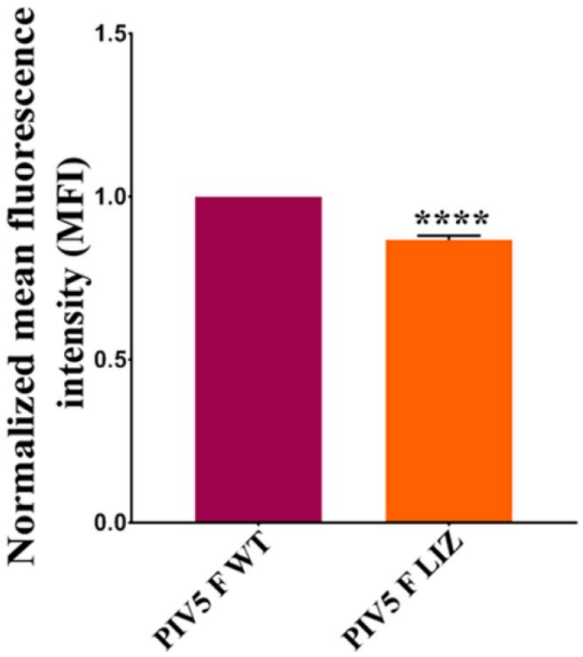

Figure 3.5. Flow cytometry to quantify expression of prefusion PIV5 F only present at the surface of cells.

Flow cytometry was performed on Vero cells transfected with WT or LIZ PIV5 F. The averages represent three independent experiments, each carried out in duplicate. The LIZ mutant was compared to WT using Student's t-test. *, $P<0.05$; **, $P<0.005$; ****$P<0.0001$

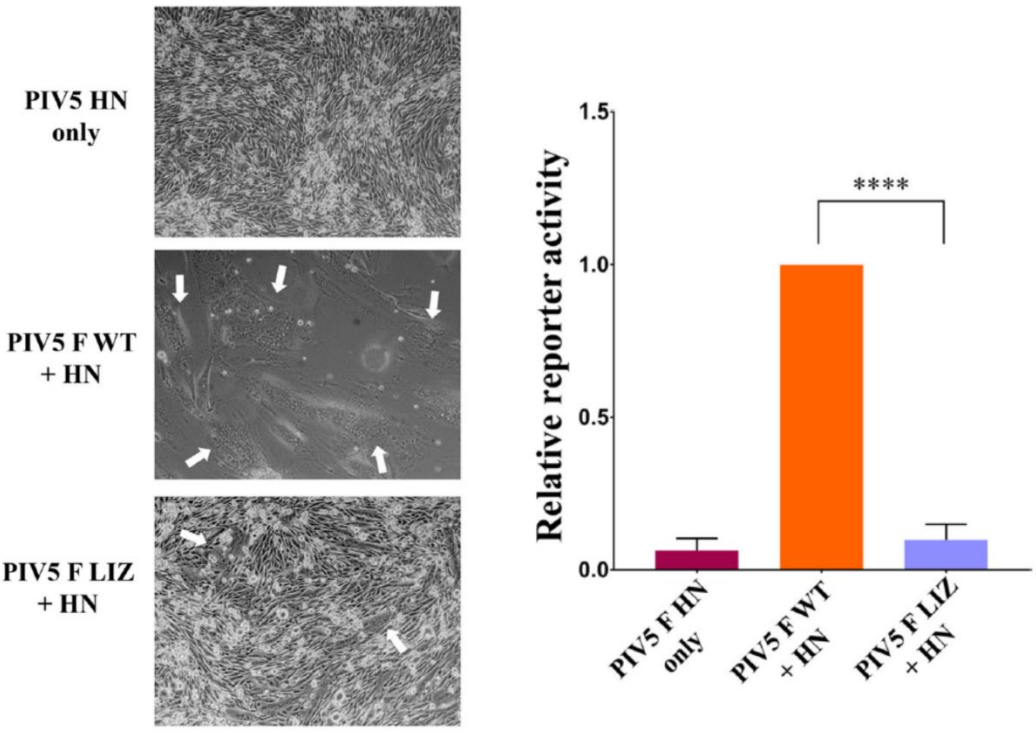

Figure 3.6. Mutations to the L/I zipper of PIV5 reduce F-mediated fusion activity.

(**Left**). Syncytia assay. BHK cells plated in six-well plates were transfected with 2.5 µg of total DNA with the PIV5 HN attachment protein alone, PIV5 WT F and HN or PIV5 LIZ F and HN. Syncytia formation was analyzed 24 h post-transfection. Images were taken with a Nikon TS100 microscope. White arrows indicate syncytia. Images are representative of two independent experiments, each carried out in triplicate. (**Right**). Luciferase reporter gene assay to quantify F fusogenic activity. Vero cells in 24-well plates were transfected with 1.0 µg total DNA with a T7 promoter plasmid and PIV5 F WT+HN or pIV5 F LIZ+HN. The following day, Vero cells were overlaid with BSR cells and incubated for 3 h to allow for luciferase production. Luciferase activity was measured using a luciferase assay system. The average represents three independent experiments, each performed in duplicate. Comparisons were performed using student's t-test, ****P<0.0001

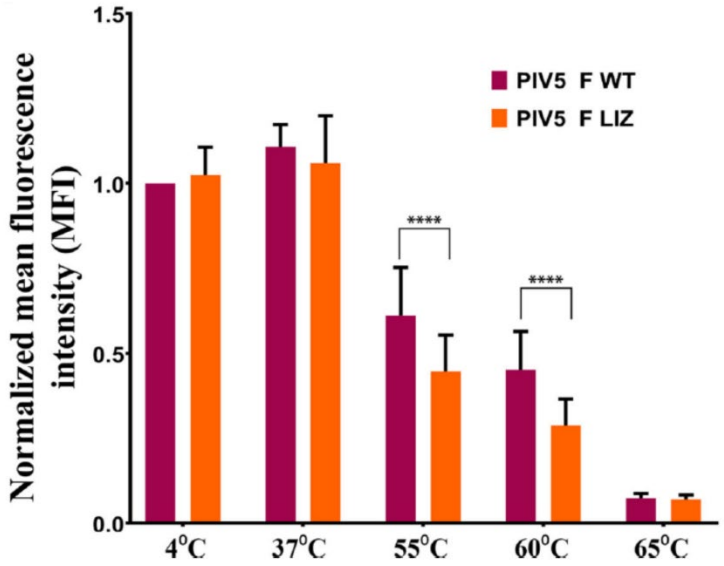

Figure 3.7. Thermal triggering assay to observe PIV5 F WT and LIZ prefusion thermostability.

Cells expressing surface PIV5 F or WT were exposed to 4, 37, 55, 60 or 65 °C for 15 min. Cells were immediately placed on ice for 15 min and prepared for flow cytometry using PIV5 mAb F1a. The average represents two independent experiments, each performed in triplicate. The LIZ mutant was compared to WT using a using Student's t-test. ****P<0.0001

Chapter 4 : ROLES OF HUMAN METAPNEUMOVIRUS MATRIX PROTEIN BEYOND ASSEMBLY

This work was performed in collaboration with Dr. David Stein and Dr. Hong Moulton (Oregon State University), who we consulted with for the design of PPMO. Drs Stein and Moulton also synthesized the arginine-rich peptide conjugated to the PPMO used in figure 4.5 – 4.9. In addition, Dr. Gaya Amarasinghe (Washington University in St. Louis) produced the IP/MS data shown in Table 1, and Dr. Cheng-Yu Wu (University of Kentucky) performed all qRT PCR experiments (Figure 4.8), as well as immunofluorescence in Figure 4.9 A and C.

Introduction

Human metapneumovirus (HMPV) is an enveloped virus that was reclassified in 2016 from the Paramyxovirdae family into the Pneumoviridae family [156]. It was discovered in 2001, although it is known to have been in circulation for several decades before its isolation—at least since 1958 [157]. Most people contract HMPV by the age of five, and reinfections are common throughout life [157, 158]. Clinically, HMPV manifests as flu-like symptoms in patients; however, for preterm infants, immunocompromised individuals and the elderly, HMPV inflicts more severe symptoms including asthma exacerbation, bronchiolitis and pneumonia, putting this category of patients at higher risk of mortality [157, 159-162]. For HMPV, there is currently no available FDA-approved therapeutic or vaccine, and much of its treatment involves supportive therapy [163]. It is therefore important to elucidate novel and effective therapeutic targets by understanding the molecular basis of HMPV infection.

The pneumovirus family contains two important human pathogens: HMPV and respiratory syncytial virus (RSV) [156]. The closely related viruses are highly heterogeneous in shape and size, with some particles bearing filamentous or asymmetric morphology, and others being spherical [157, 164-166]. HMPV viral particles feature host-derived membranes that are studded with multiple copies of the following surface glycoproteins: the attachment protein (G), which although is

necessary for attachment and entry for the closely related *Paramyxoviridae*, is dispensable in pneumoviral infection [57, 167]; the fusion protein (F), which undergoes large scale conformational changes to merge the viral and target membrane [168, 169]; and the small hydrophobic protein (SH), which is a proposed viroporin [169].

Upon entry and release of the HMPV viral genome into the host cell, discrete cytosolic pockets termed inclusion bodies (IBs) are formed [120]. HMPV IBs are membrane-less structures, and by analogy to similar viruses are thought to be formed through liquid-liquid phase separation (LLPS) [77, 80, 170, 171]. IBs are commonly formed among NNS RNA viruses and in most cases function as primary sites of efficient viral replication and transcription [76, 77, 120, 172-178]. Within IBs, there is a viral RNA-dependent RNA polymerase complex, which consists of the large protein (L) and the polymerase cofactor, phosphoprotein (P). The polymerase complex uses viral genomic (v)RNA encapsidated nucleoprotein (N) as a template for replication and transcription. The matrix 2-1 (M2-1) protein can also be associated with the polymerase and facilitates processivity, allowing for efficient transcription and translation in the IBs [179, 180].

Pneumo- and paramyxovirus vRNA is encapsidated by the nucleoprotein (N) and flanked by a *leader* (*le*) sequence at the 3' end, and a *trailer* (*tr*) region at the 5' end, with both *le* and *tr* being variable in length [32, 181]. In addition, individual genes are flanked by shorter (10-13 nt long) *gene start* (*gs*) and *gene end* (*ge*) sequences. For transcription to occur, the viral polymerase first associates with the *le* promoter sequence and scans the vRNA template for the first *gs* sequence. At the *gs*, the polymerase initiates transcription, with the *gs* playing a role in directing the capping of the RNA transcript. Transcription continues until the polymerase encounters the *ge,* where it creates a poly(A) tail and releases the nascent viral mRNA. The polymerase subsequently moves on to the next *ge* signal and transcribes each gene independently through this mechanism [32, 181-183]. The mRNA products are thought to be trafficked out of IBs into the cytosol, where they are translated into viral proteins [120, 184]. This

same encapsidated vRNA that is carried by the virus into cells is used to generate antisense genome RNA (+RNA), which is further used to generate nascent copies of vRNA. In this case, the polymerase interacts with the vRNA *le* region to start antigenome synthesis but ignores *ge* and *gs* signals to create a full antisense RNA, that in turn serves as a template for more vRNA production [32, 120, 182]. A recent report from our group showed that HMPV transcription and replication rates are increased between 6 hours post infection (h.p.i.) to 12 h.p.i. In fact, HMPV IBs coalesce in an actin-dependent manner during infection to boost the efficiency of replication and transcription [120].

Although the presence of the N and P proteins are the basic requirements for pneumovirus IB formation [174, 185], the matrix (M) proteins of RSV and the paramyxovirus NiV have been documented to be associated with inclusions [76, 95, 108]. NiV M was shown to colocalize with inclusion body species that are present at the plasma membrane later in infection [76], corroborating a longstanding observation that NNS RNA virus M proteins serve as adaptors between viral ribonucleoproteins (RNP)s and the plasma membrane [44, 166, 186, 187]. Indeed, for many non-segmented negative sense (NNS) RNA viruses, the matrix protein is thought to be a master regulator of viral infection. Viral matrix proteins are typically peripheral membrane proteins and for Newcastle disease virus (NDV), HMPV, RSV, and Ebola virus (EBOV), interact with the plasma membrane through electrostatic interactions: positively charged surfaces on the matrix proteins associate with the negatively charged inner leaflet of the plasma membrane [83, 188-190]. Underneath the plasma membrane, like I-BAR domain-containing proteins [191], M proteins polymerize to form a grid-like array and induce membrane curvature and allow for budding of nascent viral particles [44, 83, 186, 187, 189, 190, 192]. For some viruses such as EBOV, VP40 alone can form authentic virus-like particles [190]. In addition to RNPs, M is known to associate with the cytoplasmic tails of surface glycoproteins, thus M is not only important for budding but also for assembly of viral particles, particularly at late stages during infection [44, 108, 193].

Despite M having been well-established as a key player in late-stage infection, some of the function of M has proven to be enigmatic. Recent studies have shown that M may play roles in early infection: several NNS RNA matrix proteins traffic to the nucleus in early infection although NNS RNA viruses are mostly known to only involve cytosolic steps in their life cycle [95, 194-196]. Upon trafficking to the nucleus shortly after being synthesized, NiV M is ubiquitinated. This ubiquitination is not only important for nuclear exit, but also allows the matrix protein to associate with the plasma membrane upon nuclear export and facilitates its performance in assembly and budding [161]. Another unexpected feature of a pneumovirus matrix protein, HMPV M [83], is that to date, it is the only NNS RNA viral matrix protein that was co-crystalized with calcium. Although calcium is a potent signaling modulator [197], it is unclear what roles calcium binding confer to HMPV M.

In this study, we show that HMPV M is trafficked to the nucleus, and the timing of nuclear transit coincides with the previously examined height of HMPV replication and transcription [120]. Though extensive work has elucidated the mechanisms of nuclear entry and exit for some NNSV M proteins [194, 198, 199], there is a gap in our knowledge on the purpose of nuclear transit for the majority of these cases. Thus, our studies sought to bridge the gap by knocking down the matrix protein early in infection to address effects on early infection. We utilized antisense phosphorodiamidate Morpholino oligomers to selectively knock down HMPV M during infection to dissect the role of M during the course of infection. Preliminary data show that HMPV M is critical for establishing viral replication and transcription. Additionally, we address the role of calcium binding in HMPV M by examining expression and conformation of HMPV M with mutations in the calcium-coordinating residues. We find that in addition to the previously published role of calcium in thermostability of the protein [83], calcium is important in proper folding of the matrix protein.

Results

HMPV M travels in and out of the nucleus during the course of infection.

The bulk of the NNS RNA viral life cycle occurs within the cytosol. Outside of the *Bornaviridae* family, *Mononegavirales* do not require nuclear events for transcription, replication, and assembly. One of the key modulators of infection is the matrix protein, which interacts with viral and cellular proteins to play essential roles in late infection to assemble and bud virions from the host cell. Interestingly, several matrix proteins of NNS RNA viruses have been shown to associate with the nucleus and with nuclear factors [95, 194, 195, 198]. Table 4.1 shows an interactome generated from immunoprecipitation (IP) of HMPV M from transfected cells, followed mass spectrometry (MS) of host-associated proteins. Along with HMPV M transfection, cells were treated with polyinosinic:polycytidylic acid, poly (I:C), a synthetic double stranded RNA that potently mimics viral infection and induces Toll-like receptor 3 (TLR 3), MDA5, and RIG-I response [200, 201]. Among the list of interacting proteins with HMPV M is the GTP binding nucleoprotein Ran, a nuclear import factor [202] (Table 4.1). This IP/MS data supports an interaction of HMPV M with some nuclear factors, potentially consistent with HMPV M traverse to the nucleus. To follow up on the possibility of M being trafficked into the nucleus, we infected cells with wild type (WT) HMPV, at a multiplicity of infection (MOI) of 4, and fixed cells at indicated times for immunofluorescence (IF) analysis. Our data show that by 6 hours, there is evidence of matrix protein synthesis in punctate structures within the cell. By 10 hours post infection (h.p.i.), M is primarily present in the nucleus (Figure 4.1). As infection progresses from 12 h.p.i. through 30 h.p.i., the presence of M in infected cells shifts to favor a cytosolic distribution, with most of M associated in filamentous structures as infection progresses past 18 hours (Figure 4.1 D – F; I – L).

HMPV M moderately affects minigenome replication

Some NNS RNA virus matrix proteins are documented to affect viral replication and transcription. For example, in a minigenome assay, both EBOV matrix proteins (VP24 and VP40) were discovered to inhibit viral replication [109]. Previous work has shown that the highest rates of HMPV replication occur

between 6 – 12 h.p.i. [120], consistent with the hypothesis that nuclear localization of M may prevent replication inhibition, and in line with the timing of nuclear accumulation of M shown in Figure 4.1. From these observations, we hypothesized that HMPV M has a negative effect on viral replication and transcription, and is therefore sequestered away from the cytosol into the nucleus to allow viral replication to efficiently occur. To test this hypothesis, we employed a minigenome luciferase reporter gene system, kindly provided by Dr. Rachel Fearns, Boston University. BSR cells were transfected with the components required for efficient viral replication (HMPV N, P, L, and M2-1) in addition to a reporter gene plasmid containing a luciferase reporter cassette. We assessed the efficiency of reporter gene translation as a readout for the efficiency of viral transcription and replication in the context of increasing amounts of M. Our data show that at adding M to the reporter gene assay moderately affects reporter gene activity. It is noteworthy that upon addition of 2.0 µg of HMPV M to the minigenome system, we notice an inconsistency in the general trend of decreased minigenome activity in response to increasing amounts of M. It is possible that this data point is an experimental outlier. Further experimental repititions are necessary to determine if the change at this concentration of M is significant (Figure 4.2).

Given the moderate effect of M on the minigenome system, we were interested in examining the role of M the context of infection. To examine the hypothesis that HMPV M has effects on replication and transcription during the course of infection, we designed antisense peptide-linked phosphorodiamidate Morpholino oligomers (PPMOs) to knock down HMPV M protein levels (Figure 4.3 A). PMOs are nucleoside analogs that sterically inhibit protein synthesis [203]. Linking an arginine-rich sequence to the 5’ end of the PMO sequence allows for non-toxic, efficient delivery across cellular membranes [121]. PPMOs can be engineered to target the 5’untranslated region (UTR) and AUG start codon, thereby preventing the assembly of the small and large ribosomal subunits [123, 203] (Figure 4.3 C and D). Recently, PPMOs have shown to be potent, easy-to-use inhibitors of specific viral protein translation during infection [122, 170, 204].

To design a PPMO to specifically target HMPV M, we examined the 5'UTR of 44 disparate strains of HMPV (Figure 4.3; appendix i). We designed an antisense PPMO based on the conserved 13 nucleotide sequence of the 5'UTR combined with the first 12 nucleotides of the matrix protein nucleotide sequence, using CAN97-83 as our reference sequence, since it is the strain used in this study. This yielded a 25 nucleotide-long antisense PPMO for HMPV M knockdown. PPMO are incredibly specific, requiring only a five nucleotide mispairs for ablation of function [123, 205]. Our analysis shows that compared with 5'UTR regions of other viral proteins, there is not enough sequence identity for M PPMOs to have off-target effects (Figure 4.4) In addition to the M-specific PPMO, we designed a negative control scrambled PPMO, which is a nonsense PPMO with no known cellular or viral target.

PPMO cell toxicity and knockdown of M

To address the role of M early in infection, we initially examined the effect of the PPMO on cell viability with different concentrations of PPMO, up to ten times the required amount for inhibition, in 2-fold serial dilutions. Our results demonstrate that even at the highest amounts, there is no significant effect of the PPMO on cell viability (Figure 4.5). We next tested the efficiency of the PPMO to knockdown HMPV M during infection with a recombinant GFP-expressing (rg) HMPV. We found that without treatment, by 24 h.p.i, M had increased by approximately 5-fold compared to samples taken from our 6 h.p.i time point. However, when PPMO were added at 0 h.p.i, expression between 6 h.p.i and 24 h.p.i was maintained at similar levels, indicating that the PPMO was able to prevent significant translation of HMPV M (Figure 4.6 A and C).

We also addressed the effect of the M-specific PPMO on another viral protein, F. We found that surprisingly, despite lack of significant sequence similarity with the PPMO target, F synthesis was also dramatically reduced (Figure 4.6 B and D). These data suggest that knocking down M potentially affected the transcription of other viral proteins.

PPMO reduce rgHMPV titer, but not rgPIV5 or rgRSV

Based on our surprising result with HMPV F, we were interested in whether the PPMO potentially affected the establishment of infection in cells. We infected cells with rgHMPV at an MOI of 4, and then treated cells at 0, 4, and 6 h.p.i., with either the scrambled PPMO or the M-specific PPMO. At 24 h.p.i., we fixed and visualized cells, and also performed flow cytometry to quantify the number of cells that expressed GFP as a readout of the number of infected cells. Our results show that after addition of the M-PPMO at the indicated times post infection with analysis at 24 h.p.i., the number of infected cells is reduced, suggesting that M plays roles during early infection (Figure 4.7 A and D). Additionally, we wanted to address whether the effect the PPMO was specific to HMPV, so we performed the same analysis on two related viruses: RSV and the paramyxovirus, PIV5. There was no significant effect of the HMPV M-targeting PPMO on the number of infected cells present when in the case of either rgPIV5 or rgRSV, suggesting that M PPMO were specific to reducing HMPV infection (Figure 4.7 B, C, E, F).

PPMO knockdown of M shows a dramatic reduction of viral genomic and mRNA but shows no effect on cellular mRNA

Having established that the number of cells infected is reduced specifically for HMPV following PPMO treatment, we analyzed the effect of the PPMO on viral mRNA, and compared it to cellular mRNA following infection. Cells infected with HMPV at a MOI of 4 were treated with the scramble or M-specific PPMO at 0 h.p.i. At indicated times post infection, M-PPMO-treated and control cells were harvested, with RNA extracted for quantitative real time polymerase chain reaction (qRT-PCR) analysis. Our data show that for all time points, M-PPMO treatment resulted in a dramatic decrease for all viral mRNA (Figure 4.8 A-C). At 6 and 8 h.p.i., specifically, the decrease in viral mRNA occurred according to the gene order: PPMO treatment rendered N most affected, followed by P, M, F, M2-1, M2-2, SH, and G, with L being the least affected in the above order. As infection progressed, we observed by 12 h.p.i. that PPMO treated infected cells only produced approximately 10% of all viral mRNA, except for L which produced almost 50% viral mRNA compared to the control sample.

Notably, the longer infection progressed, the more dramatic the effect of M knockdown had on the efficiency of viral mRNA production. By 24 h.p.i., there was at least a 94% decrease in mRNA production per gene, contrasted with the 6-hour time point, where we observed up to a 75% decrease in mRNA production. Unlike with viral mRNA, host mRNA remained unchanged throughout the time course infection, indicating a specificity of the M PPMO knock-down in targeting viral mRNA production. Additionally, as a representative of viral genomic (v)RNA, we similarly tested the expression of P vRNA in response to PPMO during infection. Our results show that vRNA production was ablated in response to PPMO treatment (Figure 4.8 D), whereas the control cells continued to produce vRNA during infection as previously reported [120]. Taken together, these data suggest that the presence of M during infection has a significant impact on establishment of infection by positively affecting viral transcription and replication.

PPMO knockdown of M results in changes of inclusion localization during infection

IBs are sites of efficient viral replication and transcription. For HMPV, they coalesce in an actin-dependent manner during infection, a process which is postulated to increase viral genomic and mRNA production [120]. Moreover, several NNS RNA viral M proteins are known to interact with viral RNPs, priming them for assembly at the plasma membrane [44, 186]. Since our current data suggest that HMPV M informs early infection events, we sought to understand whether M affects replication and transcription by influencing inclusion body morphology and localization. To address this, we performed IF combined with fluorescence *in situ* hybridization (FISH), using probes specifically designed to detect the vRNA species in cells during a time course infection as previously designed [120]. Using two physiologically relevant cell types; human adenocarcinoma alveolar basal epithelial cells, A549 [206], and non-tumorigenic human bronchial epithelial cells BEAS-2B [207], we addressed the formation of inclusion bodies with and without M PPMO treatment (Figure 4.9). We observed that during time course of infection, as previously reported [120], HMPV IBs coalesce over time, forming larger perinuclear inclusions. By 18 h.p.i. in BEAS-2B

cells, the N protein, which is a critical component of viral ribonucleoproteins, forms filamentous structures (Figure 4.9 B), consistent with previous reports showing that M and N associate at the plasma membrane within cell-associate branched filaments and within budding filamentous viral particles [208, 209]. We also observed that by 24 h.p.i., N and vRNA were present in intercellular extensions, corroborating a previously observed result [208]. Conversely, for our time course data on M-PPMO treated cells, we were unable to identify N or vRNA in filamentous structures in both cell types. Moreover, IBs and vRNA appeared to be confined to the perinuclear region even at later time points (18 and 24 h.p.i.), suggesting a deficiency in trafficking to the plasma membrane. Together, these data indicate that HMPV M is an important mediator in trafficking vRNA to the plasma membrane. It still remains unclear whether blockade of vRNA movement to the plasma membrane as a result of M knockdown is linked to the reduction in transcription and replication, as reduced levels of other viral proteins could also influence vRNA trafficking.

Mutations to the calcium binding site of HMPV M effect protein conformation

Our studies of the matrix protein sought to understand how its unique features such as nuclear sojourn and calcium binding potentially effect HMPV infection. To this end, we also investigated the effect of mutating calcium coordinating residues. Leyrat et al. previously published a high-resolution crystal structure of HMPV M, which to date is the first NNS RNA matrix protein to have been co-crystalized with calcium. They identified residues E24, D26, L28, and K101 as directly forming a pentavalent interaction to secure calcium binding within the N-terminal region of each HMPV M monomer [83]. To examine the potential role of calcium binding for HMPV M, we made individual alanine substitutions to each calcium coordinating residue listed above, including E103, an adjacent residue to the calcium binding site. In addition, we created a quadruple mutant which featured all four calcium binding proteins mutated to alanine (Figure 4.10 A).

Our initial interest with these mutants was to investigate whether removal of calcium-coordinating residues potentially affected the localization of the matrix

protein when transfected into cells. Our results show that mutagenesis of the calcium binding site does not result in abberant localization; WT M and mutants were similarly distributed throughout the cell (Figure 4.10 B). To quantify the expression of mutants relative to WT, we expressed plasmids containing WT M or each mutant listed in Figure 4.11 A in A549 cells, and performed Western blotting. Our results support our initial finding with IF that all the mutants are detectable, and none of the mutations in residues that are involved in the direct interaction with calcium significantly change expression profiles (Figure 4.11).

Using a thermal shift assay, Leyrat et al. demonstrated that removal of calcium resulted in a 25ºC shift in melting temperature, showing that the binding of calcium to HMPV M increases thermostability and potentially contributes to its structural rigidity [83]. We were interested in testing whether this calcium binding also affected the conformation of the matrix protein when expressed in a cellular environment. To address this question, we performed radioimmunoprecipitation studies on WT M along with its mutants using a polyclonal avian metapneumovirus C matrix antibody that cross-reacts with HMPV M. This polyclonal antibody works well for Western blotting, which requires antibody interactions with a denatured protein, supporting the idea that this polyclonal antibody can recognize sequence-specific epitopes. We contrasted this with radioimmunoprecipitation studies performed with the conformation specific anti-HMPV M monoclonal antibody JOJ, which is conformational specific, as shown by its lack of reaction in Western blotting applications. Our data show that mutants of E24A, D26A, L28A, K101A, and the 4A mutant, M no longer binds the conformational antibody, but maintain binding to the sequence-specific antibody (Figure 4.12). Interestingly, we noted that the L28A and 4A mutants produced higher molecular weight M species (Figure 4. 12), suggesting that L28 potentially plays a role in regulating M oligomerization. Additionally, the mutant E103A, which is proximal to the calcium binding site but not directly involved in calcium binding also was able to bind the sequence-specific antibody, providing evidence that the calcium coordinating residues in particular are responsible for the maintenance of the matrix protein structure at the calcium binding site.

Discussion

Traditionally, our understanding of NNS RNA matrix proteins have centered on their roles in the assembly, budding, and egress of viral particles—much of which occurs at during late stages of infection [44, 186]. NNS RNA viral M proteins are known to form a highly ordered layer underneath the plasma membrane, inducing membrane curvature and facilitating the budding of new viral particles [83, 191, 192]. However, more recent reports document characteristics of M that suggest roles in addition to its mediation of late-stage infection. For example, henipavirus matrix proteins are imported into the nucleus and then exported before they arrive at the plasma membrane for assembly. For HeV M, the positive charge at position 258 is critical for nuclear transit, and specifically, the K258 residue must be ubiquitinated before the protein can exit the nucleus and associate with membrane structures [96, 194]. Both of the HeV M mutations that prevented either nuclear entry or nuclear exit also failed to associate with the plasma membrane and prevented virus budding and egress [96]. Although the lack of cytosolic distribution of nuclear-accumulated M provides a straightforward explanation for the lack of membrane association, it is less clear why mutations that prevented the import of M into the nucleus also result in a similar deficiency in assembly, since M was readily available in the cytosol. The authors speculate that in addition to monoubiquitination, M must form important associations within the nucleus that enable subsequent membrane association to occur [96].

As previous studies show that several NNS RNA viral matrix traffic to the nucleus, and our IP/MS data suggested that HMPV M associates with Ran, a nuclear GTP factor, we probed whether HMPV M also demonstrated nuclear entry during infection. Our results show that between 6 and 12 h.p.i., HMPV M is mainly localized within the nucleus, and by 18 - 24 h.p.i., becomes associated in filamentous structures consistent intercellular extensions and budding filamentous virions [208]. Previous studies of HMPV, HeV, and NiV show that when transfected alone, HMPV and henipavirus M do not demonstrate the same degree of steady-state nuclear retention that we observed for infection [96, 210, 211], indicating that infectious conditions promote nuclear accumulation, especially early in infection.

Interestingly, we note that the nuclear entry of the HMPV matrix protein coincides with the timing of exponential HMPV replication and transcription that was previously reported [120]. Our minireplicon system showed that the presence of M had a moderate yet significant inhibitory effect on HMPV minigenome replication and transcription, and thus led us to hypothesize that one consequence of HMPV M sequesteration in the nucleus is to curtail inhibition of efficient replication and transcription of the viral genome. An extension of this hypothesis is that the timely export of M would then inhibit viral replication and transcription, to favor assembly at the plasma membrane.

Infection with recombinant Sendai virus (SeV) recombinant NiV, recombinant measles virus (MeV), and recombinant RSV, all lacking M, or SeV infection with siRNA knockdown targeted against M show severe deficits in assembly and budding, but no significant effects in replication and transcription in cases where they were assessed [212-216]. Interestingly, when mutants were created to block NiV M from exiting the nucleus, NiV M was also found to be present in perinuclear IBs. The presence of NiV M presumably occurred before nuclear import, and inclusion bodies formed in this manner were hypothesized to be aggresomes [217]. Moreover, RSV lacking M results in N retention in IBs, and prevention of viral filament maturation [216]. Although the effects of M during early infection of the paramyxovirus SeV suggest that M does not affect replication and transcription during infection [214], studies on RSV show changes to IBs in the absence of M [216] and direct quantitation of viral genome and mRNA in response to M depletion had not yet been investigated in pneumoviruses until this study. Our knockdown of M resulted in considerable decreases in viral transcription and replication. We found that along with M knockdown was an accumulation of N-containing inclusion bodies at the perinuclear region, similar to results obtained for RSV [216].

Based on the interaction of M with RNPs previously discussed, it was not surprising that knocking down M would reduce the placement of N and IBs at sites closer to the plasma membrane; however, our unexpected observation of a large

decrease in efficiency of viral replication and transcription after M knockdown suggests a potential link between inclusion body dynamics mediated by M and the efficiency of vRNA and viral mRNA production. Previously, our group has shown that IBs interact with actin during infection to coalesce and boost replication and transcription [120]. During infection, M localizes within branched filamentous structures, which are also populated with actin. Actin remodels cells for efficient viral transmission [208]. It is possible that HMPV M makes contact with both actin and vRNP during infection to mediate trafficking of vRNPs to the plasma membrane for assembly. In terms of how this potentially contributes to the efficiency of viral replication, the trafficking of vRNPs away from their sites of synthesis may prevent overaccumulation of vRNPs. Indeed, recent data has shown that NiV IBs can act as aggresome-like compartments [217]. If this also occurs for HMPV inclusions in the context of overaccumulation of viral proteins, lack of trafficking of N and vRNA from IBs could inflict deleterious effects on proper IB replication and transcription function.

We cannot rule out that HMPV M contributes to the regulation of replication and transcription while it is within the nucleus. HeV M, NiV M, NDV M, SeV M, MeV M, canine distemper virus (CDV) M, influenza A, and influenza B (IAV and IBV) polymerase proteins have been shown to interact with acidic leucine-rich nuclear phosphoprotein 32 family member B (ANP32B). [210, 218-221]. ANP32B is critical for host range determination of IAV and IBV [218, 220]. Interestingly, its interaction with henipavirus M drives an increase in steady-state nuclear accumulation of ANP32B. It has been proposed that henipaviral M associations with ANP32B may help with nucleocytoplasmic shuttling or with inhibiting host responses to favor viral infection [210]. Moreover, recently, ANP32B was found to regulate immune responses in mice [222]. Although not found to directly interact with bovine RSV M, ANP32B can indirectly interact with proteins through CRM1, an adaptor protein for CD48 mRNA transport, further implicating M in associations with immune response modulators [221, 223]. The CRM1 protein has been identified to mediate nuclear shuttling of RSV M [199]. With HMPV M being closely related to RSV M, it is possible that CRM1-mediated interactions with either CRM1/CD48 mRNA

and/or ANP32B and potential downstream effectors occur during infection. Follow-up studies with IP/MS of nuclear-isolated M, in addition with chromatin immunoprecipitations (ChIP), would be helpful in identifying unique nuclear interactors and would enhance our understanding of the roles of HMPV M. In addition, with M postulated to interact with cytoplasmic tails of surface glycoproteins [44, 186], although our data show that the fusion protein is decreased in response to M knockdown, further investigation into the proportion of surface-exposed M and F would contribute to our understanding of HMPV M in viral assembly.

Our data also show that although mutations to the calcium binding region of HMPV M do not affect cytosolic localization, there is a difference in folding (Figure 4.11), although it is not known whether this difference in folding is specific to the calcium binding portion of the protein only, or whether it affects the ultrastructure of the protein, as the recognition site for the antibody is currently unknown. Follow up studies involving crystallization of the mutants are necessary to validate lack of calcium interaction, as well as changes in conformation. These results build on the previous finding that HMPV calcium binding increases thermostability [83], suggesting that the conformational changes contribute to the decrease in thermostability as a result of a lack of calcium binding.

HMPV M makes contacts with the membrane using its concave surface and the calcium binding pocket sits at the convex surface [83]. Although I hypothesize that conformational changes conferred by calcium binding likely most affect the concave surface, given its proximity to the calcium binding site, it would be important to examine whether calcium binding affects membrane association by transmitting additional conformational changes either throughout the protein or facilitates changes in interactions with currently unidentified membrane proteins and/or lipids. Moreover, the residues in HMPV M which potentially engage in contact with actin and/or vRNP association for assembly occur are currently unknown. In addition, there is a gap in our knowledge of whether HMPV M, like EBOV VP40, binds RNA directly [224]. It may be that the because the calcium

binding site, a cationic site, facing away from the membrane towards the cytosol, would mediate interactions with negatively charged molecules such as RNA. Finally, the role of calcium binding in maintaining the structural integrity of nascent virions is worth investigating.

Taken together, our data supports a model where while in the cytosol, HMPV M associates with actin to recruit vRNPs from IBs to the membrane, and recruitment of vRNPs to the membrane plays a role in maintaining the homeostasis required for efficient vRNA and viral mRNA production. This effect of maintaining inclusion body homeostasis is particularly pronounced during mid-to-late stages of infection, when IBs coalesce in an actin-dependent manner, and reach maximal transcription and replication activities. This potentially works synergistically with nuclear HMPV M, which could interact with (a) nuclear factor(s) to mediate cellular responses that are otherwise detrimental for viral infection. In addition, calcium binding of HMPV M facilitates necessary conformation of M to mediate its multitude of functions.

Table 4.1 List of host cell proteins associated with the HMPV matrix protein.

Reference	Gene Symbol	Protein	Spectral Count
sp|P23396|RS3_HUMAN	RPS3	40S ribosomal protein S3	17.1
sp|P42704|LPPRC_HUMAN	LRPPRC	Leucine-rich PPR motif-containing protein, mitochondrial	5.2
sp|P62070|RRAS2_HUMAN	RRAS2	Ras-related protein R-Ras2	4.7
sp|O95831|AIFM1_HUMAN	AIFM1	Apoptosis-inducing factor 1, mitochondrial	4.5
sp|P07437|TBB5_HUMAN	TUBB	Tubulin beta chain	4.2
sp|P68366|TBA4A_HUMAN	TUBA4A	Tubulin alpha-4A chain	4.1
sp|P10301|RRAS_HUMAN	RRAS	Ras-related protein R-Ras	3.3
sp|Q8NHP6|MSPD2_HUMAN	MOSPD2	Motile sperm domain-containing protein 2	2.9
sp|P62269|RS18_HUMAN	RPS18	40S ribosomal protein S18	2.8
sp|P62829|RL23_HUMAN	RPL23	60S ribosomal protein L23	1.8
sp|P62263|RS14_HUMAN	RPS14	40S ribosomal protein S14	1.7
sp|P35244|RFA3_HUMAN	RPA3	Replication protein A 14 kDa subunit	1.6
sp|P23284|PPIB_HUMAN	PPIB	Peptidyl-prolyl cis-trans isomerase B	1.3
sp|P42677|RS27_HUMAN	RPS27	40S ribosomal protein S27	1.1
sp|Q96CJ1|EAF2_HUMAN	EAF2	ELL-associated factor 2	1
sp|P12236|ADT3_HUMAN	SLC25A6	ADP/ATP translocase 3	1
sp|P78347|GTF2I_HUMAN	GTF2I	General transcription factor II-I	1
sp|Q13509|TBB3_HUMAN	TUBB3	Tubulin beta-3 chain	1
sp|Q15165|PON2_HUMAN	PON2	Serum paraoxonase/arylesterase 2	1
sp|P62826|RAN_HUMAN	**RAN**	**GTP-binding nuclear protein Ran**	1
sp|Q00325|MPCP_HUMAN	SLC25A3	Phosphate carrier protein, mitochondrial	1
sp|O14983|AT2A1_HUMAN	ATP2A1	Sarcoplasmic/endoplasmic reticulum calcium ATPase 1	1
sp|P07900|HS90A_HUMAN	HSP90AA1	Heat shock protein HSP 90-alpha	1
sp|P62249|RS16_HUMAN	RPS16	40S ribosomal protein S16	1
sp|P15559|NQO1_HUMAN	NQO1	NAD(P)H dehydrogenase [quinone]c 1	1
sp|P51114|FXR1_HUMAN	FXR1	Fragile X mental retardation syndrome-related protein 1	1
sp|P62820|RAB1A_HUMAN	RAB1A	Ras-related protein Rab-1A	1
sp|P46781|RS9_HUMAN	RPS9	40S ribosomal protein S9	1
sp|Q8TF66|LRC15_HUMAN	LRRC15	Leucine-rich repeat-containing protein 15	1
sp|Q58FF8|H90B2_HUMAN	HSP90AB2P	Putative heat shock protein HSP 90-beta 2	1
sp|P29966|MARCS_HUMAN	MARCKS	Myristoylated alanine-rich C-kinase substrate	1
sp|P68363|TBA1B_HUMAN	TUBA1B	Tubulin alpha-1B chain	1
sp|P62834|RAP1A_HUMAN	RAP1A	Ras-related protein Rap-1A	1

Cells were transfected with HMPV M and subjected to poly(I:C) treatment to mimic viral infection. Interactome includes Ran, a GTP-binding nuclear protein that is

associated with nucleocytoplasmic transport. **This data was generated by Dr. Gaya Amarasinghe (Washington University in St. Louis).**

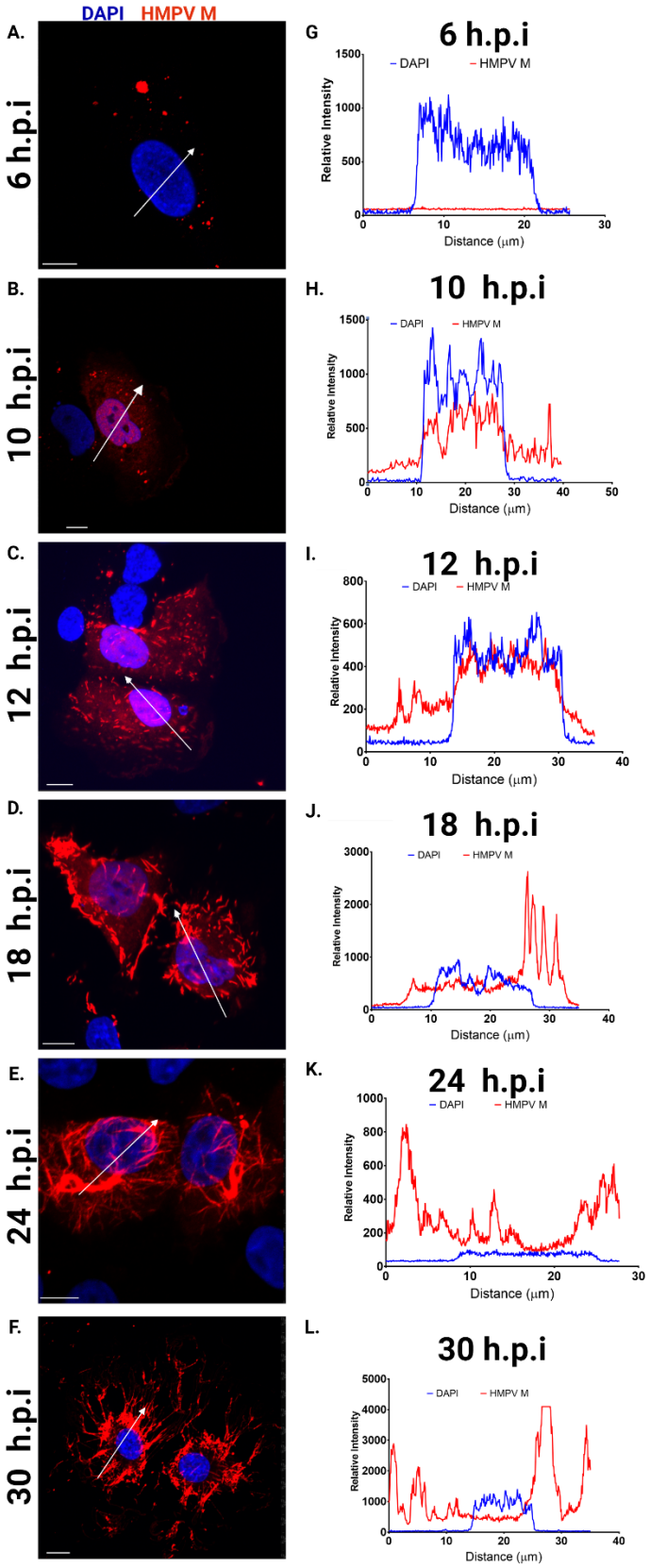
DAPI HMPV M
A.
6 h.p.i
B.
10 h.p.i
C.
12 h.p.i
D.
18 h.p.i
E.
24 h.p.i
F.
30 h.p.i
G
6 h.p.i
H.
10 h.p.i
I.
12 h.p.i
J.
18 h.p.i
K.
24 h.p.i
L.
30 h.p.i
DAPI
HMPV M
Relative Intensity
Distance (μm)

Figure 4.1. Localization of human metapneumovirus matrix protein (HMPV M) during infection.

BEAS-2B cells were infected with HMPV at multiplicity of infection (MOI) of 4. Cells were fixed at 6, 10, 12, 18, 24, and 30 hours post infection (h.p.i) for immunofluorescence with the monoclonal anti-HMPV antibody JOJ x (**A-F**). Colocalization profiles of DAPI, representing nuclei, and HMPV M (red; **G-L**). Images were taken with a Nikon A1 confocal microscope. Images are representative of at least 10 images taken for each condition. Scale bars represent 10μm.

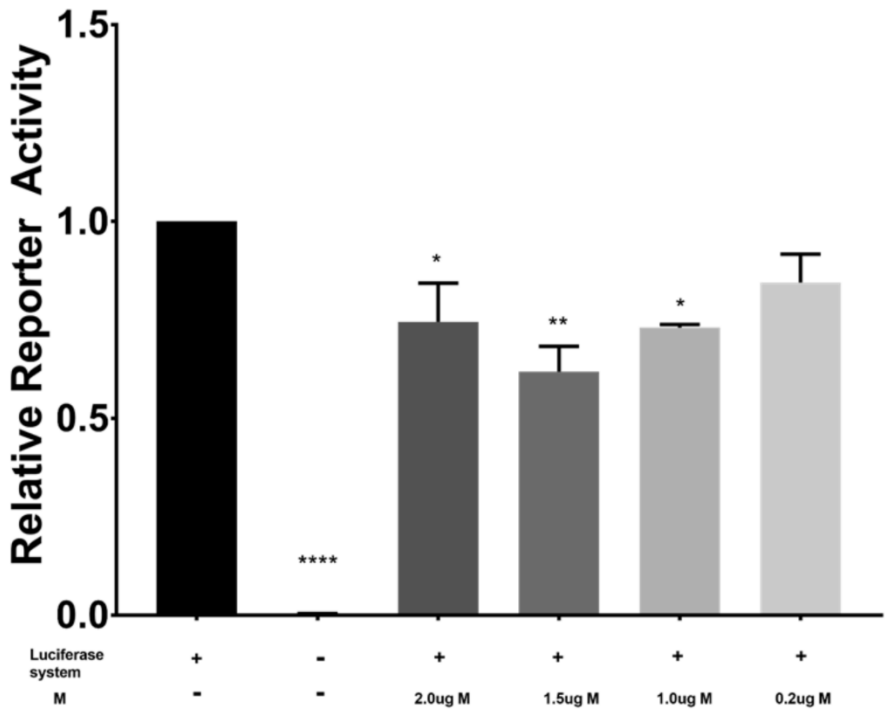

Figure 4.2. ***HMPV Matrix protein effect on minigenome activity.***

BSR cells constitutively expressing T7 polymerase were transfected with HMPV N, P, L, M2-1, and a luciferase-encoding minigenome. Altogether, these components termed here as the luciferase minigenome system. In the context of varying HMPV matrix (M) concentration (0.2 - 2μg), the minigenome reporter activity was examined. Experiment was performed in triplicate. n=1. Two-way ANOVA was performed to assess significance. *p<0.05, **p<0.005, ****p<0.0001

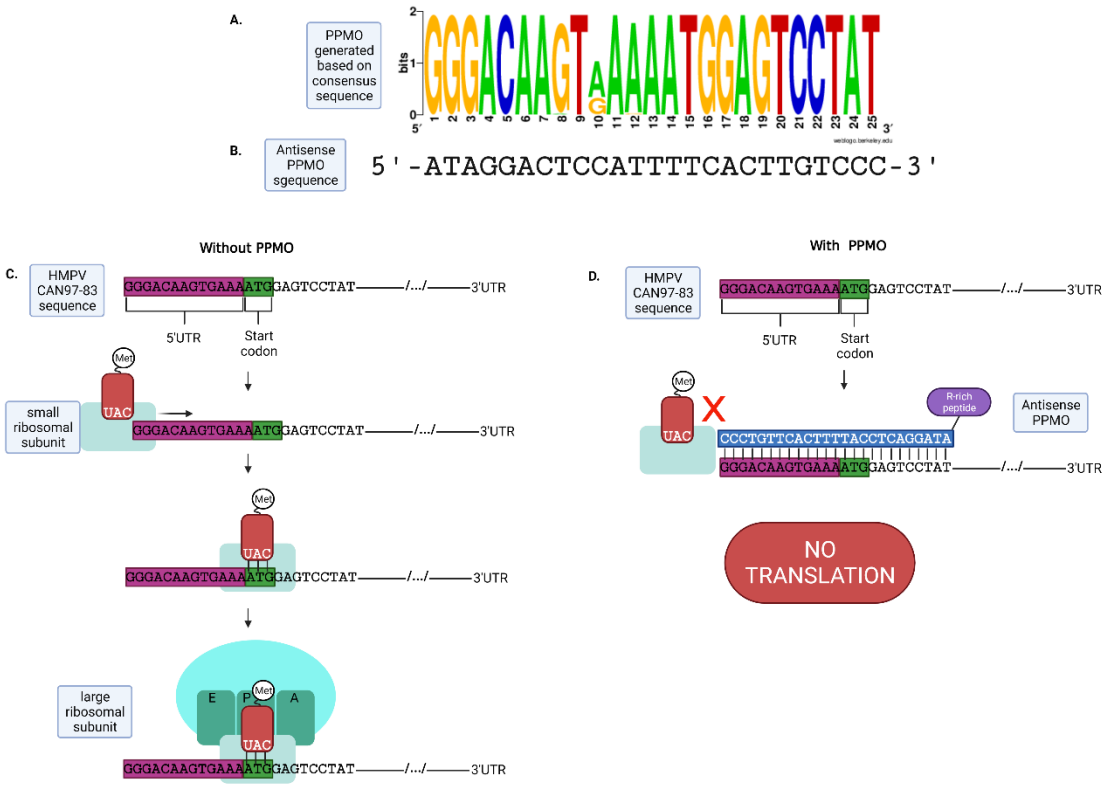

Figure 4.3. Peptide-linked phosphorodiamidate Morpholino oligomer (PPMO) mechanism of action.

A. Consensus sequence generated based on cDNA of first 25 nucleotides (13 nucleotides comprising of the 5'untranslated region, and the first 12 nucleotides of HMPV coding region) based 44 disparate HMPV strains. Accession numbers and individual sequences included in appendix. **B.** Antisense PPMO generated based on consensus sequence, with particular emphasis on HMPV M strain CAN97-83 (GenBank accession number AY297749.1). **C**. Simplified mechanism of viral translation initiation by cellular ribosomal machinery in absence of PPMO. Small ribosomal subunit containing t-RNA scans 5' untranslated region (UTR) for start codon. After initiation, elongation occurs, allowing for the translation of mRNA into viral proteins. **D.** PPMO hybridize to 5'UTR of HMPV M, sterically blocking access of small ribosomal subunit from the start codon. Translation is not initiated, and M protein is knocked down.

A.

```
Scrambled      --TATAAATTGTAACTGAGGTAAGAGG      25
L              gagacaaatagcaatggatcctctt--      25
SH             gggataagtgacaatgataacatta--      25
M2-2           gcaggcgctgacaatgactcttcat--      25
G              gggacaagtagttatggaggtgaaa--      25
M              gggacaagtgaaaatggagtcctat--      25
P              gggacaagtcaaaatgtcattccct--      25
M2-1           gggacaaatcataatgtctcgcaag--      25
N              gggacaagtgaaaatgtctcttcaa--      25
F              gggacaaataaaaatgtcttggaaa--      25
                        *    *
```

B.

```
L          gagacaaatagcaatggatcctctt     25
SH         gggataagtgacaatgataacatta     25
M2-2       gcaggcgctgacaatgactcttcat     25
G          gggacaagtagttatggaggtgaaa     25
M          gggacaagtgaaaatggagtcctat     25
P          gggacaagtcaaaatgtcattccct     25
M2-1       gggacaaatcataatgtctcgcaag     25
N          gggacaagtgaaaatgtctcttcaa     25
F          gggacaaataaaaatgtcttggaaa     25
           *        *    ***
```

C.

```
 1: Scrambled   100.00   43.48   39.13   17.39   60.87   39.13   30.43   39.13   34.78   39.13
 2: L            43.48  100.00   52.00   48.00   56.00   60.00   52.00   56.00   60.00   56.00
 3: SH           39.13   52.00  100.00   40.00   48.00   64.00   56.00   48.00   60.00   52.00
 4: M2-2         17.39   48.00   40.00  100.00   28.00   40.00   44.00   44.00   60.00   40.00
 5: G            60.87   56.00   48.00   28.00  100.00   64.00   52.00   56.00   60.00   64.00
 6: M            39.13   60.00   64.00   40.00   64.00  100.00   72.00   60.00   68.00   64.00
 7: P            30.43   52.00   56.00   44.00   52.00   72.00  100.00   68.00   76.00   68.00
 8: M2-1         39.13   56.00   48.00   44.00   56.00   60.00   68.00  100.00   72.00   80.00
 9: N            34.78   60.00   60.00   60.00   60.00   68.00   76.00   72.00  100.00   76.00
10: F            39.13   56.00   52.00   40.00   64.00   64.00   68.00   80.00   76.00  100.00
```

Figure 4.4. Sequence alignments of designed PPMO on 5'untranslated regions of HMPV genes.

A. Sequence alignment of scrambled (nonsense PPMO with no known cellular or viral targets) antisense PPMO target sequence against viral genes. **B**. Sequence alignment of antisense PPMO target (M) against 5'untranslated regions of other viral genes. **C**. Percent identity matrix of Scrambled and M-specific gene targets. All analyses were performed using ClustalW2

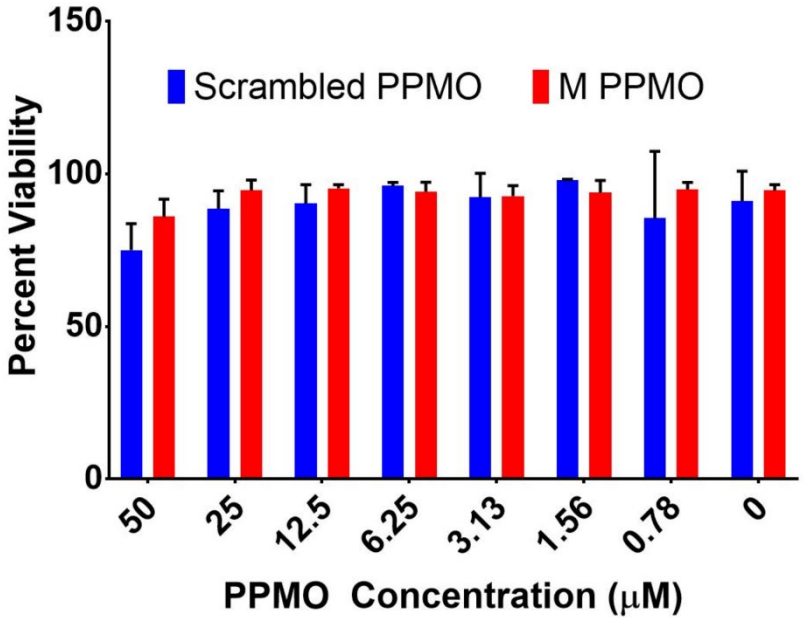

Figure 4.5. Cell viability after exposure to varying concentrations of the PPMO.

Results of a flow cytometry experiment on A549 cells treated with indicated concentrations of scrambled PPMO (blue) or M-specific PPMO (red). Cell viability was assessed with propidium iodide. The experiment was carried out in duplicate. n=1.

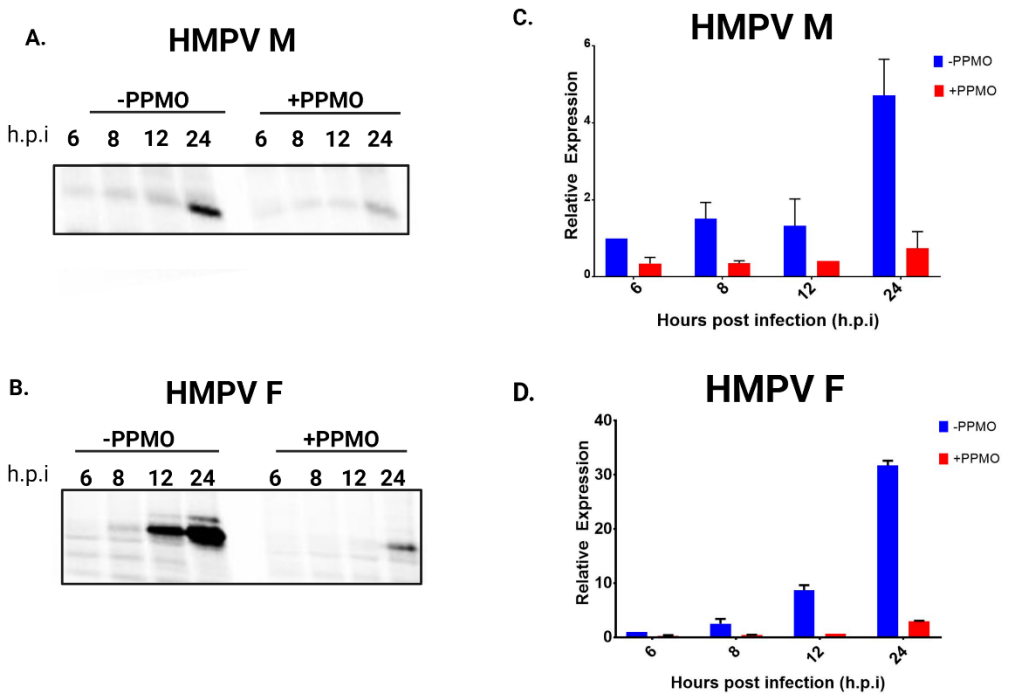

Figure 4.6. Expression of HMPV viral proteins after PPMO treatment.

A. A549 cells were treated with either 5 μM of scrambled PPMO (-PPMO), or 5 μM of M-specific PPMO (+PPMO). PPMO were added at 0 h.p.i. Radioimmunoprecipitation of cell lysate collected at indicated times show matrix protein (F) expression during infection with and without M-specific PPMO treatment. **B**. A549 cells treated with or without M-specific PPMO were assessed for fusion protein (F) expression in time course. **C** and **D**, quantitation of A and B. The experiments were carried out in duplicate. n=2

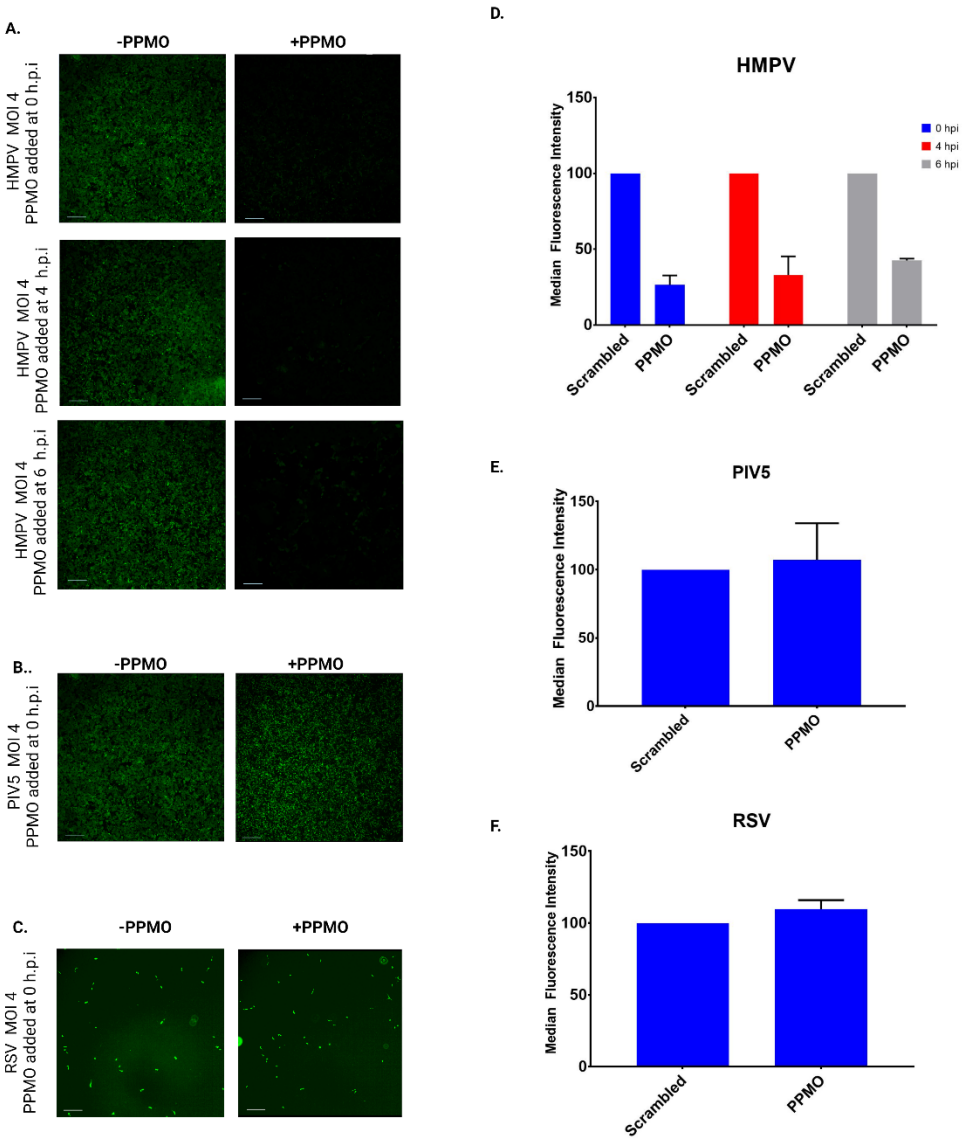

Figure 4.7. Effect of HMPV M-targeting PPMO on HMPV, PIV5, and RSV.

A549 cells were infected with either rgHMPV, rgPIV5, or rgRSV at a multiplicity of infection (MOI) of 4. Cells were either treated with 5 μM of scrambled PPMO (-PPMO) or 5 μM of HMPV M-targeting PPMO (+PPMO) at indicated times post infection. Cells were visualized at 24 hours post infection (h.p.i.) (**A-C**) Images were acquired with a Zeiss Axiovert 100 microscope. Scale bars represent 50 μm. Images are representative. **D-F** flow cytometry to quantify infection of cells in A-C. A-C were carried out in duplicate, n=2. Flow cytometry was performed in duplicate; n=1.

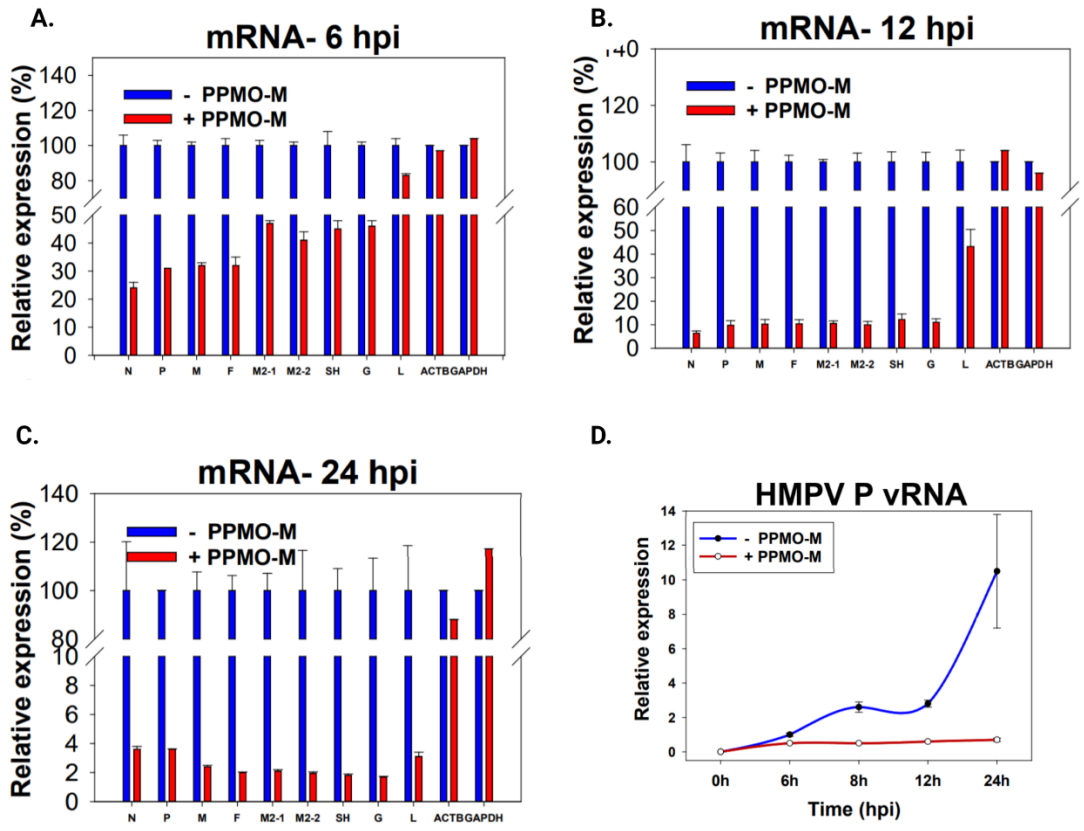

Figure 4.8. Quantitation of viral genomic (v)RNA and viral mRNA following M-targeting PPMO knockdown.

A-C. A549 cells were infected with WT HMPV at an MOI of 4. At 0 h.p.i, cells were treated with either 5 μM of scrambled PPMO (-PPMO-M) or 5 μM of M-targeting PPMO (+PPMO-M). RNA was isolated for quantitative RT PCR at indicated time points. In addition to viral mRNA, host cellular actin and GAPDH mRNA expression levels were also examined. **D**. Effect of PPMO treatment as performed in time course for A-C was also performed using primers against vRNA. The experiment was carried out in triplicate. n=1. **This experiment was performed by Dr. Cheng-yu Wu.**

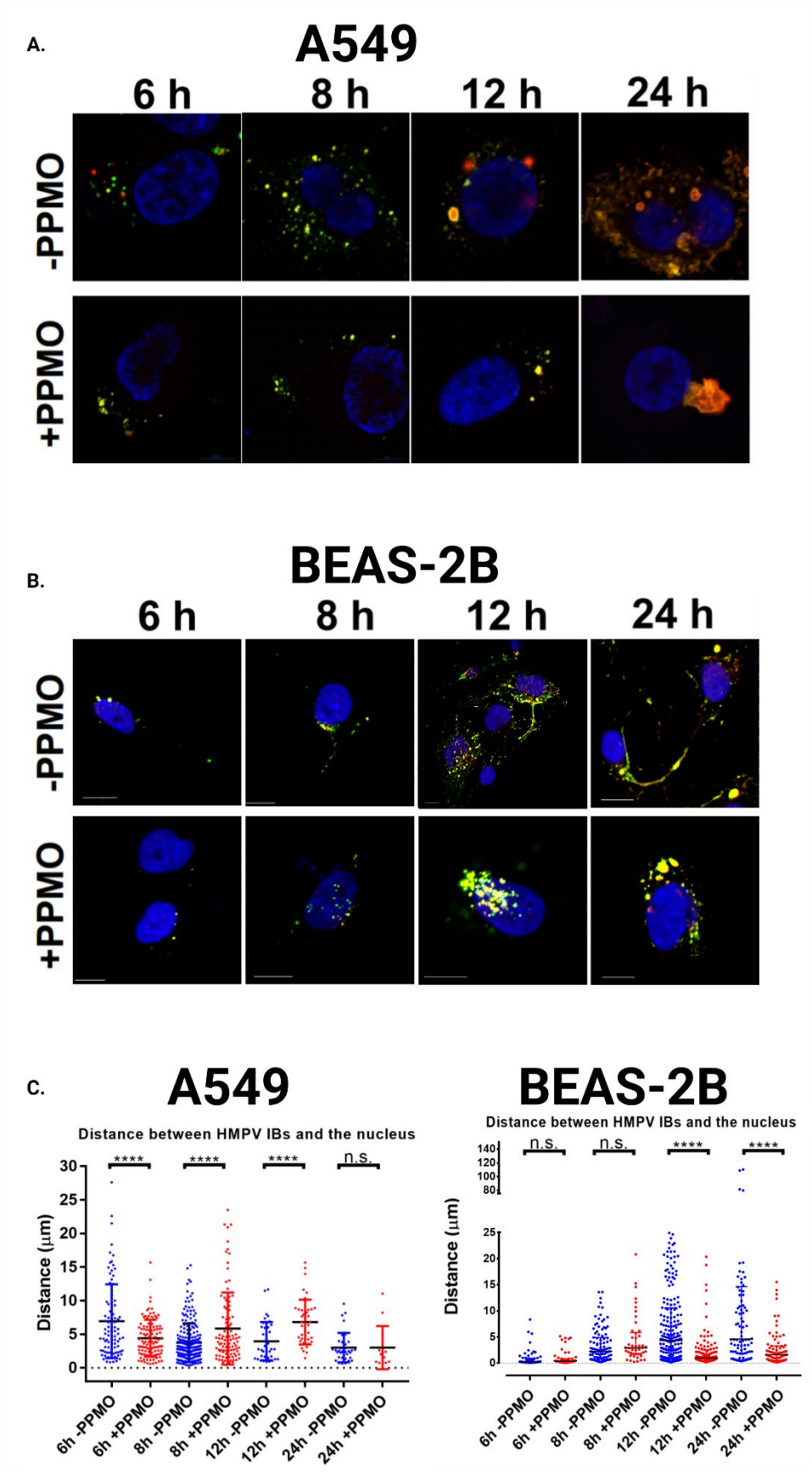
A.
A549
6 h
8 h
12 h
24 h
-PPMO
+PPMO
B.
BEAS-2B
6 h
8 h
12 h
24 h
-PPMO
+PPMO
C.
A549
Distance between HMPV IBs and the nucleus
Distance (μm)
****
****
****
n.s.
6h -PPMO
6h +PPMO
8h -PPMO
8h +PPMO
12h -PPMO
12h +PPMO
24h -PPMO
24h +PPMO
BEAS-2B
Distance between HMPV IBs and the nucleus
Distance (μm)
n.s.
n.s.
****
****
6h -PPMO
6h +PPMO
8h -PPMO
8h +PPMO
12h -PPMO
12h +PPMO
24h -PPMO
24h +PPMO

Figure 4.9. ***Effect of M-targeting PPMO on inclusion body localization*****.** A549 (**A**) and BEAS-2B cells (**B**) were infected with WT HMPV at an MOI of 4. At 0 h.p.i, cells were treated with either 5 μM of scrambled PPMO (-PPMO) or 5 μM of M-specific PPMO (+PPMO). Cells were fixed in 4% PFA at indicated times post infection and visualized using a Nikon A1 confocal microscope. Scale bars represent 10 μm. Images are representative. **C**. Quantitation of distance of IBs from nuclei in absence or presence of M-specific PPMO of at least 10 cells per condition. **Experiments and figure preparation of A and C were performed by Dr. Cheng-Yu Wu.**

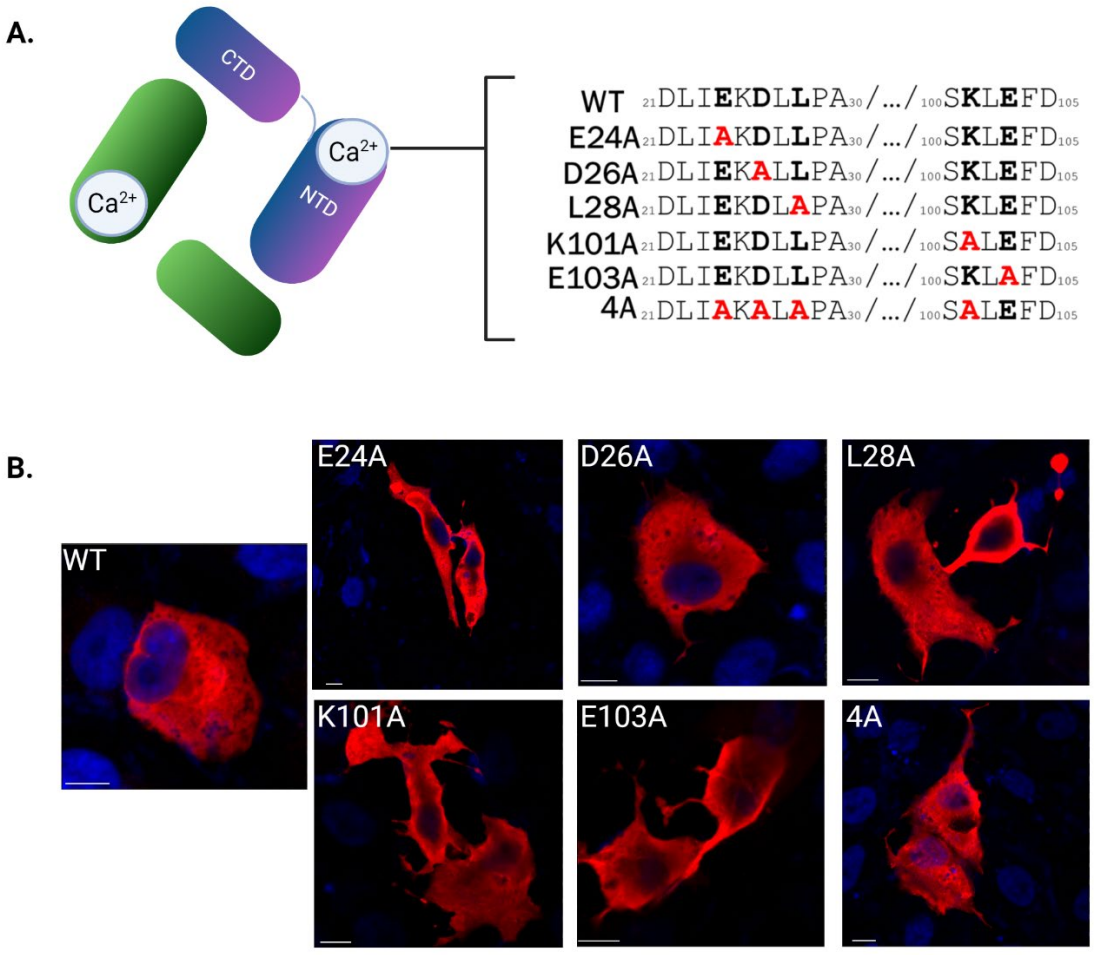

Figure 4.10. Effect of mutating calcium-coordinating residues on HMPV M localization.

A. Schematic of mutations performed to the calcium binding site of HMPV M. **B**. Immunofluorescence images taken with a Nikon A1 confocal microscope, showing localization of HMPV M mutant proteins compared to wild type (WT). Scale bars represent 10 μm. Images are representative. n=1

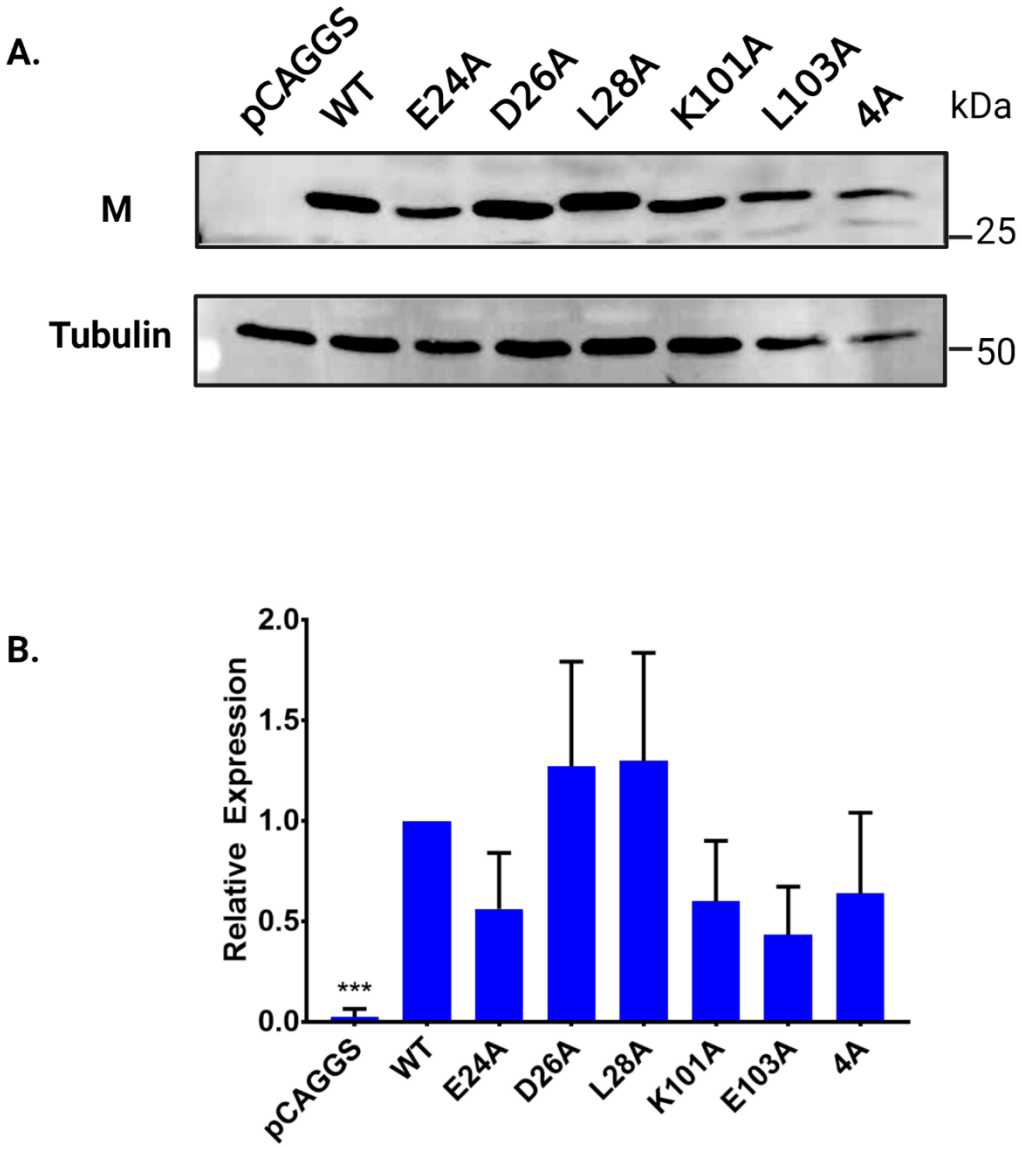

Figure 4.11. Effect of mutagenesis of calcium coordinating mutants on HMPV M expression.

A. Western blot from cell lysates of cells transfected with HMPV M. **B.** Quantitation of A with standardization to tubulin. n=2

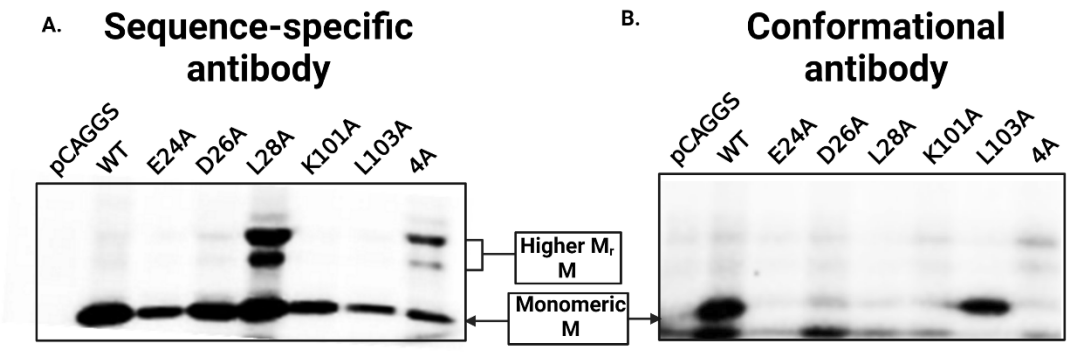

Figure 4.12. Radioimmunoprecipitation of HMPV M following mutagenesis to calcium binding site with conformational and sequence-specific antibodies.

A. Detection of immunoprecipitated WT HMPV matrix protein sequence-specific and **B**. conformation specific antibodies. Experiments were performed in triplicate. n=1.

Chapter 5 :DISCUSSION AND FUTURE DIRECTIONS

Overview

Generating effective preventative and treatment measures to battle viral infections requires a thorough understanding of the molecular details of viral infection. The work in this dissertation focuses on infectious mechanisms of non-segmented negative sense (NNS) RNA viruses with particular emphasis on the factors that govern the mechanisms of viral entry facilitation. In addition, this work addresses an unlikely key player in early infection, and how it may function in eventually generating viral progeny. Previous studies on paramyxo- and pneumoviruses that have focused on how viral fusion (F) and attachment proteins (G) start infection established the foundation for the first part of this dissertation work. These have provided a basis for our understanding that the F protein is triggered in a timely manner to mediate the merger of the viral and target cell membranes. The factors that contribute to the metastability of the F protein before it is triggered include a transmembrane domain (TMD) that trimerizes with the help of a leucine/isoleucine (L/I) zipper. For Hendra virus (HeV), the L/I zipper is critical for the proper expression of HeV F in its fusogenically active form. In Chapter 3, we address whether this observation is relevant within the paramyovirus family by studying the TMD L/I zipper in the context of another paramyxovirus, parainfluenza virus 5 (PIV5). We establish that the TMD L/I zipper does not affect the surface or total expression of PIV5 F, but it is key in its functionality. This thesis also includes the study of a pneumovirus, human metapneumovirus (HMPV), and the early events after entry. In Chapter 4, the effects of the viral matrix protein, traditionally thought to be solely a major drive of events associated with late infection, are discussed in the context of establishing infection. This work has identified potential additional roles of the matrix protein in promoting efficient viral replication and transcription. This work contributes to our understanding of NNS RNA viruses but also highlights unanswered questions that would contribute to understanding the molecular basis of infection for identification of new antiviral targets.

Transmembrane domain interactions facilitate functionality of paramyxovirus fusion proteins.

Enveloped viruses require carefully orchestrated events to merge their membranes with host cell membranes. Membrane mergers are processes that require repulsive “hydration forces” to be overcome in a kinetically costly process, as distinct membranes approach each other. Viral surface glycoproteins provide the basis through which membrane mergers occur between viruses and their target cells [225]. Paramyxoviruses and the closely related pneumoviruses typically engage attachment proteins for adsorption of viral particles to host cells. They also possess fusion proteins which undertake a major part of the membrane merging process by undergoing dramatic conformational changes down an energy gradient. Proper functionality of these surface glycoproteins serves as a critical jumping point of establishing viral infection [44, 134, 186].

Paramyo- and pneumoviral fusion proteins are classical class I fusion proteins: they fold into homotrimers within the endoplasmic reticulum, require a cleavage process to expose their fusion peptide before they become functionally active, and refold portions of their ectodomain into a six-helix bundle of α-helices. Importantly, these proteins are held in a metastable conformational state until the signal for triggering occurs [226]. Initial contacts during the fusion process involve fusion protein ectodomains, thus implicating them as important players in driving membrane merging [53, 143]. As such, the fusion peptides and heptad repeat regions have been heavily probed as therapeutic targets. The HIV drug Enfuvirtide, is a robust example of the outcome of such works. Enfuvirtide is an HR2-derived peptide that outcompetes HR2 to bind the HR1 of gp41, blocking progression of the fusion protein from its pre-hairpin intermediate to the six-helix bundle form [227]. In addition, peptides directed at the heptad repeats of henipaviruses, measles virus (MeV), and RSV have shown promise [228-230].

Given the complexity of the membrane fusion process, it is important that all domains of fusion proteins are well studied if effective targets are to be generated. While the external domains of fusion proteins have been historically examined, it was not until recently that these studies extended to their

transmembrane domains [231, 232]. Their hydrophobicity makes TMDs difficult to crystalize; however, development of potent biochemical assays has allowed the scientific community to piece together important features of fusion protein TMDs that affect functionality [231]. One of the most widely studied class I fusion proteins is influenza HA. Reports document that replacement of the HA TMD with a glycosylphosphatidylinositol (GPI) anchor resulted in loss of HA functionality in merging membranes. Specifically, the influenza HA-GPI chimeric protein was only able to partially drive membrane fusion, resulting in hemifusion, a process where the outer and not inner membrane leaflets fuse [233, 234]. These studies suggested a potential role of the length of the TMD, and its spanning across both leaflets as important in completion of membrane fusion. Indeed, when the TMD was truncated, influenza HA also formed a hemifusion intermediate [235]. Moreover, VSV G, which is a class III fusion protein also demonstrated a length requirement for proper fusogenic activity—truncation mutants similarly resulted in hemifusion intermediates [235]. In addition to length, recent work demonstrates that the dissociation of the trimeric TMDs of HeV F is required to facilitate fusion. Introduced disulfide bonds to the N-terminus of the TMD that locked the TMD in trimeric state resulted in loss of fusion activity, despite some of the mutants being expressed at surface levels sufficient for fusion [236]. Similarly, experiments were carried out with PIV5 F, where the membrane proximal external region (MPER) was locked together using introduced disulfide bonds. The data from this work also shows that dissociation of trimeric interactions is important for F fluidity and subsequent transitions from pre-to-post-fusion conformation [237].

In the VSV G example listed above where truncation resulted in loss of functionality, a single glycine residue reintroduced to the truncation mutant restored 80% functionality. This example is one of the studies that showed that the specific amino acids present in the TMD are critical for its function [238]. The potential importance of individual residues in the context of viral fusion protein TMDs therefore spurred follow up studies from several groups that identified specific amino acids within individual fusion proteins as playing a role. Using sedimentation equilibrium ultracentrifugation, our lab determined that in isolation,

the transmembrane domains of several class I and class II fusion proteins trimerize [41, 145]. The presence of an AXXG motif within the TMD of HeV F led to an investigation of whether this motif plays roles in trimerization and fusogenic activity of the full protein. This work showed that upon mutation of the AXXG glycine residue, G508 to alanine, leucine, or isoleucine, the surface expression and fusogenic activity were reduced. Interestingly, it was found that these mutations strengthened TMD-TMD interactions, thus pointing to a role of the G508 in maintaining protein expression and functionality [41]. The recent work on the locking of TMDs in trimers using disulfide bonds demonstrated that the mutant F proteins lost fusogenic activity, but where able to undergo at least initial triggering of conformational changes, as they lost binding to a pre-fusion specific antibody. [236]. Together, these studies indicate a requirement of flexibility in TMD trimeric interactions underline a very delicate balance in the triggering of fusion proteins.

The presence of a proteinaceous TMD is required for trimerization of the protein, with specific residues playing key roles. But what is the nature of residues that support the maintenance of the metastable pre-fusion structure such that it can still be triggered when signaled? On investigation of other potential interaction motifs within the TMD, a leucine/isoleucine (L/I) zipper in frame with the heptad repeat B L/I zipper was identified [66]. On further investigation, this L/I zipper or similar repeats of β-branched residues were identified in TMDs of 140 other paramyxo-and pneumovirus F proteins, suggesting a conserved importance across the viral families. Studies with HeV F identified the L/I zipper as critical in pre-fusion stability of the protein, as mutations to the L/I zipper resulted in misfolding and loss of functionality. In isolation, the TMD of HeV F was found to associate in trimers as determined by sedimentation equilibrium analytical ultracentrifugation (SE-AUC) [74].

In chapter 3, we addressed the L/I zipper of another paramyxovirus F protein, parainfluenza virus 5, a paramyxovirus model system. Previously, the L/I zipper of HeV F was found to be important for properly maintaining prefusion conformation. Surface biotinylation experiments elucidated a reduction surface

expression of the L/I zipper mutant, suggesting a role for the L/I zipper in proper folding and/or trafficking the fusion protein. Our initial experiments visualized the placement of HeV F, and found that as suspected, the decrease in HeV F surface expression was because it was retained in structures close to the nucleus consistent with the endoplasmic reticulum (ER). ER retention reflects a defect in folding, which can lead to degradation in the unfolded protein response pathway [239], thus explaining the decrease in overall protein expression for HeV F L/I zipper mutants. The previous analytical ultracentrifugation data, together with the surface biotinylation and immunofluorescence data, show that the TMD L/I zipper strongly impacts trimerization of the protein as it is being synthesized, and that disruptions of these TMD L/I zipper interactions causes adverse effects during the very early stages following synthesis. In Chapter 3 our paramyxovirus model conversely suggests that the L/I zipper is not critical for surface expression in PIV5, as IF and surface biotinylation data show only a modest decrease in surface expression following mutations to the L/I zipper. We also used a conformation-specific antibody to show that L/I zipper mutants were still stable in the prefusion form, and thermal triggering assays demonstrated a loss of prefusion conformation after exposure to heat, indicating that these mutants are capable of being triggered.

Despite the difference in effects of the TMD L/I zipper on surface expression between HeV F and PIV5 F, an interesting parallel exists for these proteins: the L/I zipper contributes to the functionality of the F protein. In Chapter 3, we showed using syncytial and reporter gene assays that, despite the presence of the mutants on the surface in pre-fusion form and despite the ability of these mutants to be triggered, TMD L/I zipper mutations rendered the protein non-functional. Our work corroborates a previous study that showed that one of the leucine residues present in the L/I zipper, L486, is an important driver of fusion. Further mutagenesis work in dissecting the individual roles of the other L/I residues within the zipper would enhance our understanding of the strength of these interactions in the context of functionality. It would be important to also examine PIV5 F L493, and PIV5 F L500 independently for surface expression, syncytial formation and fusogenic activity in

a reporter gene assay. Given that our triple mutant, L486A + L493A + L500A readily expresses its pre-fusion form on the surface of cells, I hypothesize that with each of these individual mutants, there would not be severe deficits in surface expression and should facilitate functional studies. Within the L/I zipper, the position at 507 is a valine residue. Mutating this residue to alanine, leucine or isoleucine in the context of the wild type protein would also be important to include in the study of how these residues affect protein functionality. Additionally, like the G508 example for HeV F [41], it would be important to perform single and combination mutagenesis on isolated TMDs of PIV5 F for TMD-TMD oligomeric analyses. These studies would be helpful in investigating the mechanisms through which L/I zippers contribute to functionality through the lens of TMD associations.

Although our study identified that fusion is blocked when the L/I zipper is mutated to alanine, we are limited in our knowledge of the stage of fusion that is affected. Weakened interactions of the TMD could result in prematurely triggered F; however, our results in Chapter 3 that show only a modest decrease in pre-fusion F at the surface of cells in response to L/I zipper mutations, refuting this idea. Moreover, Chapter 3 shows that F loses binding affinity to the pre-fusion conformational antibody upon triggering, suggesting that F is at least able to start the triggering process in absence of the L/I zipper. These observations beg the question of how fusion is then prevented in the TMD L/I zipper PIV5 mutants. Studies show that the TMD forms critical interactions with HN to secure the formation of the six-helix bundle. Further studies addressing whether a post-fusion F can be formed, whether a six-helix bundle can be formed, or alternatively studying the presence of pre-fusion intermediates in absence of the L/I zipper will assist in our understanding of the L/I zipper function.

Therapeutic targeting of paramyxo- and pneumovirus fusion transmembrane domains

As with the Enfuvirtide example of a designed peptide inhibiting fusogenic activity [227], our lab group recently generated an exogenous HeV TMD-based peptide. The rationale behind this approach is that an exogenous TMD peptide would outcompete and displace native TMD trimerization, resulting in the

premature triggering or misfolding of the full protein. When examined, co-expression of HeV F with the HeV F TMD-targeted peptide resulted in reduction in F protein expression and fusogenic activity. Co-expression of peptides designed against PIV5 F TMD did not inhibit HMPV infection, although significantly reduced PIV5 F infection, suggesting sequence specificity as a factor [146]. These promising data suggest that in addition to ectodomains, the TMDs of viral fusion proteins potentially present as potent drug targets.

The HMPV matrix protein in early infection

Once entry is successfully executed, enveloped viruses release their contents into host cells for propagation. As discussed in the introduction (Chapter 1), HMPV induces formation of inclusion body structures, where the bulk of replication and transcription events of viral genes occur. Once genes are translated, the viral proteins are assembled at the plasma membrane, during what is termed late-stage infection for budding and egress. The matrix protein has been postulated for many viruses to be the main organizer of assembly, budding and egress [44, 193]. Although HMPV M is not involved in the ESCRT pathway, there is a conserved YAGL motif that facilitates higher order oligomerization necessary for the formation of the grid-like array underneath the plasma membrane that enables viral assembly and budding [211]. Like the Ebola virus (EBOV) VP40 matrix protein, transiently expressed in 293-F cells, HMPV M has been reported to form virus-like particles (VLP)s [240].

Since its discovery in 2001, there have been a limited number of studies on functions of the HMPV matrix protein; however, closely related viral matrix protein functions may shed light on some of the unknown functions of HMPV M. Despite low sequence similarity among *Mononegavirales*, there is a high degree of structural similarity (Chapter 1), suggesting convergent evolutionary mechanisms in guiding function of the protein. One of the most extensively studied *Mononegavirales* matrix proteins is EBOV VP40. EBOV VP40 consists of two domains: the N-terminal domain (NTD), which is responsible for dimerization of the

protein, and the C-terminal domain (CTD), responsible for interactions that lead to and with the plasma membrane [190]. The HMPV matrix protein was also recently crystalized and similarly shown to have distinct CTD and NTD domains, forming dimers in solution; however, unlike with EBOV VP40, HMPV M has a dimerization interface that spans both the CTD and NTDs [83, 190].

Although heavily involved in the processes of assembly and budding, recent studies have implicated the viral matrix protein in earlier processes during infection. EBOV VP40 forms an octameric ring that has RNA-binding capabilities, and when transiently expressed in a reporter gene system, was found to have inhibitory effects on viral genomic and RNA synthesis [224]. In fact, several Mononegavirales matrix proteins have either reported associations with RNPs, or directly with RNA [44, 186], and in some cases inhibit viral replication and transcription [241-244]; a clue that the viral matrix proteins of these viruses play key roles at different infectious stages. In chapter 4, we found that like many other viral matrix proteins, HMPV M first marks its presence in the nucleus shortly after synthesis, before it traverses to viral filaments. As reviewed in Chapter 1, for NiV M, this nuclear transit is important for the membrane association and budding features of M [96, 194]. One important difference between EBOV VP40 and paramyxo- and pneumovirus matrix proteins is that VP40 contains a series of hydrophobic residues that deeply penetrate the plasma membrane from the cytosolic side [245]. The paramyxovirus Nipah virus (NiV) M provides evidence that at least one Mononegaviral M proteins traffics to the nucleus to gain access to a currently unknown factor, which may be a posttranslational modification, that allows for membrane association [194]. In addition, though HMPV M is known to interact with the viral membrane through its concave surface [83], there is currently no established posttranslational modification that facilitates the associations of HMPV M and the viral membrane contrary to what has been observed with EBOV VP40. Further studies into nuclear isolated M contrasted with cytosol-retained M may provide further evidence of the nuclear factors necessary for M functionality.

Similar to EBOV VP40 and MeV M [224, 244], our data in Chapter 4 provided evidence that in a minigenome system, HMPV M exerts inhibitory effects on vRNA replication and transcription. Surprisingly, in the context of a knockdown, there were severe deficits in the number of cells where infection had progressed enough for GFP expression, and with the expression of another viral protein, F. On further investigation, work in Chapter 4 established that HMPV M positively contributes to the synthesis of all viral mRNA products as well as to the efficiency in vRNA production, potentially leading to the observed decrease in HMPV F as a result of M knockdown. These studies establish a previously unidentified role in the process of infection of Mononegavirales: M is key in efficient transcription and translation of viral RNA. The use of a PPMO as a tool for knockdown is extremely specific [122, 204], and our analyses show no significant homology to the other genes to allow for cross-reaction of the PPMO with off-targets. However, out of an abundance of caution, we have designed a second unique PPMO to target HMPV M. Further studies will examine whether this second PPMO knockdown of M exerts the same universal effects in viral infection. In addition, extending these knockdown studies to RSV M would enhance our understanding of the roles pneumovirus matrix proteins play.

In Chapter 4, we also showed that IB dynamics are severely affected by M knockdown. When M is knocked down, the movement of IBs and vRNPs towards the plasma membrane was thwarted. IBs and IB-like structures have long been studied as critical components of viral replication and transcription, and recent work from our lab showed that this observation is consistent with HMPV M, with actin driving coalescence of IBs to promote transcription and replication [120]. A single-particle tracking study showed that EBOV VP40 traffics along actin towards the plasma membrane, with plasma membrane contacts serving as an important modulator of assembly and budding processes [246]. Interestingly, HMPV M has been shown to associate in branched filaments, and these branched filaments are at least in part formed through remodeling of actin during infection, suggesting a potential link between actin and HMPV M. RSV M, Sendai virus M and Newcastle disease M are also associated with actin, with actin playing positive roles in RNA

synthesis [247-249]. Further investigations with M and actin would be necessary to identify whether M acts in concert with actin to positively affect viral RNA production.

IBs are membrane-less structures and on recent analysis, were shown to be formed through liquid-liquid phase separation (LLPS), with P as an important driver of droplet formation. Recent work from our lab group is the first to identify that HMPV N and P proteins are able to form LLPS, with P as an important driver. In addition, P forms direct associations with RNA (Boggs, unpublished data). To carry out these *in vitro* phase separation assays, our group has developed protocols for the effective purification of HMPV viral proteins including HMPV M purification, which is currently being optimized. Future studies will focus on the effects of HMPV M on the formation of these LLPS structures. In addition, testing whether HMPV M, like HMPV P, can directly modulate RNA binding would enhance our understanding of the roles of HMPV M in viral replication and transcription.

Calcium binding in the functions of HMPV M

Leyrat et al. published in 2014 that HMPV M is a calcium binding protein. [83]. In Chapter 4, we investigated the role of calcium binding residues in the expression and folding of HMPV M. We found that single and combination alanine mutations to the HMPV M calcium-coordinating did not affect expression. However, we observed loss of conformational antibody binding with alanine mutants of residues that directly coordinate calcium binding. These studies suggest that HMPV M calcium binding is essential for proper folding of the protein; however, our studies are limited as we have not directly shown that these mutations result in lack of calcium binding. Further studies using purified M or M mutants could be utilized to verify loss of calcium binding, including and crystallization of HMPV M mutants would verify whether the changes we observed result from lack of calcium binding.

Additionally, it would be important to determine the effects of calcium binding in the context of infection. To examine this, I propose the creation of a

recombinant virus with M mutants. Since M is heavily involved in budding and assembly of nascent viral particles, the potential challenge to overcome lies in whether improperly folded M would yield enough viral titer for subsequent experiments. In the situation that the recombinant HMPV M cannot be rescued, I propose transcomplementation of HMPV M either using transient transfection of plasmid-encoded wild type M, or with a stable cell line that expresses wild type M for the recombinant calcium-binding-mutant HMPV M viral growth. A similar strategy was employed for the closely related RSV virus, where M was completely removed from the genome [216]. Using these recombinant viruses, the effect of the mutations to the calcium binding residues on nuclear localization, membrane association, replication, transcription, and inclusion body dynamics could be studied. In addition, immunoprecipitation coupled with mass spectrometry of calcium-binding mutants compared to wild type could establish potential host interactions mediated through calcium binding.

Altogether, the work discussed in this dissertation contribute to our understanding of NNS RNA viral infection. Continuing research in the field, including the outlined future directions would serve to create a framework for identifying factors that in the long term may serve as effective therapeutic targets.

Appendix i

Sequences used in the design of M-specific PPMO

ACCESSION #	SEQUENCE	
MF104608.1	GGGACAAGTGAAAATGGAGTCCTAT	25
MK588635.1	GGGACAAGTGAAAATGGAGTCCTAT	25
KJ627433.1	GGGACAAGTGAAAATGGAGTCCTAT	25
KJ627407.1	GGGACAAGTGAAAATGGAGTCCTAT	25
KJ627427.1	GGGACAAGTGAAAATGGAGTCCTAT	25
KJ627425.1	GGGACAAGTGAAAATGGAGTCCTAT	25
KJ627394.1	GGGACAAGTGAAAATGGAGTCCTAT	25
KY474534.1	GGGACAAGTGAAAATGGAGTCCTAT	25
AB503857.1	GGGACAAGTGAAAATGGAGTCCTAT	25
KC403981.1	GGGACAAGTGAAAATGGAGTCCTAT	25
MH150889.1	GGGACAAGTGAAAATGGAGTCCTAT	25
KC403979.1	GGGACAAGTGAAAATGGAGTCCTAT	25
KF686742.1	GGGACAAGTGAAAATGGAGTCCTAT	25
AY297749.1	GGGACAAGTGAAAATGGAGTCCTAT	25
KY474537.1	GGGACAAGTAAGAATGGAGTCCTAT	25
GQ153651.1	GGGACAAGTAAAAATGGAGTCCTAT	25
MN745084.1	GGGACAAGTAAAAATGGAGTCCTAT	25
MK087726.1	GGGACAAGTAAAAATGGAGTCCTAT	25
MN745087.1	GGGACAAGTAAAAATGGAGTCCTAT	25
MK167039.1	GGGACAAGTAAAAATGGAGTCCTAT	25
KY474539.1	GGGACAAGTAAAAATGGAGTCCTAT	25
MF104609.1	GGGACAAGTAAAAATGGAGTCCTAT	25
MK167040.1	GGGACAAGTAAAAATGGAGTCCTAT	25
MN306028.1	GGGACAAGTAAAAATGGAGTCCTAT	25
MN745085.1	GGGACAAGTAAAAATGGAGTCCTAT	25
MF104602.1	GGGACAAGTAAAAATGGAGTCCTAT	25
MF104594.1	GGGACAAGTAAAAATGGAGTCCTAT	25
MF104610.1	GGGACAAGTAAAAATGGAGTCCTAT	25
KC562233.1	GGGACAAGTAAAAATGGAGTCCTAT	25
AY530090.1	GGGACAAGTAAAAATGGAGTCCTAT	25
AY530095.1	GGGACAAGTAAAAATGGAGTCCTAT	25
KC562221.1	GGGACAAGTAAAAATGGAGTCCTAT	25
KC562240.1	GGGACAAGTAAAAATGGAGTCCTAT	25
KJ627417.1	GGGACAAGTAAAAATGGAGTCCTAT	25
KJ627379.1	GGGACAAGTAAAAATGGAGTCCTAT	25
KJ627422.1	GGGACAAGTAAAAATGGAGTCCTAT	25
KJ627430.1	GGGACAAGTAAAAATGGAGTCCTAT	25
KJ627406.1	GGGACAAGTAAAAATGGAGTCCTAT	25
KC403978.1	GGGACAAGTAAAAATGGAGTCCTAT	25
KC403984.1	GGGACAAGTAAAAATGGAGTCCTAT	25
KC562243.1	GGGACAAGTAAAAATGGAGTCCTAT	25
MF104611.1	GGGACAAGTAAAAATGGAGTCCTAT	25
JN184400.1	GGGACAAGTAAAAATGGAGTCCTAT	25
DQ843659.1	GGGACAAATAAAAATGGAGTCCTAT	25
	******* * * *************	

Appendix ii

List of abbreviations

6HB	six-helix bundle
ANP32B	acidic leucine-rich nuclear phosphoprotein 32 family member B
BDV	Borna disease virus
CD	cluster of differentiation
CDV	canine distemper virus
ChIP	chromatin immunoprecipitation
CPE	cytopathic effects
CRM1	chromosomal maintenance 1 (exportin 1)
CT	cytoplasmic tail
CTD	C-terminal domain
EBOV	Ebola virus
ER	endoplasmic reticulum
F	fusion protein
FISH	fluorescence in situ hybridization
FP	fusion peptide
G/GP	glycoprotein
G/GP/H/HN	attachment protein
GPI	glycosylphosphatidylinositol
H/HA	hemagglutinin
HeV	Hendra virus
HMPV	human metapneumovirus
HN	hemagglutinin/neuraminidase
hpi	hours post infection
hPIV	human parainfluenza virus
HRA/B	heptad repeat A/B
IAV	influenza A virus
IB	inclusion body
IBV	influenza B virus
ICAM	intercellular adhesion molecule
IP	immunoprecipitation
JPV	J paramyxovirus
L	large protein
LIZ	leucine/isoleucine zipper
LLPS	liquid-liquid phase separation
M	matrix protein
M2-1	matrix 2-1 protein
MDA5	melanoma differentiation-associated protein 5
MeV	measles virus
MOI	multiplicity of infection
MPER	membrane proximal external region
MS	mass spectrometry
MuV	mumps virus

N/NP	nucleoprotein
NDV	Newcastle disease virus
NES	nuclear export signal
NiV	Nipah virus
NNS	non-segmented negative sense
NPC	nuclear pore complex
Npm	nucleophosmin
NS	non structural protein
NTD	N-terminal domain
P	phosphoprotein
PIV5	parainfluenza virus 5
poly (I:C)	polyinosinic:polycytidylic acid
PPMO	peptide-conjugated phosphorodiamidate Morpholino oligomer
PS	phosphatidylserine
RdRp	RNA dependent RNA polymerase
RIG-I	retinoic acid-inducible gene I
RNP	ribonucleoprotein
RSV	respiratory syncytial virus
RV	rabies virus
SE-AUC	sedimentation equilibrium analytical ultracentrifugation
SeV	Sendai virus
SH	small hydrophobic protein
SLAM	signalling lymphocyte-activation molecule
TGN	*trans* Golgi network
TLR 3	Toll-like receptor 3
TMD	transmembrane domain
TNF-α	tumor necrosis factor alpha
TRV	Tupaia rhabdovirus
UBF	upstream binding factor F
UTR	untranslated region
VLP	virus-like particle
VP24	viral protein 24
VP40	viral protein 40
vRNA	viral genomic RNA
VSV	vesicular stomatitis virus
WT	wild type

REFERENCES

1. Weyer, J., A. Grobbelaar, and L. Blumberg, *Ebola virus disease: history, epidemiology and outbreaks.* Curr Infect Dis Rep, 2015. **17**(5): p. 480.
2. Aguilar, H.C. and B. Lee, *Emerging paramyxoviruses: molecular mechanisms and antiviral strategies.* Expert Rev Mol Med, 2011. **13**: p. e6.
3. Singh, R., et al., *Rabies - epidemiology, pathogenesis, public health concerns and advances in diagnosis and control: a comprehensive review.* Vet Q, 2017. **37**(1): p. 212-251.
4. Cui, J. and L.F. Wang, *Genomic Mining Reveals Deep Evolutionary Relationships between Bornaviruses and Bats.* Viruses, 2015. **7**(11): p. 5792-800.
5. Crowe, J.E., Jr. and J.V. Williams, *Paramyxoviruses: Respiratory Syncytial Virus and Human Metapneumovirus.* Viral Infections of Humans: Epidemiology and Control, 2014: p. 601-627.
6. van Doorn, H.R. and H. Yu, *Viral Respiratory Infections.* Hunter's Tropical Medicine and Emerging Infectious Diseases, 2020: p. 284-288.
7. Esposito, S. and M.V. Mastrolia, *Metapneumovirus Infections and Respiratory Complications.* Semin Respir Crit Care Med, 2016. **37**(4): p. 512-21.
8. Reiche, J., et al., *Human metapneumovirus: insights from a ten-year molecular and epidemiological analysis in Germany.* PLoS One, 2014. **9**(2): p. e88342.
9. Schildgen, V., et al., *Human Metapneumovirus: lessons learned over the first decade.* Clin Microbiol Rev, 2011. **24**(4): p. 734-54.
10. Couch, R.B., J.A. Englund, and E. Whimbey, *Respiratory viral infections in immunocompetent and immunocompromised persons.* Am J Med, 1997. **102**(3a): p. 2-9; discussion 25-6.
11. Han, L.L., J.P. Alexander, and L.J. Anderson, *Respiratory syncytial virus pneumonia among the elderly: an assessment of disease burden.* J Infect Dis, 1999. **179**(1): p. 25-30.
12. Aggarwal, M. and R.K. Plemper, *Structural Insight into Paramyxovirus and Pneumovirus Entry Inhibition.* Viruses, 2020. **12**(3): p. 342.
13. Branttie, J.M. and R.E. Dutch, *Parainfluenza virus 5 fusion protein maintains pre-fusion stability but not fusogenic activity following mutation of a transmembrane leucine/isoleucine domain.* J Gen Virol, 2020. **101**(5): p. 467-472.
14. Abdella, R., et al., *Structure of a paramyxovirus polymerase complex reveals a unique methyltransferase-CTD conformation.* Proc Natl Acad Sci U S A, 2020. **117**(9): p. 4931-4941.
15. Ertl, H.C.J., *New Rabies Vaccines for Use in Humans.* Vaccines, 2019. **7**(2): p. 54.
16. La Torre, G., et al., *The effectiveness of measles-mumps-rubella (MMR) vaccination in the prevention of pediatric hospitalizations for targeted and untargeted infections: A retrospective cohort study.* Human vaccines & immunotherapeutics, 2017. **13**(8): p. 1879-1883.
17. Hayman, D.T.S., *Measles vaccination in an increasingly immunized and developed world.* Human vaccines & immunotherapeutics, 2019. **15**(1): p. 28-33.
18. Kitanovski, L., et al., *Treatment of severe human metapneumovirus (hMPV) pneumonia in an immunocompromised child with oral ribavirin and IVIG.* J Pediatr Hematol Oncol, 2013. **35**(7): p. e311-3.
19. Eiland, L.S., *Respiratory syncytial virus: diagnosis, treatment and prevention.* The journal of pediatric pharmacology and therapeutics : JPPT : the official journal of PPAG, 2009. **14**(2): p. 75-85.

20. Broder, C.C., et al., *A treatment for and vaccine against the deadly Hendra and Nipah viruses.* Antiviral research, 2013. **100**(1): p. 8-13.
21. Geisbert, T.W., et al., *A single dose investigational subunit vaccine for human use against Nipah virus and Hendra virus.* npj Vaccines, 2021. **6**(1): p. 23.
22. El-Sayed, A., *Advances in rabies prophylaxis and treatment with emphasis on immunoresponse mechanisms.* International journal of veterinary science and medicine, 2018. **6**(1): p. 8-15.
23. Markham, A., *REGN-EB3: First Approval.* Drugs, 2021. **81**(1): p. 175-178.
24. Gaafar, Y.Z.A., et al., *Characterisation of a novel nucleorhabdovirus infecting alfalfa (Medicago sativa).* Virol J, 2019. **16**(1): p. 55.
25. Liu, L., et al., *Fungal negative-stranded RNA virus that is related to bornaviruses and nyaviruses.* Proc Natl Acad Sci U S A, 2014. **111**(33): p. 12205-10.
26. Arcos Gonzalez, P., et al., *The Epidemiological Presentation Pattern of Ebola Virus Disease Outbreaks: Changes from 1976 to 2019.* Prehosp Disaster Med, 2020: p. 1-7.
27. Jorquera, P.A. and R.A. Tripp, *Respiratory syncytial virus: prospects for new and emerging therapeutics.* Expert Rev Respir Med, 2017. **11**(8): p. 609-615.
28. Ferren, M., B. Horvat, and C. Mathieu, *Measles Encephalitis: Towards New Therapeutics.* Viruses, 2019. **11**(11).
29. ME, J.W., K. Adair, and L. Brierley, *RNA Viruses: A Case Study of the Biology of Emerging Infectious Diseases.* Microbiol Spectr, 2013. **1**(1).
30. Parrish, C.R., et al., *Cross-species virus transmission and the emergence of new epidemic diseases.* Microbiol Mol Biol Rev, 2008. **72**(3): p. 457-70.
31. Afonso, C.L., et al., *Taxonomy of the order Mononegavirales: update 2016.* Arch Virol, 2016. **161**(8): p. 2351-60.
32. Whelan, S.P., J.N. Barr, and G.W. Wertz, *Transcription and replication of nonsegmented negative-strand RNA viruses.* Curr Top Microbiol Immunol, 2004. **283**: p. 61-119.
33. Latorre, V., F. Mattenberger, and R. Geller, *Chaperoning the Mononegavirales: Current Knowledge and Future Directions.* Viruses, 2018. **10**(12).
34. Ruigrok, R.W., T. Crépin, and D. Kolakofsky, *Nucleoproteins and nucleocapsids of negative-strand RNA viruses.* Curr Opin Microbiol, 2011. **14**(4): p. 504-10.
35. Alayyoubi, M., et al., *Structure of the paramyxovirus parainfluenza virus 5 nucleoprotein-RNA complex.* Proc Natl Acad Sci U S A, 2015. **112**(14): p. E1792-9.
36. Cleveland, S.B., J. Davies, and M.A. McClure, *A bioinformatics approach to the structure, function, and evolution of the nucleoprotein of the order mononegavirales.* PLoS One, 2011. **6**(5): p. e19275.
37. Cox, R., et al., *Structural and functional characterization of the mumps virus phosphoprotein.* J Virol, 2013. **87**(13): p. 7558-68.
38. Liu, X., et al., *Host protein ABCE1 interacts with the viral phosphoprotein and promotes rabies virus replication.* Biosafety and Health, 2020. **2**(3): p. 157-163.
39. Jiang, Y., Y. Qin, and M. Chen, *Host-Pathogen Interactions in Measles Virus Replication and Anti-Viral Immunity.* Viruses, 2016. **8**(11): p. 308.
40. Fuentes, S.M., et al., *Phosphorylation of paramyxovirus phosphoprotein and its role in viral gene expression.* Future Microbiol, 2010. **5**(1): p. 9-13.
41. Smith, E.C., et al., *Trimeric transmembrane domain interactions in paramyxovirus fusion proteins: roles in protein folding, stability, and function.* J Biol Chem, 2013. **288**(50): p. 35726-35.
42. Aguilar, H.C., et al., *Paramyxovirus Glycoproteins and the Membrane Fusion Process.* Curr Clin Microbiol Rep, 2016. **3**(3): p. 142-154.

43. Martens, S. and H.T. McMahon, *Mechanisms of membrane fusion: disparate players and common principles.* Nat Rev Mol Cell Biol, 2008. **9**(7): p. 543-56.
44. El Najjar, F., A.P. Schmitt, and R.E. Dutch, *Paramyxovirus glycoprotein incorporation, assembly and budding: a three way dance for infectious particle production.* Viruses, 2014. **6**(8): p. 3019-54.
45. Kim, Y.H., et al., *Capture and imaging of a prehairpin fusion intermediate of the paramyxovirus PIV5.* Proc Natl Acad Sci U S A, 2011. **108**(52): p. 20992-7.
46. Chang, A. and R.E. Dutch, *Paramyxovirus fusion and entry: multiple paths to a common end.* Viruses, 2012. **4**(4): p. 613-36.
47. Bajramovic, J.J., et al., *Borna disease virus glycoprotein is required for viral dissemination in neurons.* Journal of virology, 2003. **77**(22): p. 12222-12231.
48. Barrett, C.T., S.R. Webb, and R.E. Dutch, *A Hydrophobic Target: Using the Paramyxovirus Fusion Protein Transmembrane Domain To Modulate Fusion Protein Stability.* J Virol, 2019. **93**(17).
49. Martin, B., et al., *Filovirus proteins for antiviral drug discovery: A structure/function analysis of surface glycoproteins and virus entry.* Antiviral Res, 2016. **135**: p. 1-14.
50. Masante, C., et al., *The human metapneumovirus small hydrophobic protein has properties consistent with those of a viroporin and can modulate viral fusogenic activity.* Journal of virology, 2014. **88**(11): p. 6423-6433.
51. Gan, S.W., et al., *The small hydrophobic protein of the human respiratory syncytial virus forms pentameric ion channels.* J Biol Chem, 2012. **287**(29): p. 24671-89.
52. Schlesinger, M.J. and S. Schlesinger, *Domains of virus glycoproteins.* Advances in virus research, 1987. **33**: p. 1-44.
53. Aguilar, H.C., et al., *Paramyxovirus Glycoproteins and the Membrane Fusion Process.* Current clinical microbiology reports, 2016. **3**(3): p. 142-154.
54. Dörig, R.E., et al., *The human CD46 molecule is a receptor for measles virus (Edmonston strain).* Cell, 1993. **75**(2): p. 295-305.
55. Tatsuo, H., et al., *SLAM (CDw150) is a cellular receptor for measles virus.* Nature, 2000. **406**(6798): p. 893-7.
56. Chang, A., et al., *Human metapneumovirus (HMPV) binding and infection are mediated by interactions between the HMPV fusion protein and heparan sulfate.* J Virol, 2012. **86**(6): p. 3230-43.
57. Biacchesi, S., et al., *Recombinant human Metapneumovirus lacking the small hydrophobic SH and/or attachment G glycoprotein: deletion of G yields a promising vaccine candidate.* Journal of virology, 2004. **78**(23): p. 12877-12887.
58. Lin, Y., et al., *Induction of apoptosis by paramyxovirus simian virus 5 lacking a small hydrophobic gene.* Journal of virology, 2003. **77**(6): p. 3371-3383.
59. Klimyte, E.M., et al., *Inhibition of Human Metapneumovirus Binding to Heparan Sulfate Blocks Infection in Human Lung Cells and Airway Tissues.* J Virol, 2016. **90**(20): p. 9237-50.
60. Cox, R.G., et al., *Human Metapneumovirus Is Capable of Entering Cells by Fusion with Endosomal Membranes.* PLoS Pathog, 2015. **11**(12): p. e1005303.
61. Krzyzaniak, M.A., et al., *Host cell entry of respiratory syncytial virus involves macropinocytosis followed by proteolytic activation of the F protein.* PLoS Pathog, 2013. **9**(4): p. e1003309.
62. Straus, M.R., et al., *SPINT2 inhibits proteases involved in activation of both influenza viruses and metapneumoviruses.* Virology, 2020. **543**: p. 43-53.

63. Schowalter, R.M., S.E. Smith, and R.E. Dutch, *Characterization of human metapneumovirus F protein-promoted membrane fusion: critical roles for proteolytic processing and low pH.* Journal of virology, 2006. **80**(22): p. 10931-10941.
64. Yin, H.S., et al., *Structure of the uncleaved ectodomain of the paramyxovirus (hPIV3) fusion protein.* Proc Natl Acad Sci U S A, 2005. **102**(26): p. 9288-93.
65. Yin, H.-S., et al., *Structure of the parainfluenza virus 5 F protein in its metastable, prefusion conformation.* Nature, 2006. **439**(7072): p. 38-44.
66. Popa, A., et al., *Residues in the Hendra Virus Fusion Protein Transmembrane Domain Are Critical for Endocytic Recycling.* Journal of Virology, 2012. **86**(6): p. 3014-3026.
67. Cifuentes-Muñoz, N., et al., *Mutations in the Transmembrane Domain and Cytoplasmic Tail of Hendra Virus Fusion Protein Disrupt Virus-Like-Particle Assembly.* Journal of virology, 2017. **91**(14): p. e00152-17.
68. Gravel, K.A., et al., *The Transmembrane Domain Sequence Affects the Structure and Function of the Newcastle Disease Virus Fusion Protein.* Journal of Virology, 2011. **85**(7): p. 3486-3497.
69. Brock, S.C., et al., *The transmembrane domain of the respiratory syncytial virus F protein is an orientation-independent apical plasma membrane sorting sequence.* Journal of virology, 2005. **79**(19): p. 12528-12535.
70. Smith, E.C., et al., *Trimeric transmembrane domain interactions in paramyxovirus fusion proteins: roles in protein folding, stability, and function.* The Journal of biological chemistry, 2013. **288**(50): p. 35726-35735.
71. Smith, E.C., et al., *Beyond anchoring: the expanding role of the hendra virus fusion protein transmembrane domain in protein folding, stability, and function.* Journal of virology, 2012. **86**(6): p. 3003-3013.
72. Yao, H., et al., *Viral fusion protein transmembrane domain adopts β-strand structure to facilitate membrane topological changes for virus–cell fusion.* Proceedings of the National Academy of Sciences, 2015. **112**(35): p. 10926-10931.
73. Lee, M., et al., *Conformation and Trimer Association of the Transmembrane Domain of the Parainfluenza Virus Fusion Protein in Lipid Bilayers from Solid-State NMR: Insights into the Sequence Determinants of Trimer Structure and Fusion Activity.* Journal of molecular biology, 2018. **430**(5): p. 695-709.
74. Webb, S., et al., *Hendra virus fusion protein transmembrane domain contributes to pre-fusion protein stability.* J Biol Chem, 2017. **292**(14): p. 5685-5694.
75. Cifuentes-Munoz, N., et al., *Human Metapneumovirus Induces Formation of Inclusion Bodies for Efficient Genome Replication and Transcription.* J Virol, 2017. **91**(24).
76. Ringel, M., et al., *Nipah virus induces two inclusion body populations: Identification of novel inclusions at the plasma membrane.* PLoS Pathog, 2019. **15**(4): p. e1007733.
77. Zhou, Y., et al., *Measles Virus Forms Inclusion Bodies with Properties of Liquid Organelles.* Journal of Virology, 2019. **93**(21): p. e00948-19.
78. Hoenen, T., et al., *Inclusion bodies are a site of ebolavirus replication.* J Virol, 2012. **86**(21): p. 11779-88.
79. !!! INVALID CITATION !!! {}.
80. Nevers, Q., et al., *Negri bodies and other virus membrane-less replication compartments.* Biochimica et biophysica acta. Molecular cell research, 2020. **1867**(12): p. 118831-118831.
81. Del Vecchio, K., et al., *A cationic, C-terminal patch and structural rearrangements in Ebola virus matrix VP40 protein control its interactions with phosphatidylserine.* J Biol Chem, 2018. **293**(9): p. 3335-3349.

82. Bornholdt, Z.A., et al., *Structural rearrangement of ebola virus VP40 begets multiple functions in the virus life cycle.* Cell, 2013. **154**(4): p. 763-74.
83. Leyrat, C., et al., *Structure and self-assembly of the calcium binding matrix protein of human metapneumovirus.* Structure, 2014. **22**(1): p. 136-48.
84. Atreya, P.L., M.E. Peeples, and P.L. Collins, *The NS1 protein of human respiratory syncytial virus is a potent inhibitor of minigenome transcription and RNA replication.* Journal of virology, 1998. **72**(2): p. 1452-1461.
85. Sedeyn, K., B. Schepens, and X. Saelens, *Respiratory syncytial virus nonstructural proteins 1 and 2: Exceptional disrupters of innate immune responses.* PLoS pathogens, 2019. **15**(10): p. e1007984-e1007984.
86. Chatterjee, S., et al., *Structural basis for human respiratory syncytial virus NS1-mediated modulation of host responses.* Nature microbiology, 2017. **2**: p. 17101-17101.
87. Ghildyal, R., A. Ho, and D.A. Jans, *Central role of the respiratory syncytial virus matrix protein in infection.* FEMS Microbiol Rev, 2006. **30**(5): p. 692-705.
88. Forster, A., et al., *Dimerization of matrix protein is required for budding of respiratory syncytial virus.* J Virol, 2015. **89**(8): p. 4624-35.
89. Pentecost, M., et al., *Evidence for ubiquitin-regulated nuclear and subnuclear trafficking among Paramyxovirinae matrix proteins.* PLoS pathogens, 2015. **11**(3): p. e1004739-e1004739.
90. Watkinson, R.E. and B. Lee, *Nipah virus matrix protein: expert hacker of cellular machines.* FEBS letters, 2016. **590**(15): p. 2494-2511.
91. Terry, L.J., E.B. Shows, and S.R. Wente, *Crossing the nuclear envelope: hierarchical regulation of nucleocytoplasmic transport.* Science, 2007. **318**(5855): p. 1412-6.
92. Chase, G., et al., *Borna disease virus matrix protein is an integral component of the viral ribonucleoprotein complex that does not interfere with polymerase activity.* J Virol, 2007. **81**(2): p. 743-9.
93. Honda, T. and K. Tomonaga, *Nucleocytoplasmic Shuttling of Viral Proteins in Borna Disease Virus Infection.* Viruses, 2013. **5**(8): p. 1978-1990.
94. Neumann, P., et al., *Crystal structure of the Borna disease virus matrix protein (BDV-M) reveals ssRNA binding properties.* Proceedings of the National Academy of Sciences, 2009. **106**(10): p. 3710-3715.
95. Ghildyal, R., et al., *The matrix protein of Human respiratory syncytial virus localises to the nucleus of infected cells and inhibits transcription.* Arch Virol, 2003. **148**(7): p. 1419-29.
96. Wang, Y.E., et al., *Ubiquitin-regulated nuclear-cytoplasmic trafficking of the Nipah virus matrix protein is important for viral budding.* PLoS Pathog, 2010. **6**(11): p. e1001186.
97. Oliveira, A.P., et al., *Human respiratory syncytial virus N, P and M protein interactions in HEK-293T cells.* Virus Res, 2013. **177**(1): p. 108-12.
98. Rawlinson, S.M., et al., *Viral regulation of host cell biology by hijacking of the nucleolar DNA-damage response.* Nature Communications, 2018. **9**(1): p. 3057.
99. Prakash, V., et al., *Ribosome biogenesis during cell cycle arrest fuels EMT in development and disease.* Nature Communications, 2019. **10**(1): p. 2110.
100. Deffrasnes, C., et al., *Genome-wide siRNA Screening at Biosafety Level 4 Reveals a Crucial Role for Fibrillarin in Henipavirus Infection.* PLoS Pathog, 2016. **12**(3): p. e1005478.
101. Black, B.L. and D.S. Lyles, *Vesicular stomatitis virus matrix protein inhibits host cell-directed transcription of target genes in vivo.* Journal of Virology, 1992. **66**(7): p. 4058-4064.

102. Fresco, L.D., M.G. Kurilla, and J.D. Keene, *Rapid inhibition of processing and assembly of small nuclear ribonucleoproteins after infection with vesicular stomatitis virus.* Mol Cell Biol, 1987. **7**(3): p. 1148-55.
103. Black, B.L., et al., *The role of vesicular stomatitis virus matrix protein in inhibition of host-directed gene expression is genetically separable from its function in virus assembly.* Journal of Virology, 1993. **67**(8): p. 4814-4821.
104. Petersen, J.M., et al., *The Matrix Protein of Vesicular Stomatitis Virus Inhibits Nucleocytoplasmic Transport When It Is in the Nucleus and Associated with Nuclear Pore Complexes.* Molecular and Cellular Biology, 2000. **20**(22): p. 8590-8601.
105. Finke, S., R. Mueller-Waldeck, and K.-K. Conzelmann, *Rabies virus matrix protein regulates the balance of virus transcription and replication.* Journal of General Virology, 2003. **84**(6): p. 1613-1621.
106. Yu, X., et al., *Measles Virus Matrix Protein Inhibits Host Cell Transcription.* PLoS One, 2016. **11**(8): p. e0161360.
107. Conzelmann, K.K., *Nonsegmented negative-strand RNA viruses: genetics and manipulation of viral genomes.* Annu Rev Genet, 1998. **32**: p. 123-62.
108. Ghildyal, R., et al., *Respiratory syncytial virus matrix protein associates with nucleocapsids in infected cells.* J Gen Virol, 2002. **83**(Pt 4): p. 753-757.
109. Hoenen, T., et al., *Both matrix proteins of Ebola virus contribute to the regulation of viral genome replication and transcription.* Virology, 2010. **403**(1): p. 56-66.
110. Watanabe, K., et al., *Mechanism for inhibition of influenza virus RNA polymerase activity by matrix protein.* Journal of Virology, 1996. **70**(1): p. 241-247.
111. Ghildyal, R., et al., *Nuclear import of the respiratory syncytial virus matrix protein is mediated by importin beta1 independent of importin alpha.* Biochemistry, 2005. **44**(38): p. 12887-95.
112. Rodriguez, L., et al., *Human respiratory syncytial virus matrix protein is an RNA-binding protein: binding properties, location and identity of the RNA contact residues.* J Gen Virol, 2004. **85**(Pt 3): p. 709-19.
113. Collins, P.L. and J.A. Melero, *Progress in understanding and controlling respiratory syncytial virus: still crazy after all these years.* Virus Res, 2011. **162**(1-2): p. 80-99.
114. Shahrabadi, M.S. and P.W. Lee, *Calcium requirement for syncytium formation in HEp-2 cells by respiratory syncytial virus.* Journal of clinical microbiology, 1988. **26**(1): p. 139-141.
115. Hoffmann, H.H., et al., *Diverse Viruses Require the Calcium Transporter SPCA1 for Maturation and Spread.* Cell Host Microbe, 2017. **22**(4): p. 460-470.e5.
116. Kamata, M., A. Hiraki, and J. Kim, *Effect of Ca2+ on morphogenesis of HVJ (Sendai virus) virion in LLC-MK2 cells: suppression of viral production.* Cell Struct Funct, 1994. **19**(5): p. 315-23.
117. Amarasinghe, G.K. and R.E. Dutch, *A calcium-fortified viral matrix protein.* Structure, 2014. **22**(1): p. 5-7.
118. Buchholz, U.J., S. Finke, and K.-K. Conzelmann, *Generation of Bovine Respiratory Syncytial Virus (BRSV) from cDNA: BRSV NS2 Is Not Essential for Virus Replication in Tissue Culture, and the Human RSV Leader Region Acts as a Functional BRSV Genome Promoter.* Journal of Virology, 1999. **73**(1): p. 251.
119. Hitoshi, N., Y. Ken-ichi, and M. Jun-ichi, *Efficient selection for high-expression transfectants with a novel eukaryotic vector.* Gene, 1991. **108**(2): p. 193-199.

120. Cifuentes-Muñoz, N., et al., *Human Metapneumovirus Induces Formation of Inclusion Bodies for Efficient Genome Replication and Transcription.* Journal of Virology, 2017. **91**(24): p. e01282-17.
121. Moulton, H.M., et al., *Cellular uptake of antisense morpholino oligomers conjugated to arginine-rich peptides.* Bioconjug Chem, 2004. **15**(2): p. 290-9.
122. Rosenke, K., et al., *Inhibition of SARS-CoV-2 in Vero cell cultures by peptide-conjugated morpholino-oligomers.* bioRxiv, 2020.
123. Moulton, J.D., *Using morpholinos to control gene expression.* Current protocols in nucleic acid chemistry, 2007. **Chapter 4**(1): p. 4301-4.30.
124. Rima, B., et al., *Problems of classification in the family Paramyxoviridae.* Arch Virol, 2018. **163**(5): p. 1395-1404.
125. Cox, R.M. and R.K. Plemper, *Structure and organization of paramyxovirus particles.* Curr Opin Virol, 2017. **24**: p. 105-114.
126. Harrison, M.S., T. Sakaguchi, and A.P. Schmitt, *Paramyxovirus assembly and budding: building particles that transmit infections.* Int J Biochem Cell Biol, 2010. **42**(9): p. 1416-29.
127. Kuehn, B.M., *Drop in Vaccination Causes Surge in Global Measles Cases, Deaths.* JAMA, 2021. **325**(3): p. 213.
128. Sanyaolu, A., et al., *Measles Outbreak in Unvaccinated and Partially Vaccinated Children and Adults in the United States and Canada (2018-2019): A Narrative Review of Cases.* Inquiry : a journal of medical care organization, provision and financing, 2019. **56**: p. 46958019894098-46958019894098.
129. Broder, C.C., D.L. Weir, and P.A. Reid, *Hendra virus and Nipah virus animal vaccines.* Vaccine, 2016. **34**(30): p. 3525-3534.
130. Halpin, K., et al., *Pteropid bats are confirmed as the reservoir hosts of henipaviruses: a comprehensive experimental study of virus transmission.* The American journal of tropical medicine and hygiene, 2011. **85**(5): p. 946-951.
131. Snary, E.L., et al., *Qualitative release assessment to estimate the likelihood of henipavirus entering the United Kingdom.* PLoS One, 2012. **7**(2): p. e27918.
132. Loney, C., et al., *Paramyxovirus ultrastructure and genome packaging: cryo-electron tomography of sendai virus.* Journal of virology, 2009. **83**(16): p. 8191-8197.
133. Terrier, O., et al., *Parainfluenza virus type 5 (PIV-5) morphology revealed by cryo-electron microscopy.* Virus Research, 2009. **142**(1): p. 200-203.
134. Chang, A. and R.E. Dutch, *Paramyxovirus fusion and entry: multiple paths to a common end.* Viruses, 2012. **4**(4): p. 613-636.
135. Martens, S. and H.T. McMahon, *Mechanisms of membrane fusion: disparate players and common principles.* Nature Reviews Molecular Cell Biology, 2008. **9**(7): p. 543-556.
136. Dutch, R.E. and R.A. Lamb, *Deletion of the cytoplasmic tail of the fusion protein of the paramyxovirus simian virus 5 affects fusion pore enlargement.* Journal of virology, 2001. **75**(11): p. 5363-5369.
137. Yao, H. and M. Hong, *Membrane-dependent conformation, dynamics, and lipid interactions of the fusion peptide of the paramyxovirus PIV5 from solid-state NMR.* J Mol Biol, 2013. **425**(3): p. 563-76.
138. Smith, E.C., et al., *Role of sequence and structure of the Hendra fusion protein fusion peptide in membrane fusion.* The Journal of biological chemistry, 2012. **287**(35): p. 30035-30048.
139. Pager, C.T., et al., *A mature and fusogenic form of the Nipah virus fusion protein requires proteolytic processing by cathepsin L.* Virology, 2006. **346**(2): p. 251-7.

140. Welch, B.D., et al., *Structure of the cleavage-activated prefusion form of the parainfluenza virus 5 fusion protein.* Proc Natl Acad Sci U S A, 2012. **109**(41): p. 16672-7.
141. Leyrer, S., et al., *Sendai virus-like particles devoid of haemagglutinin-neuraminidase protein infect cells via the human asialoglycoprotein receptor.* J Gen Virol, 1998. **79 (Pt 4)**: p. 683-7.
142. Smith, E.C., et al., *Viral entry mechanisms: the increasing diversity of paramyxovirus entry.* Febs j, 2009. **276**(24): p. 7217-27.
143. Lee, J.K., et al., *Functional interaction between paramyxovirus fusion and attachment proteins.* J Biol Chem, 2008. **283**(24): p. 16561-72.
144. Bose, S., et al., *Mutations in the Parainfluenza Virus 5 Fusion Protein Reveal Domains Important for Fusion Triggering and Metastability.* Journal of Virology, 2013. **87**(24): p. 13520.
145. Webb, S.R., et al., *Transmembrane Domains of Highly Pathogenic Viral Fusion Proteins Exhibit Trimeric Association In Vitro.* mSphere, 2018. **3**(2).
146. Barrett, C.T., S.R. Webb, and R.E. Dutch, *A Hydrophobic Target: Using the Paramyxovirus Fusion Protein Transmembrane Domain To Modulate Fusion Protein Stability.* Journal of Virology, 2019. **93**(17): p. e00863-19.
147. Bissonnette, M.L., et al., *Functional analysis of the transmembrane domain in paramyxovirus F protein-mediated membrane fusion.* J Mol Biol, 2009. **386**(1): p. 14-36.
148. Donald, J.E., et al., *Transmembrane orientation and possible role of the fusogenic peptide from parainfluenza virus 5 (PIV5) in promoting fusion.* Proceedings of the National Academy of Sciences, 2011. **108**(10): p. 3958.
149. Porotto, M., et al., *Viral entry inhibitors targeted to the membrane site of action.* J Virol, 2010. **84**(13): p. 6760-8.
150. Poor, T.A., et al., *Probing the paramyxovirus fusion (F) protein-refolding event from pre- to postfusion by oxidative footprinting.* Proceedings of the National Academy of Sciences, 2014. **111**(25): p. E2596-E2605.
151. Jardetzky, T.S. and R.A. Lamb, *Activation of paramyxovirus membrane fusion and virus entry.* Current opinion in virology, 2014. **5**: p. 24-33.
152. Mirza, A.M., et al., *Triggering of the newcastle disease virus fusion protein by a chimeric attachment protein that binds to Nipah virus receptors.* J Biol Chem, 2011. **286**(20): p. 17851-60.
153. Lai, A.L. and J.H. Freed, *The Interaction between Influenza HA Fusion Peptide and Transmembrane Domain Affects Membrane Structure.* Biophysical journal, 2015. **109**(12): p. 2523-2536.
154. Lee, J., et al., *Structure of the Ebola virus envelope protein MPER/TM domain and its interaction with the fusion loop explains their fusion activity.* Proceedings of the National Academy of Sciences, 2017. **114**(38): p. E7987-E7996.
155. Kwon, B., et al., *Oligomeric Structure and Three-Dimensional Fold of the HIV gp41 Membrane-Proximal External Region and Transmembrane Domain in Phospholipid Bilayers.* J Am Chem Soc, 2018. **140**(26): p. 8246-8259.
156. Rima, B., et al., *ICTV Virus Taxonomy Profile: Pneumoviridae.* The Journal of general virology, 2017. **98**(12): p. 2912-2913.
157. van den Hoogen, B.G., et al., *A newly discovered human pneumovirus isolated from young children with respiratory tract disease.* Nat Med, 2001. **7**(6): p. 719-24.
158. Panda, S., et al., *Human metapneumovirus: review of an important respiratory pathogen.* Int J Infect Dis, 2014. **25**: p. 45-52.

159. van den Hoogen, B.G., D.M. Osterhaus, and R.A. Fouchier, *Clinical impact and diagnosis of human metapneumovirus infection.* Pediatr Infect Dis J, 2004. **23**(1 Suppl): p. S25-32.
160. Williams, J.V., et al., *Human metapneumovirus and lower respiratory tract disease in otherwise healthy infants and children.* The New England journal of medicine, 2004. **350**(5): p. 443-450.
161. Wang, X., et al., *Global burden of acute lower respiratory infection associated with human metapneumovirus in children under 5 years in 2018: a systematic review and modelling study.* Lancet Glob Health, 2021. **9**(1): p. e33-e43.
162. Haas, L.E.M., et al., *Human metapneumovirus in adults.* Viruses, 2013. **5**(1): p. 87-110.
163. Kumar, P. and M. Srivastava, *Prophylactic and therapeutic approaches for human metapneumovirus.* Virusdisease, 2018. **29**(4): p. 434-444.
164. Jumat, M.R., et al., *Imaging analysis of human metapneumovirus-infected cells provides evidence for the involvement of F-actin and the raft-lipid microdomains in virus morphogenesis.* Virology Journal, 2014. **11**(1): p. 198.
165. Peret, T.C., et al., *Characterization of human metapneumoviruses isolated from patients in North America.* J Infect Dis, 2002. **185**(11): p. 1660-3.
166. Ke, Z., et al., *The Morphology and Assembly of Respiratory Syncytial Virus Revealed by Cryo-Electron Tomography.* Viruses, 2018. **10**(8): p. 446.
167. Biacchesi, S., et al., *Infection of nonhuman primates with recombinant human metapneumovirus lacking the SH, G, or M2-2 protein categorizes each as a nonessential accessory protein and identifies vaccine candidates.* Journal of virology, 2005. **79**(19): p. 12608-12613.
168. Battles, M.B., et al., *Structure and immunogenicity of pre-fusion-stabilized human metapneumovirus F glycoprotein.* Nature Communications, 2017. **8**(1): p. 1528.
169. Masante, C., et al., *The human metapneumovirus small hydrophobic protein has properties consistent with those of a viroporin and can modulate viral fusogenic activity.* J Virol, 2014. **88**(11): p. 6423-33.
170. Heinrich, B.S., et al., *Phase Transitions Drive the Formation of Vesicular Stomatitis Virus Replication Compartments.* mBio, 2018. **9**(5): p. e02290-17.
171. Su, J.M., et al., *Formation and Function of Liquid-Like Viral Factories in Negative-Sense Single-Stranded RNA Virus Infections.* Viruses, 2021. **13**(1).
172. Zhang, S., et al., *Inclusion Body Fusion of Human Parainfluenza Virus Type 3 Regulated by Acetylated α-Tubulin Enhances Viral Replication.* J Virol, 2017. **91**(3).
173. Carlos, T.S., et al., *Parainfluenza virus 5 genomes are located in viral cytoplasmic bodies whilst the virus dismantles the interferon-induced antiviral state of cells.* The Journal of general virology, 2009. **90**(Pt 9): p. 2147-2156.
174. García, J., et al., *Cytoplasmic Inclusions of Respiratory Syncytial Virus-Infected Cells: Formation of Inclusion Bodies in Transfected Cells That Coexpress the Nucleoprotein, the Phosphoprotein, and the 22K Protein.* Virology, 1993. **195**(1): p. 243-247.
175. Lahaye, X., et al., *Functional characterization of Negri bodies (NBs) in rabies virus-infected cells: Evidence that NBs are sites of viral transcription and replication.* J Virol, 2009. **83**(16): p. 7948-58.
176. Heinrich, B.S., et al., *Protein expression redirects vesicular stomatitis virus RNA synthesis to cytoplasmic inclusions.* PLoS pathogens, 2010. **6**(6): p. e1000958-e1000958.
177. Dolnik, O., et al., *Marburg virus inclusions: A virus-induced microcompartment and interface to multivesicular bodies and the late endosomal compartment.* Eur J Cell Biol, 2015. **94**(7-9): p. 323-31.

178. Hoenen, T., et al., *Inclusion bodies are a site of ebolavirus replication.* Journal of virology, 2012. **86**(21): p. 11779-11788.
179. Hardy, R.W. and G.W. Wertz, *The Cys₃-His₁ Motif of the Respiratory Syncytial Virus M2-1 Protein Is Essential for Protein Function.* Journal of Virology, 2000. **74**(13): p. 5880.
180. Fearns, R. and P.L. Collins, *Role of the M2-1 Transcription Antitermination Protein of Respiratory Syncytial Virus in Sequential Transcription.* Journal of Virology, 1999. **73**(7): p. 5852.
181. Wignall-Fleming, E.B., et al., *Analysis of Paramyxovirus Transcription and Replication by High-Throughput Sequencing.* Journal of Virology, 2019. **93**(17): p. e00571-19.
182. Noton, S.L. and R. Fearns, *Initiation and regulation of paramyxovirus transcription and replication.* Virology, 2015. **479-480**: p. 545-554.
183. Ruigrok, R.W.H., T. Crépin, and D. Kolakofsky, *Nucleoproteins and nucleocapsids of negative-strand RNA viruses.* Current Opinion in Microbiology, 2011. **14**(4): p. 504-510.
184. Rincheval, V., et al., *Functional organization of cytoplasmic inclusion bodies in cells infected by respiratory syncytial virus.* Nat Commun, 2017. **8**(1): p. 563.
185. Derdowski, A., et al., *Human metapneumovirus nucleoprotein and phosphoprotein interact and provide the minimal requirements for inclusion body formation.* J Gen Virol, 2008. **89**(Pt 11): p. 2698-2708.
186. Harrison, M.S., T. Sakaguchi, and A.P. Schmitt, *Paramyxovirus assembly and budding: building particles that transmit infections.* The international journal of biochemistry & cell biology, 2010. **42**(9): p. 1416-1429.
187. Liljeroos, L., et al., *Electron cryotomography of measles virus reveals how matrix protein coats the ribonucleocapsid within intact virions.* Proc Natl Acad Sci U S A, 2011. **108**(44): p. 18085-90.
188. !!! INVALID CITATION !!! [].
189. Money, V.A., et al., *Surface features of a Mononegavirales matrix protein indicate sites of membrane interaction.* Proceedings of the National Academy of Sciences, 2009. **106**(11): p. 4441.
190. Stahelin, R.V., *Membrane binding and bending in Ebola VP40 assembly and egress.* Frontiers in microbiology, 2014. **5**: p. 300-300.
191. Saarikangas, J., et al., *Molecular mechanisms of membrane deformation by I-BAR domain proteins.* Curr Biol, 2009. **19**(2): p. 95-107.
192. Shtykova, E.V., et al., *Solution Structure, Self-Assembly, and Membrane Interactions of the Matrix Protein from Newcastle Disease Virus at Neutral and Acidic pH.* Journal of Virology, 2019. **93**(6): p. e01450-18.
193. Ke, Z., et al., *Promotion of virus assembly and organization by the measles virus matrix protein.* Nature Communications, 2018. **9**(1): p. 1736.
194. Pentecost, M., et al., *Evidence for ubiquitin-regulated nuclear and subnuclear trafficking among Paramyxovirinae matrix proteins.* PLoS Pathog, 2015. **11**(3): p. e1004739.
195. Duan, Z., et al., *Nuclear localization of Newcastle disease virus matrix protein promotes virus replication by affecting viral RNA synthesis and transcription and inhibiting host cell transcription.* Veterinary Research, 2019. **50**(1): p. 22.
196. Petersen, J.M., L.-S. Her, and J.E. Dahlberg, *Multiple vesiculoviral matrix proteins inhibit both nuclear export and import.* Proceedings of the National Academy of Sciences, 2001. **98**(15): p. 8590.
197. Berridge, M.J., P. Lipp, and M.D. Bootman, *The versatility and universality of calcium signalling.* Nature Reviews Molecular Cell Biology, 2000. **1**(1): p. 11-21.

198. Glodowski, D.R., J.M. Petersen, and J.E. Dahlberg, *Complex nuclear localization signals in the matrix protein of vesicular stomatitis virus.* J Biol Chem, 2002. **277**(49): p. 46864-70.
199. Ghildyal, R., et al., *The Respiratory Syncytial Virus Matrix Protein Possesses a Crm1-Mediated Nuclear Export Mechanism.* Journal of Virology, 2009. **83**(11): p. 5353.
200. Field, A.K., et al., *Inducers of interferon and host resistance. II. Multistranded synthetic polynucleotide complexes.* Proceedings of the National Academy of Sciences of the United States of America, 1967. **58**(3): p. 1004-1010.
201. Frank-Bertoncelj, M., et al., *TLR3 Ligand Poly(I:C) Exerts Distinct Actions in Synovial Fibroblasts When Delivered by Extracellular Vesicles.* Front Immunol, 2018. **9**: p. 28.
202. Moore, M.S. and G. Blobel, *A G protein involved in nucleocytoplasmic transport: the role of Ran.* Trends Biochem Sci, 1994. **19**(5): p. 211-6.
203. Summerton, J. and D. Weller, *Morpholino antisense oligomers: design, preparation, and properties.* Antisense Nucleic Acid Drug Dev, 1997. **7**(3): p. 187-95.
204. Nan, Y. and Y.-J. Zhang, *Antisense Phosphorodiamidate Morpholino Oligomers as Novel Antiviral Compounds.* Frontiers in microbiology, 2018. **9**: p. 750-750.
205. Khokha, M.K., et al., *Techniques and probes for the study of Xenopus tropicalis development.* Dev Dyn, 2002. **225**(4): p. 499-510.
206. Giard, D.J., et al., *In vitro cultivation of human tumors: establishment of cell lines derived from a series of solid tumors.* J Natl Cancer Inst, 1973. **51**(5): p. 1417-23.
207. Reddel, R.R., et al., *Transformation of human bronchial epithelial cells by infection with SV40 or adenovirus-12 SV40 hybrid virus, or transfection via strontium phosphate coprecipitation with a plasmid containing SV40 early region genes.* Cancer Res, 1988. **48**(7): p. 1904-9.
208. El Najjar, F., et al., *Human metapneumovirus Induces Reorganization of the Actin Cytoskeleton for Direct Cell-to-Cell Spread.* PLoS pathogens, 2016. **12**(9): p. e1005922-e1005922.
209. Loo, L.H., et al., *Evidence for the interaction of the human metapneumovirus G and F proteins during virus-like particle formation.* Virology Journal, 2013. **10**(1): p. 294.
210. Bauer, A., et al., *ANP32B is a nuclear target of henipavirus M proteins.* PloS one, 2014. **9**(5): p. e97233-e97233.
211. Sabo, Y., M. Ehrlich, and E. Bacharach, *The conserved YAGL motif in human metapneumovirus is required for higher-order cellular assemblies of the matrix protein and for virion production.* Journal of virology, 2011. **85**(13): p. 6594-6609.
212. Runkler, N., et al., *Measles virus nucleocapsid transport to the plasma membrane requires stable expression and surface accumulation of the viral matrix protein.* Cell Microbiol, 2007. **9**(5): p. 1203-14.
213. Inoue, M., et al., *A new Sendai virus vector deficient in the matrix gene does not form virus particles and shows extensive cell-to-cell spreading.* Journal of virology, 2003. **77**(11): p. 6419-6429.
214. Mottet-Osman, G., et al., *Suppression of the Sendai virus M protein through a novel short interfering RNA approach inhibits viral particle production but does not affect viral RNA synthesis.* Journal of virology, 2007. **81**(6): p. 2861-2868.
215. Dietzel, E., et al., *Nipah Virus Matrix Protein Influences Fusogenicity and Is Essential for Particle Infectivity and Stability.* Journal of virology, 2015. **90**(5): p. 2514-2522.
216. Mitra, R., et al., *The human respiratory syncytial virus matrix protein is required for maturation of viral filaments.* Journal of virology, 2012. **86**(8): p. 4432-4443.
217. Ringel, M., et al., *Replication of a Nipah Virus Encoding a Nuclear-Retained Matrix Protein.* J Infect Dis, 2020. **221**(Suppl 4): p. S389-s394.

218. Staller, E., et al., *A rare variant in Anp32B impairs influenza virus replication in human cells.* bioRxiv, 2020: p. 2020.04.06.027482.
219. Zhang, Z., et al., *Selective usage of ANP32 proteins by influenza B virus polymerase: Implications in determination of host range.* PLoS Pathog, 2020. **16**(10): p. e1008989.
220. Staller, E., et al., *ANP32 Proteins Are Essential for Influenza Virus Replication in Human Cells.* Journal of virology, 2019. **93**(17): p. e00217-19.
221. Günther, M., et al., *Interaction of host cellular factor ANP32B with matrix proteins of different paramyxoviruses.* J Gen Virol, 2020. **101**(1): p. 44-58.
222. Chemnitz, J., et al., *The acidic protein rich in leucines Anp32b is an immunomodulator of inflammation in mice.* Scientific Reports, 2019. **9**(1): p. 4853.
223. Fries, B., et al., *Analysis of nucleocytoplasmic trafficking of the HuR ligand APRIL and its influence on CD83 expression.* J Biol Chem, 2007. **282**(7): p. 4504-4515.
224. Hoenen, T., et al., *VP40 octamers are essential for Ebola virus replication.* Journal of virology, 2005. **79**(3): p. 1898-1905.
225. !!! INVALID CITATION !!! [223, 224].
226. White, J.M., et al., *Structures and mechanisms of viral membrane fusion proteins: multiple variations on a common theme.* Critical reviews in biochemistry and molecular biology, 2008. **43**(3): p. 189-219.
227. Greenberg, M., et al., *HIV fusion and its inhibition in antiretroviral therapy.* Rev Med Virol, 2004. **14**(5): p. 321-37.
228. Bossart, K.N., et al., *Inhibition of Henipavirus fusion and infection by heptad-derived peptides of the Nipah virus fusion glycoprotein.* Virology journal, 2005. **2**: p. 57-57.
229. Lambert, D.M., et al., *Peptides from conserved regions of paramyxovirus fusion (F) proteins are potent inhibitors of viral fusion.* Proceedings of the National Academy of Sciences of the United States of America, 1996. **93**(5): p. 2186-2191.
230. Cianci, C., et al., *Orally active fusion inhibitor of respiratory syncytial virus.* Antimicrob Agents Chemother, 2004. **48**(2): p. 413-22.
231. Barrett, C.T. and R.E. Dutch, *Viral Membrane Fusion and the Transmembrane Domain.* Viruses, 2020. **12**(7): p. 693.
232. Langosch, D., M. Hofmann, and C. Ungermann, *The role of transmembrane domains in membrane fusion.* Cell Mol Life Sci, 2007. **64**(7-8): p. 850-64.
233. Nüssler, F., M.J. Clague, and A. Herrmann, *Meta-stability of the hemifusion intermediate induced by glycosylphosphatidylinositol-anchored influenza hemagglutinin.* Biophys J, 1997. **73**(5): p. 2280-91.
234. Kemble, G.W., T. Danieli, and J.M. White, *Lipid-anchored influenza hemagglutinin promotes hemifusion, not complete fusion.* Cell, 1994. **76**(2): p. 383-91.
235. Armstrong, R.T., A.S. Kushnir, and J.M. White, *The transmembrane domain of influenza hemagglutinin exhibits a stringent length requirement to support the hemifusion to fusion transition.* J Cell Biol, 2000. **151**(2): p. 425-37.
236. Slaughter, K.B. and R.E. Dutch, *Transmembrane Domain Dissociation Is Required for Hendra Virus F Protein Fusogenic Activity.* Journal of Virology, 2019. **93**(22): p. e01069-19.
237. Zokarkar, A., et al., *Reversible inhibition of fusion activity of a paramyxovirus fusion protein by an engineered disulfide bond in the membrane-proximal external region.* Journal of virology, 2012. **86**(22): p. 12397-12401.
238. Cleverley, D.Z. and J. Lenard, *The transmembrane domain in viral fusion: Essential role for a conserved glycine residue in vesicular stomatitis virus G protein.* Proceedings of the National Academy of Sciences, 1998. **95**(7): p. 3425.

239. Hetz, C., *The unfolded protein response: controlling cell fate decisions under ER stress and beyond.* Nature Reviews Molecular Cell Biology, 2012. **13**(2): p. 89-102.
240. Cox, R.G., et al., *Human Metapneumovirus Virus-Like Particles Induce Protective B and T Cell Responses in a Mouse Model.* Journal of Virology, 2014. **88**(11): p. 6368.
241. Suryanarayana, K., et al., *Transcription inhibition and other properties of matrix proteins expressed by M genes cloned from measles viruses and diseased human brain tissue.* Journal of virology, 1994. **68**(3): p. 1532-1543.
242. Madara, J.J., et al., *The multifunctional Ebola virus VP40 matrix protein is a promising therapeutic target.* Future virology, 2015. **10**(5): p. 537-546.
243. Finke, S., R. Mueller-Waldeck, and K.K. Conzelmann, *Rabies virus matrix protein regulates the balance of virus transcription and replication.* J Gen Virol, 2003. **84**(Pt 6): p. 1613-1621.
244. Iwasaki, M., et al., *The matrix protein of measles virus regulates viral RNA synthesis and assembly by interacting with the nucleocapsid protein.* Journal of virology, 2009. **83**(20): p. 10374-10383.
245. Adu-Gyamfi, E., et al., *The Ebola virus matrix protein penetrates into the plasma membrane: a key step in viral protein 40 (VP40) oligomerization and viral egress.* The Journal of biological chemistry, 2013. **288**(8): p. 5779-5789.
246. Adu-Gyamfi, E., et al., *Single-particle tracking demonstrates that actin coordinates the movement of the Ebola virus matrix protein.* Biophysical journal, 2012. **103**(9): p. L41-L43.
247. Giuffre, R.M., et al., *Evidence for an interaction between the membrane protein of a paramyxovirus and actin.* Journal of Virology, 1982. **42**(3): p. 963.
248. Takimoto, T. and A. Portner, *Molecular mechanism of paramyxovirus budding.* Virus Res, 2004. **106**(2): p. 133-45.
249. Shahriari, S., K.-J. Wei, and R. Ghildyal, *Respiratory Syncytial Virus Matrix (M) Protein Interacts with Actin In Vitro and in Cell Culture.* Viruses, 2018. **10**(10): p. 535.

VITA

JEAN BRANTTIE

EDUCATION

Ph.D. University of Kentucky, College of Medicine May 2016-Present
Department of Molecular and Cellular Biochemistry
Graduate Research Advisor: Rebecca E. Dutch, Ph.D.
Cumulative GPA: 4.00/4.00

B.S. Kentucky State University, Frankfort, Kentucky August 2012- May 2016
Bachelor of Science in Biology
Minor in Chemistry
Summa cum laude: 3.96/4.00

RESEARCH EXPERIENCE

University of Kentucky, Lexington, KY May 2017-Present
Graduate Research Assistant – Molecular and Cellular Biochemistry
Advisor: Dr. Rebecca Dutch

Eli Lilly and Company June 2020-August 2020
Medicines Innovation Hub – Bioproduct Research and Development
Summer Intern

LEADERSHIP EXPERIENCE

University of Kentucky
Students Embracing Equity in Medical Sciences January 2019-Present
Founding President.

University of Kentucky
Graduate Student Congress May 2019-May 2020
Chair of Institutional Advocacy,

University of Kentucky
Biochemistry 401G January 2019-May 2019
Teaching Assistant

Kentucky State University
Academic Center for Excellence August 2013-May 2016
Academic Peer Tutor and Mentor

PUBLICATIONS

Barrett CT, Neal HE, Edmonds K, Moncman CL, Thompson R, **Branttie JM**, Boggs KB, Wu CY, Leung DW, and Dutch RE (2021). *Effect of clinical isolate or cleavage site mutations in the SARS-CoV-2 spike protein on protein stability, cleavage, and cell-cell fusion function*. Resubmitted to J. Biol. Chem. on June 6, 2021.

Branttie JM, Dutch RE. *Parainfluenza virus 5 fusion protein maintains pre-fusion stability but not fusogenic activity following mutation of a transmembrane leucine/isoleucine domain*. J Gen Virol. 2020;101(5):467-472. doi:10.1099/jgv.0.001399

Cifuentes-Muñoz, N., **Branttie, J**., Slaughter, K., & Dutch, R. (2017). *Human Metapneumovirus Induces Formation of Inclusion Bodies for Efficient Genome Replication and Transcription*. Journal of Virology: JVI. 91(24), Journal of virology: JVI. , 2017, Vol.91 (24).

PRESENTATIONS

Branttie, J., & Dutch, R. (2020). Parainfluenza virus 5 fusion protein maintains pre-fusion stability but not fusogenic activity following mutation of a transmembrane leucine/isoleucine domain. Oral presentation scheduled for the Southeast Regional Virology Conference (Atlanta, GA). Event canceled due to COVID.

Branttie, J., & Dutch, R. (2019). A Transmembrane Domain Leucine/Isoleucine Zipper is Important for Fusogenic Activity of the PIV5 Fusion Protein. Poster presentation at the American Society for Virology Conference, Minneapolis MN.

Branttie, J., & Dutch, R. (2018). A Transmembrane Domain Leucine/Isoleucine Zipper is Important for Fusogenic Activity of the PIV5 Fusion Protein. Poster presented at the American Society for Virology Conference, College Park, MD.

Branttie, J., & Dutch, R. (2018). A Transmembrane Domain Leucine/Isoleucine Zipper is Important for Fusogenic Activity of the PIV5 Fusion Protein. Poster presented at the Experimental Biology Conference, San Diego, CA

Branttie, J., Caine, V., Lai, A. (2015). Survey of microbial sedimentation from indoor air in a campus setting. Poster presented at the Kentucky Academy of Science Symposium, Highland Heights, Kentucky.

Branttie, J., Sluss, T., (2015). Analysis of Long-term Discharge trends in Lotic Systems of Kentucky. Poster presented at the International Environmental Youth Symposium, Atlanta, Georgia.

FELLOWSHIPS & FUNDING

College of Medicine Fellowship for Graduate Research August 2017-August 2018
Lyman T. Johnson Fellowship August 2016-Present

HONORS AND AWARDS

Emerging Scholar, Faculty of Color Network
Selected by the Faculty of Color Network at the University of Kentucky based on work in diversity and inclusion, academic achievement, and research excellence.

Pillar Award for Belonging and Engagement
Awarded by the Graduate Student Congress at the University of Kentucky for work in planning, advocacy, and fundraising for highlighting and celebrating diversity on campus.

Lloyd E. Alexander Memorial Award
Selected by the Biology faculty at Kentucky State University—based on academic performance, research, leadership qualities and service to the unit and peers.

President's Senior Award
Awarded to seniors with the highest cumulative grade point average at Kentucky State University.

Dean's Outstanding Student in Mathematics and Science Award
Awarded for excellence in Mathematics and Science at Kentucky State University.

Outstanding Biology Student Award
Awarded for excellence in major or study at Kentucky State University.